AGRONOMIC PERFORMANCE AND MODELING OF BIOENERGY FEEDSTOCK CROP GROWTH AND DEVELOPMENT IN THE TEXAS ROLLING PLAINS

A Dissertation

by

PRAMOD POKHREL

Submitted to the Office of Graduate and Professional Studies of
Texas A&M University
in partial fulfillment of the requirements for the degree of

DOCTOR OF PHILOSOPHY

Chair of Committee,	Nithya Rajan
Co-Chair of Committee,	John L. Jifon
Committee Members,	Russell W. Jessup
	William L. Rooney
Head of Department,	David D. Baltensperger

August 2020

Major Subject: Agronomy

ABSTRACT

Energy canes (*Saccharum spp.* hybrid) and energy sorghum (S*orghum bicolor* L. Moench) have the potential to adapt in broader agroclimatic conditions and produce higher biomass yield. The first study was conducted to evaluate the agronomic performance of four energy cane genotypes (TUS11-62, TUS11-58, TCP10-4928, and Ho 02-113) in the Texas Rolling Plains. The results showed that the average biomass yield of plant cane, first ratoon, and the second ratoon were 20.16 t ha^{-1}, 40.37 t ha^{-1}, 26.4 t ha^{-1} respectively. Feedstock genotype did not affect biomass yield except plant cane in 2016. Severe winter kill resulted in the yield decline in the second ratoon. The second study was conducted to test the feasibility of the Decision Support System for Agrotechnology Transfer (DSSAT) – CANEGRO model to simulate the growth and development of energy canes**.** Among all variables measured, model predictions were best for stalk height and aboveground biomass yield. The simulated biomass yield and stalk height were within ±15% to observed values. The third study was performed to simulate the effect of change in climatic variables on biomass yield of energy cane in the Texas Rolling Plains. An increase in temperature and decrease in precipitation decreased biomass yield. Simulation results showed that the aboveground biomass yield of plant cane ranged from 11- 14 t ha^{-1} in irrigated and 4-9 t ha^{-1} in rainfed conditions and first ratoon ranged from 24 - 38 t ha^{-1} in irrigated and 10 – 21 t ha^{-1} in rainfed conditions respectively. Yield loss was higher when daily maximum and minimum temperature increased by 2°C and precipitation decreased by 20%. The fourth study was conducted

to evaluate the biomass yield and canopy characteristics of energy sorghum cultivars; ES 5140 and ES 5200. Additional water input (67%) in high irrigation treatment increased the plant height by 30%, water use efficiency (WUE) by 42%, and final biomass by 100% compared to low irrigation treatment. A strong linear relationship between leaf area index (LAI) ($R^2 = 0.82$) and exponential relationship between LAI and normalized difference vegetation index (NDVI) ($R^2 = 0.82$) were observed. Both sorghum hybrids showed similar light interception characteristics (light extinction coefficient of 0.41 in ES 5140 and 0.42 in ES 5022).

DEDICATION

I dedicate this dissertation to my late grandmother who taught me the value of education. I also dedicate this dissertation to my dad Mr. Krishna Prasad Pokhrel and mom Mrs. Ishwori Pokhrel.

ACKNOWLEDGEMENTS

This dissertation is one of the significant milestones in my academic career. Several people have contributed from their side to prepare this dissertation. Without their support, the writing of this dissertation would have not been possible. I would like to remember and thank each of them from the core of my heart.

I would like to express my sincere gratitude to my major advisor Dr. Nithya Rajan for her insightful comments and support throughout the study period. I would always be grateful for her constructive criticism and consistent encouragement. Also, I am sincerely thankful to my committee co-chair Dr. John Jifon and my committee members Dr. Russel W Jessup, and Dr. William L. Rooney for their guidance and invaluable suggestions.

I would like to thank all fellow graduate students from Rajan Crop Physiology Lab and staff at the Texas A&M AgriLife Research Station in Chillicothe, Texas. I also extend my thanks to department faculty and staff for making time at Texas A&M University a great experience.

Finally, I thank my wife, Puspa Ghimire, for her patience, love, care, and encouragement.

CONTRIBUTORS AND FUNDING SOURCES

This work was supervised by a dissertation committee consisting of Dr. Nithya Rajan, Dr. Russel W. Jessup, and Dr. William L. Rooney of the Department of Soil and Crop Sciences and Dr. John L. Jifon of the Department of Horticulture.

All works conducted for the dissertation was completed by the student independently.

This work is supported by the AFRI Sustainable Bioenergy Challenge Program [grant no. 2013-67009-21353, project accession no. 1001289] from the USDA National Institute of Food and Agriculture. Its contents are solely the responsibility of the authors and do not necessarily represents the official view of funding agency.

TABLE OF CONTENTS

Page

LIST OF FIGURES

Page

LIST OF TABLES

Page

CHAPTER I

INTRODUCTION

Demand and supply of bioethanol reached a record high in the US in 2017 (RFA, 2018b). Bioethanol production in the US increased rapidly from 40 billion liters in 2009 to 60 billion liters in 2017, accounting for about 10% of total 540 billion liters of refined motor gas (Figure 1.1) (EIA, 2018). Further, the US exported 5.2 billion and while importing 291 million liters of bioethanol in 2017 (RFA, 2018a). Bioethanol was imported to fulfill the standard of the Renewable Fuel Standard (RFS) program and low carbon fuel standard of California, which requires the use biofuel with low greenhouse gas (GHG) emission during its production lifecycle (Sharma et al., 2017; Whistance et al., 2017). Bioethanol is mostly produced from corn although a modest proportion is derived from sorghum and other grain starch. RFA (2018b) reported 98.5% of total bioethanol was produced from grain starch, and only 1.1% was produced from cellulosic biomass in 2017. The US RFS requires at least 44% of targeted 136 billion liters renewable fuel production by 2022 must be derived from cellulosic sources to reduce the greenhouse gas (GHG) footprint associated with bioethanol production in the US (EPA, 2018b).

Biomass production mainly depends on available inputs, environmental conditions, and management practices. Suitability and sustainability of the feedstock production depend on adaptability and profitability in the growing regions. Therefore, appropriate inputs are necessary to maximize the return and sustain the production. Corn

and sugarcane are widely known first generation feedstocks that contribute most of the biofuel production on global scale (Naik et al., 2010). Cultivation of these feedstocks relies heavily on high input and intensively managed production systems. These feedstocks not only require higher amount of water during production, but they also require significant amount of water post-harvest handling and industrial processes to produce ethanol. (Chiu et al., 2009; Wu et al., 2012). Chiu et al. (2009) estimated that 5 to 2138 L water is required to produce a liter of ethanol from field to the pump. The water requirement varies from region and methods of irrigation in the production site. Rainfed lignocellulosic feedstock production is one of the efficient biofuel production system because of the lower input requirement for biomass production (Rooney et al., 2007). Therefore, lignocellulosic feedstocks are considered as a better alternative energy source to reduce the competition for resources between food and fuel production.

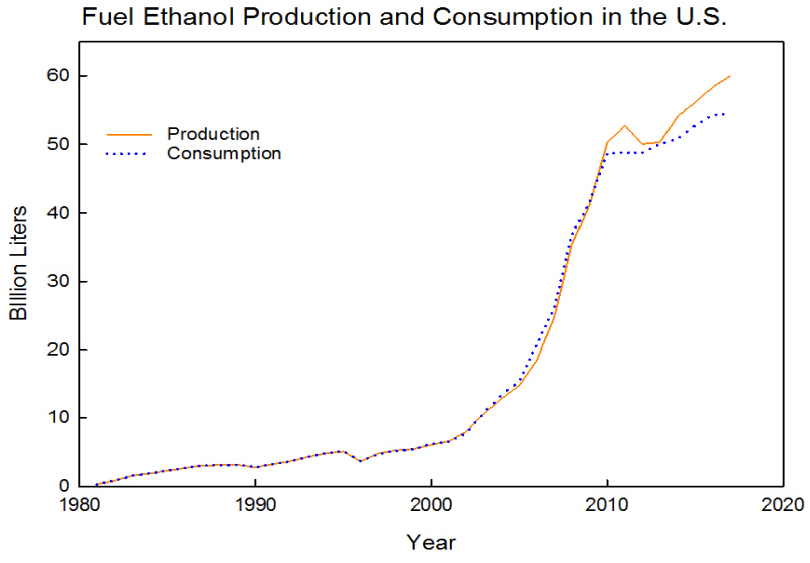

Figure 1.1. Bioethanol production and consumption in the US since 1982 (Adapted from Energy Information Administration, 2018).

Studies have shown that newly developed second-generation energy cane (*Saccharum spp.* hybrid) dry biomass yield as high as 45 t ha^{-1} (Erickson et al., 2012; Naik et al., 2010). Energy canes are interspecific hybrids of *S. officinarum* and *S. spontaneum* and perform better than sugarcanes especially on marginal land (Matsuoka et al., 2014), and are more persistent in colder environments (Khan et al., 2013). Compared to other feedstocks, energy canes have higher fiber content (cellulose 30-35%, hemicellulose 18-22%, and lignin 20-25%) which makes them suitable for biomass production (Fageria et al., 2013). Energy cane accumulates significant amount of belowground biomass in rhizomes during its active growth phase and it helps them to regrow for multiple years (Tew and Cobill, 2008). The rhizomes also help to recycle nutrients and store moisture, making them nutrient and water use efficient under marginal production conditions (Matsuoka et al., 2014). These grasses could contribute to sustainable production of bioethanol not only by reducing the competition for resources over grain-based ethanol production but also by utilizing the marginal lands by decreasing runoff, soil erosion, and nutrient losses from those lands. Site specific crop performance data together with economic and growth and development modeling analyses are required to match feedstocks with appropriate production regions to maximize productivity, optimize feedstock quality and conversion efficiency, and minimize the risks associated with successful operation of biofuels production chain.

The overall goal of this research is to evaluate recently developed second-generation energy cane feedstocks in the Texas Rolling Plains. The outcomes of this research will also provide an improved decision support system tools to benefit the production of

feedstocks in a specific growing and management conditions. It also offers a regional assessment of the sustainability of crops in the changing climatic condition in the Texas Rolling Plains. Specific objectives of the study are:

1. Compare and evaluate the agronomic performance and biomass yield of energy cane genotypes in the Texas Rolling Plains.
2. Calibrate and evaluate the DSSAT/ CANEGRO-Sugarcane model to simulate growth and yield of energy cane genotypes in the Texas Rolling Plains.
3. Evaluate the impact of future climate variability on biomass production of energy canes in the Texas Rolling Plains.
4. Compare and evaluate growth and light interception characteristics of energy sorghum hybrids.

This dissertation consists of six chapters. Chapter 1 is about general introduction about the feedstocks, growing region, and research objectives. Chapter 2 address the first objective. The research presented in chapter discuss the result of the field study. It consists of comparison of biomass and growth characteristics data of energy cane genotypes. Chapter 3 discusses about the adapting a DSSAT- CANEGRO- Sugarcane model to predict the biomass yield of energy cane genotypes in the Texas Rolling Plains to address the objective 2. After model calibration and evaluation, the CANEGRO – Sugarcane model was used to simulate the growth and biomass yield of remaining genotypes used in the study. Chapter 4 discuss about simulating the growth and biomass yield of energy cane in future climate change scenarios using calibrated and validated model. Chapter 5 discuss about the growth characteristics and light interception

characteristics such as leaf area index, light extinction coefficient and biomass yield of energy sorghum hybrids in the semi-arid Texas Rolling Plains to address the objective 4 of the study. The final chapter, Chapter 6 summarize the important findings of individual study objectives.

CHAPTER II

AGRONOMIC PERFORMANCE OF THE LIGNOCELLULOSIC FEEDSTOCK CROP ENERGY CANE IN THE TEXAS ROLLING PLAINS

INTRODUCTION

Energy Independence and Security Act of 2007 (EISA 2007) recognize lignocellulosic feedstock production as a major contributor to sustainable fuel production in the U.S. (Langholtz et al., 2016; Sissine, 2007). The act is committed to increase the energy independence of the U.S. by increasing the use of renewable fuels. To reduce greenhouse gas (GHG) emissions and ensure the future of clean energy, the U.S. Renewable Fuel Standard Program (US-RFS) mandates production of at least 44% of the targeted 136 billion liters of renewable fuel production from cellulosic sources by 2022 (DOE, 2020) However, the current cellulosic biofuel production in the U.S. has been less than the mandated production requirement set forth by EISA 2007. As a result, the Environmental Protection Agency (EPA) has exercised its cellulosic waiver authority and reduced the cellulosic biofuel target every year. In 2019, the cellulosic biofuel mandate was decreased to 1.6 billion liters from the original target of 32 billion liters (EPA, 2018a). Although the cellulosic biofuels sector has shown steady growth every year, domestic production was much lower than the original goal. Increasing cellulosic biofuel production in the U.S. requires advancements in several technology-related sectors including production of high yielding cellulosic biofuel feedstocks without affecting the national and global food security (Sohl et al., 2012).

Biofuels produced from lignocellulosic crops have the potential to enhance energy and food security and mitigate greenhouse gas emissions (OECD/FAO, 2015) Historically, biofuel production in the U.S. was dominated by grain-based feedstocks (Solomon et al., 2007). Approximately 40% of corn grains (*Zea mays* L.) produced during 2010-2015 was used for ethanol production in the U.S. (DOE, 2019a). However, using grains from corn and sorghum (*Sorghum bicolor* L.) for fuel production competes with increasing food and feed demands nationally and globally (Propheter et al., 2010). An alternate solution is to use lignocellulosic crops for biofuel production. Using perennial grasses and high biomass feedstock crops for fuel production may decrease the competition for prime croplands as these biofuel crops could be grown in marginal lands (Sanford et al., 2017). Growing feedstock crops in marginal lands also helps to decrease runoff, soil erosion, and nutrient losses that ultimately improve the landscape.

High biomass yield is one of the desirable characteristics of biofuel feedstock crops. Perennial tall grasses are well known for their ability to accumulate higher biomass, have a broader range of geographical adaptation, and are tolerant to a wider range of climatic conditions (Wang et al., 2017). Besides their adaptability, these perennial grasses help to improve soil health by increasing soil organic carbon, nutrient cycling, and biodiversity (Das et al., 2018). These beneficial properties make them a sustainable and promising source of lignocellulosic feedstocks. Switchgrass (*Panicum virgatum* L.) and miscanthus (*Miscanthus spp.*) are the potential bioenergy feedstocks in humid temperate to cool temperate regions (Sanford et al., 2017; Wang et al., 2017). Perennial

napier grass (*Pennisetum purpureum* S.) and annual energy sorghums are among the highest yielding feedstocks in the tropical and subtropical regions (Na et al., 2016b).

As the demand for biofuels is growing, many promising grasses are undergoing intensive breeding and agronomic research (Casler et al., 2017). Energy cane (*Saccharum spp*. hybrids) is one of the high biomass feedstocks developed by crossing sugarcane (*Saccharum spp*.) with a wild sugarcane relative (*S. spontaneum*) (Leon et al., 2015; Matsuoka et al., 2014). Both sugarcane and energy cane share the common ancestry of *S. officinarum* and *S. Spontaneum*. Sugarcane genome consist 85% genes from S. *officinarum* and 15% from *S. spontaneum.* Genetically, energy cane shares more genetic material from *S. Spontaneum* which results more tissue fiber (16% to 30%) and low sugar content (<10%) (Fageria et al., 2013; Matsuoka et al., 2014). Growing interest in energy cane for its biomass has led to the development of several high yielding genotypes in the last decade (Gordon et al., 2016; Waclawovsky et al., 2010).

Energy canes are classified into two different categories, type I and type II. Type I energy cane has low sugar (10-14%) and high fiber (14-20%) content than conventional sugarcane. Type II energy cane has even lower sugar content (<10%) than type I, but high fiber (>20%), which makes it appropriate for biomass production. Due to high sugar content, type I energy cane is cultivated for dual purpose of sugar and biomass but, type II energy cane is developed for lignocellulosic biomass production (Matsuoka et al., 2014). The extensive research and breeding efforts also increased disease resistance, adaptability, and biomass yield of energy canes that ultimately make them highly suitable for biomass production for a wide range of production regions.

To avoid the food versus fuel conflict, production of second-generation lignocellulosic feedstocks must utilize agriculturally degraded and marginal lands instead of prime farmlands (Chiluwal et al., 2019; Matsuoka et al., 2014). High biomass yield potential under limited input (marginal conditions) is a necessary prerequisite to ensure economic and environmental sustainability of the expanding biofuels and bioproducts economy. Texas Rolling Plains located in the northern Texas is an ecological region characterized by marginal production conditions. Average annual precipitation in the region from west to east ranges from 460 to 760 mm (Modala, 2014). Increasing crop water demand, frequent droughts, warmer summer temperatures, and decreasing precipitation are affecting crop production and economic revenues in this semi-arid region. As farmers in this region seek alternate crop options, high-biomass producing biofuel feedstocks may emerge as a viable opportunity in the future. However, only limited information is available about the performance of newly developed feedstock crops in semi-arid regions such as the Texas Rolling Plains.

The goal of this study was to characterize the growth, biomass yield of energy cane feedstock hybrids in the semi-arid Texas Rolling Plains. This three-year field study (2015 to 2017) evaluated the performance of four newly developed energy cane feedstocks under high and low irrigation conditions. Understanding the performance of these promising genotypes in the Texas Rolling Plains will contribute to a better understanding of their growth, development, and yield performance in marginal growing environments.

MATERIALS AND METHODS

Field Experiment

The study was conducted from 2015 to 2017 at the Texas A&M AgriLife Research Station in Chillicothe, Texas. The experimental plots were located in the research facility [34° 11' 46.99" N & 99° 31' 51.83" W, 437 m elevation] on an Abilene clay loam soil (Fine, mixed, thermic Pachic Argiustolls). This part of the Texas Rolling Plains has a semi-arid climate with an average annual precipitation of approximately 640 mm. Two-third of the annual precipitation occurs during May - October and dry freezing events are common from December to February.

Four energy cane type II genotypes (TUS11-62, TUS11-58, TCP10-4928, and Ho 02-113) were evaluated during the study. The first three energy cane genotypes were derived from crosses and selections as part of the Texas A&M AgriLife sugarcane breeding program in Weslaco, Texas, and are intended for biomass production in the U.S. Gulf Coast region (da Silva et al., 2020; da Silva et al., 2018). Ho 02-113 was developed and released by the USDA-ARS Sugarcane Research Unit in Houma, Louisiana as a feedstock for biofuel production (Hale et al., 2013). Energy cane plots were established in May 2015 using cane billets and maintained until November 2017. The second set of energy cane plots were established in May 2016. The 2016 planted energy cane did not survive the severe freezing during the 2016-17 winter and regrowth did not occur in 2017. Only one year of data is available from this second field experiment.

The experimental design was a randomized complete block with a split plot arrangement with four replications. The main plots consisted of two irrigation treatments and subplots consisted of energy cane genotypes (TUS11-62, TUS11-58, TCP10-4928, and Ho 02-113). Irrigation water was applied using the furrow method. The main plot was 72 m long and 32 m wide with ~1% slope. Individual plots were 5.5 m long and 4 m wide with four rows at 1 m distance. Plots were maintained with 1.5 m alleys between individual plots and 3 m alleys between blocks. Ridges and furrows were created a week before planting. Nitrogen fertilizer (Urea 46-0-0) was applied at 67 kg N ha^{-1} a day before planting. Cane billets were planted manually on ridges at a plant spacing of 33 cm. Planting was done on 20 May 2015. The second energy cane experiment was established in 2016 near the first study. In this experiment, plots were arranged in a randomized complete block design (RCBD) with only high irrigation treatment. Plots were 6 m long and 4 m wide with four rows at 1 m distance. The separation between plots and blocks were similar to the energy cane plots established in 2015. Nitrogen fertilizer (Urea, 46-0-0) was applied in August at 67 kg ha^{-1} by broadcasting. Weeds were managed whenever required in all experimental plots.

In 2015, irrigation water was applied ten times in high irrigation plots and six times in low irrigation plots from June to August. High irrigation plots received a total of 601 mm of irrigation water and low irrigation plots receive a total of 359 mm of irrigation water. An additional 257 mm of precipitation was received during the plant growing season from June to October. During the first ratoon phase in 2016, irrigation water was applied eight times in high irrigation plots (420 mm total irrigation) and six

times (265 mm total irrigation) in low irrigation plots. The cane billets that were planted in 2016 (plant cane) was maintained with high irrigation and received 420 mm of irrigation water, similar to the first ratoon plots. These plant cane plots received an additional 683 mm of precipitation from May until the final harvest in October. Similarly, the first ratoon received an additional 764 mm precipitation from March until October. During the second ratoon phase in 2017, irrigation water was applied four times in high irrigation plots and three times in low irrigation plots. High irrigation plots received a total of 358 mm of irrigation water and low irrigation plots received a total of 245 mm. An additional 1114 mm precipitation was received in the second ratoon growing season from March until October.

Weather

A weather station was established on site. Air temperature was collected using a temperature/RH sensor (Model HMP50, Campbell Scientific Inc., Logan, UT, USA). Precipitation was measured using a tipping bucket rain gauge (Model TE525, Campbell Scientific Inc., Logan, UT, USA). All data were collected at 10-second intervals using a CR1000 datalogger (Campbell Scientific Inc., Logan, UT, USA), which was used for hourly calculations. Daily values were obtained using hourly data for maximum and minimum air temperatures and cumulative precipitation.

Data Collection and Analysis

Field data was collected in 2016 and 2017. Within season field data collected include stalk height, stalk density, leaf area index (LAI), and the normalized difference vegetation index (NDVI). Data were collected from the middle two rows of each plot.

Stalk height was measured by randomly selecting 12 stalks per plot. Height was measured from soil surface to the visible collar of the uppermost leaf. Stalk density was measured by counting the number of stalks in a meter of crop row. Leaf area index was measured using a hand-held plant canopy analyzer (Model LI-COR 2200C; LI-COR Biosciences, Lincoln, NE). Measurements of LAI were taken during early morning between 6:30 am to 7:30 am when the sun was low on the horizon. View cap with 45° field of view was used during the LAI measurement. Two measurements were taken from each plot. A multispectral radiometer (Model MSR5; CROPSCAN Inc, Rochester, MN) was used for measuring reflected sunlight in the red (670 nm) and near-infrared (NIR; 830 nm) wavelengths. The NDVI was calculated using the equation (NIR - Red)/ (NIR + Red). These measurements were taken during solar noon (± 1 hour) time when the sky was clear. Measurements were taken by placing the sensor directly over the canopy. Approximately 1m distance was maintained between the sensor and top of plant canopy.

Final aboveground biomass measurements were taken on 28 October in 2016 and 11 November in 2017. Five representative stalks from each plot were harvested manually to obtain biomass yield. Stalk numbers were also obtained at the time of biomass harvest by counting the number of stalks in 2 m length of middle two crop rows. Samples were weighed immediately after harvesting and leaves and stalks were separated. Stalk diameter for each stalk was measured at three places: 10 cm above the bottom end, middle of the stalk, and 10 cm below the top end. Average of these three measurements were taken as the stalk diameter for an individual stalk. Separated leaves

and stalks were oven dried at 60°C until biomass weight remains unchanged. Biomass weight of 5 stalks was then multiplied by the average number of stalks, and final biomass was obtained on an area basis.

Leaf and stem tissues from the final harvest were analyzed for lignin, cellulose, and hemicellulose contents. Oven-dried plant parts (stem and leaves) were used to prepare separate samples for stem and green leaves. Stems were broken down into smaller chips (3-5 cm) using a wood chipper before grinding. All leaf and stem tissue were ground using a Wiley Mill (Thomas Scientific, NJ) and passed through a 1 mm screen to prepare final samples for analysis. Structural carbohydrates (cellulose, hemicellulose, and lignin) were estimated using Near-infrared spectroscopy (NIRs) (SpectraStar analyzer, Model 2500X RTW, Unity Scientific, Inc., Purcellville, VA). The NIR method was optimized to analyze the tissue components of bioenergy feedstocks (sugarcane, energy cane, and miscanthus). Non-structural components (i.e. extractives) such as sucrose, chlorophyll etc. were estimated using high performance liquid chromatography (Model UltiMate® 3000 HPLC; Thermo Scientific Dionex, Sunnyvale, California) or inductively coupled plasma spectroscopy (Model: Optima 7300 DV ICP-OES, PerkinElmer, Inc., Waltham, MA, USA).

Statistical analysis was conducted using a mixed model procedure in SAS v 9.4 (SAS, 2016). Field data were analyzed by analysis of variance (ANOVA) for repeated measures. Replication was considered a random variable, irrigation and genotypes were considered as fixed effects. Treatment means were separated by the Tukey method at $p \leq 0.05$ significance level.

RESULTS AND DISCUSSION

Weather Conditions

Average annual temperature at the study site was similar in all three years (18.4°C in 2015 and 2016, and 18.3° C in 2017), which was about 0.8°C higher than the 30-year average of 17.6°C. Figure 2.1 presents the monthly average maximum and minimum air temperature, and cumulative precipitation for the study period from 2015-2017 (Figure 2.1A-C). Long-term average (1984-2017) of these weather variables are presented in Figure 2.1D. Among the three years of this study, December 2016 and January 2017 had several days with minimum daily temperature reaching up to -14 to -16ºC. This was of particular importance as November through March was the dormancy period of energy cane in the Texas Rolling Plains. Survival of energy cane rhizomes during this period depends on the temperature conditions (Matsuoka and Franco-Garcia, 2011; Na et al., 2014; Sladden et al., 1991) and the cold hardiness trait each genotype (Khan et al., 2013).

Cumulative annual precipitation and its distribution during the growing season were substantially different between the study years. The average annual precipitation during 2015 (815 mm), 2016 (961 mm), and 2017 (1247 mm) were higher by 26%, 49% and 94% respectively compared to the 34-years average annual precipitation of 642 mm. In 2015, 51% of the annual precipitation was received before initiating the study (January to May) (Figure 2.1A). Only 33% of the total precipitation was received from June to October when energy cane was growing in the field. In 2016, January to March were the dry months. Only 6% of annual precipitation was received during this period

before the first ratoon emergence (Figure 2.1B). Majority of the annual precipitation (~79%) was received during the first ratoon growing season from April to October. Plant cane growing season in 2016 was from mid-May to October. About 63% of total precipitation was received during this period. Annual precipitation in 2017 was substantially higher than 2015 and 2016. About 23% of the total precipitation was received from January to March before the second ratoon emergence (Figure 2.1C). About 77% of the annual precipitation was received during the second ratoon growing season from April to mid-November. Nearly one third (28%) of annual precipitation in 2017 was received during the month of August.

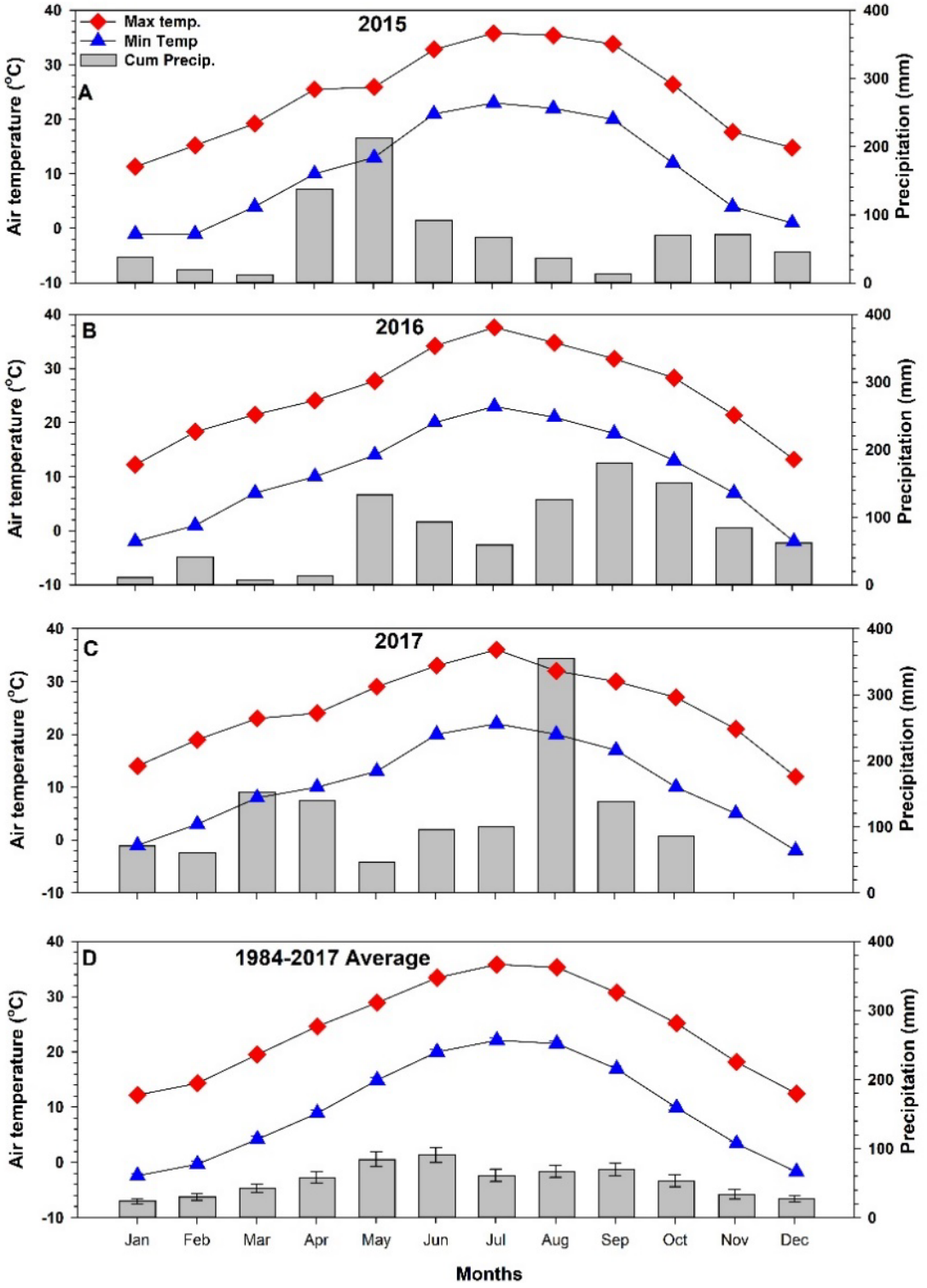

Figure 2.1. Average monthly maximum air temperature, average monthly minimum air temperature, and monthly cumulative precipitation for (A) 2015 (B) 2016 (C) 2017 and (D) 1984-2017. Error bars are the standard error of the mean.

Stalk Density

Stalk density of plant cane (billets planted in 2016) varied significantly among genotypes ($p \leq 0.01$) and crop growth stage ($p \leq 0.01$). Stalk density also showed a significant genotype x crop growth stage interaction ($p \leq 0.05$) (Table 2.1). Number of stalks increased rapidly during the first three months after planting of cane billets. Stalk density during mid-August was the highest for TCP10-4928 (average of 45 stalks m^{-2}) and the lowest for TUS11-62 (average of 26 stalks m^{-2}). The average stalk density of Ho 02-113, and TUS11-58 were 41±1.4 stalks m^{-2} and 36±2.5 stalks m^{-2} respectively. A decrease in stalk density was observed after mid-August for TCP10-4928, Ho 02-113 and TUS11-58. By October, the average stalk density declined to 38.9±1.7 stalks m^{-2} (decreased by 14%), 34.9±3.4 stalks m^{-2} (decreased by 18%), and 29.4±1.3 stalks m^{-2} (decreased by 15%) respectively for TCP10-4928, Ho 02-113 and TUS11-58. Although TUS11-62 had lower stalk density in mid-August, it continued to produce additional tillers and the average stalk density increased to 30±3.2 stalks m^{-2} (increased by 15%) at harvest in by October.

Stalk density of first ratoon (billet planted in 2015) showed a significant difference among genotypes ($p \leq 0.05$) and crop growth stage ($p \leq 0.01$) (Table 2.1). No significant difference was observed between irrigation treatments. Stalk density of first ratoon was much higher than the plant cane. Similar to plant cane, stalk density during July was the highest for TCP10-4928 with an average of 83.3±5.3 stalks m^{-2}. Genotype TUS11-58 had the lowest stalk density (67.8±5.1 stalks m^{-2}). Average stalk density of genotype Ho 02-113 and TUS11-62 were 78±5.1stalks m^{-2} and 74.4±4.3 stalks m^{-2}

respectively. Stalk density decreased as the season progressed. At final harvest (October 28), genotype Ho 02-113 had an average stalk density of 60.5±2.6 stalks m^{-2} (decreased by 23%), TUS11-62 had an average of 57.8±3.4 stalks m^{-2} (decreased by 22%), TCP10-4928 had an average of 56.6±1.7 stalks m^{-2} (decreased by 32%), and TUS11-58 had an average of 50.4±2.6 stalks m^{-2} (decreased by 26%). During the second ratoon season in 2017, stalk density was measured only at harvest and showed a significant difference among genotypes ($P \leq 0.01$) (Table 2.1). However, stalk density declined substantially during the second ratoon period. Genotype TCP10-4928 had the highest stalk density (average of 26.6±1.1 stalks m^{-2}) and TUS11-58 had the lowest (average of 17.4±1.1 stalks m^{-2}). Stalk density of genotype Ho 02-113 was 21.3±2 stalks m^{-2}. Genotype TUS11-62 had regrowth only in high irrigation plots and had an average stalk density of 17.3±1.3 stalks m^{-2}.

Table 2.1. Analysis of variance for stalk growth parameters of energy cane affected by genotype, irrigation, and growth stage. Results are presented for plant cane (2016), first ratoon (2016) and second ratoon (2017).

Source	Stalk density	Stalk height
Plant cane (2016)		
Genotype	**	**
Growth stage	**	**
Genotype x Growth Stage	*	NS
First ratoon (2016)		
Irrigation	NS	*
Genotype	*	**
Irrigation x Genotype	NS	NS
Growth Stage	**	**
Genotype x Growth Stage	NS	**
Irrigation x Genotype x Growth Stage	NS	NS
Second Ratoon (2017)		
Irrigation	NS	NS
Genotype	**	**
Irrigation x Genotype	NS	NS
Growth Stage	-	**
Genotype x Growth Stage	-	NS
Irrigation x Genotype x Growth Stage	-	NS

* significant at $p < 0.05$, ** significant at $p<0.01$, and NS: non-significant at $p = 0.05$

Overall, stalk density increased in the early growth phase, reached a peak, and started to decrease towards the end of the growing season. Peak tillering at our study site occurred in July-August. Yang et al. (2018) reported similar trends at different locations of coastal Texas. In their study, stalk density of plant cane varied from 10-25 stalks m^{-2}. In case of first and second ratoons, stalk density varied from 10-30 stalks m^{-2} and 10-15 stalks m^{-2} respectively. In a study conducted in Georgia, Chiluwal et al. (2018) reported an average stalk density of 24.5 stalks m^{-2} for plant cane, 32.3 stalks m^{-2} for first ratoon, and 27.3 stalks m^{-2} for second ratoon. In another study conducted in Louisiana, Viator et al. (2012) reported an average stalk density of 17.3 stalks m^{-2} for both plant cane and first ratoon. The stalk density of plant cane recorded in our study was similar to these

previously reported studies. However, stalk density during the first ratoon period was substantially higher at our study site. This higher tiller density at our site may have been due to narrow row spacing and lower plant to plant spacing compared to the other reported studies discussed above.

In the second ratoon cycle, TUS11-62 in low irrigation plots had very high mortality rates (~100%). As discussed earlier, December 2016 and January 2017 had several days with minimum daily temperature reaching as low as -16°C (Figure 2.1). These extreme low temperature days might have affected re-emergence and tiller production in the subsequent 2017 growing season. Rhizome survival during the over-wintering period is a key factor in many sugarcane species that determines tiller production in the next growing season (Matsuoka and Franco-Garcia, 2011). In a growth chamber study, when cold sensitive energy cane clones were exposed to 0°C for a week, they exhibited stunted growth and did not produce new tillers (Khan et al., 2013). Similar results were reported in miscanthus by Fonteyne et al. (2016). In their study, rhizome mortality due to below freezing temperature (up to -5.6°C) was about 50%. Therefore, extreme low temperature events during the winter of 2016 in our study site might have significantly reduced the ratoon vigor of all genotypes. Among the four genotypes, TUS11-62 showed the highest cold-sensitivity.

Stalk Height

Similar to stalk density, stalk height of plant cane (billets planted in 2016) showed significant difference among genotypes ($p \leq 0.01$) (Table 2.1). A sigmoid growth pattern characterized by slow early growth, rapid mid-season growth, and slow growth

in late season was observed (Figure 2.2). Genotype TUS11-62 had significantly taller stalks (138±3 cm) at harvest. Stalk height of first ratoon (billet planted in 2015) showed significant differences among irrigation treatment ($p \leq 0.05$) and genotypes ($p \leq 0.01$). In-season stalk height was higher in high irrigation treatment. Stalk height increased rapidly from July to mid-August and continued to increase at a slower rate until harvest (Figure 2.3A and B). Similar to plant cane, genotype TUS11-62 was significantly taller (232±3 cm at final harvest) in the first ratoon phase. Stalk height during the second ratoon period was lower than the first ratoon. Stalk height of genotypes at harvest was not significantly different and was averaged at 163 cm.

The final stalk height of plant cane in our study was less than observed values in other studies. Viator et al. (2012) reported stalk height of plant cane up to 240 cm in Louisiana and Yang et al. (2018) reported stalk height reaching up to 300 cm in the coastal region of Texas. Our study site in the Texas Rolling Plains region had shorter plant cane growing season (about 5.5 months) compared to the sub-tropical locations in the above-mentioned studies (12 months). In the first ratoon phase, final stalk height at our site was at comparable levels to those reported by Viator et al (2012). All genotypes in our study showed a decline in stalk height in the second ratoon phase which might have been affected by reduced plant vigor due to winter freezing as discussed in the previous section.

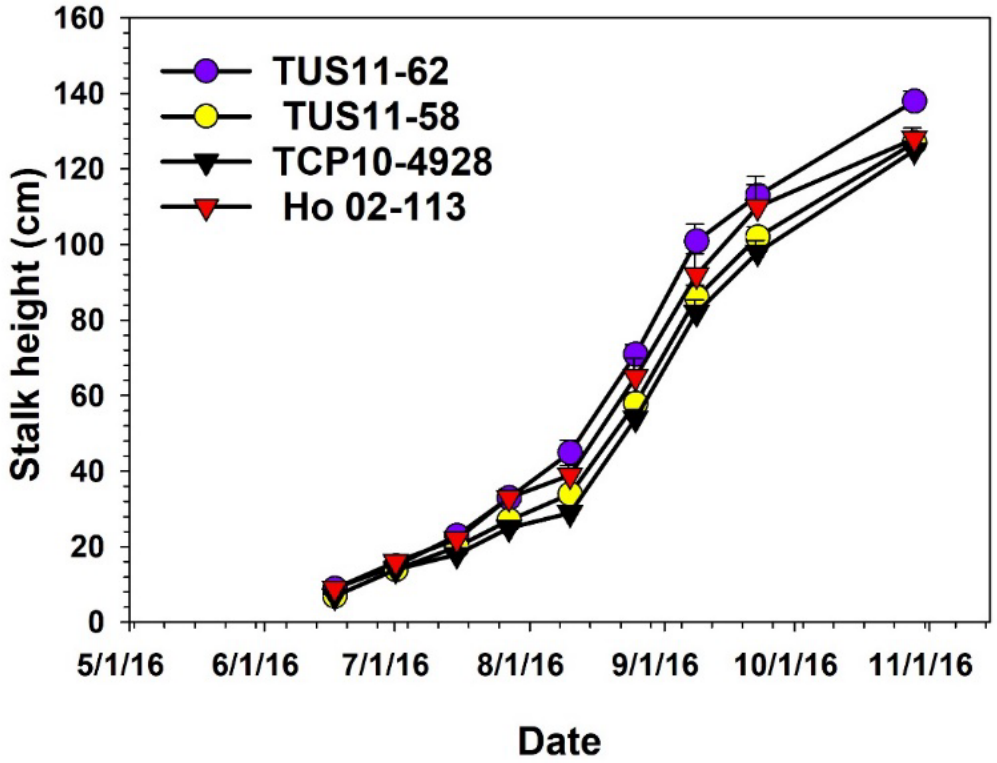

Figure 2.2 Stalk height of energy cane genotypes during the plant cane growing season (May to October) in 2016. Error bars are the standard error or the mean.

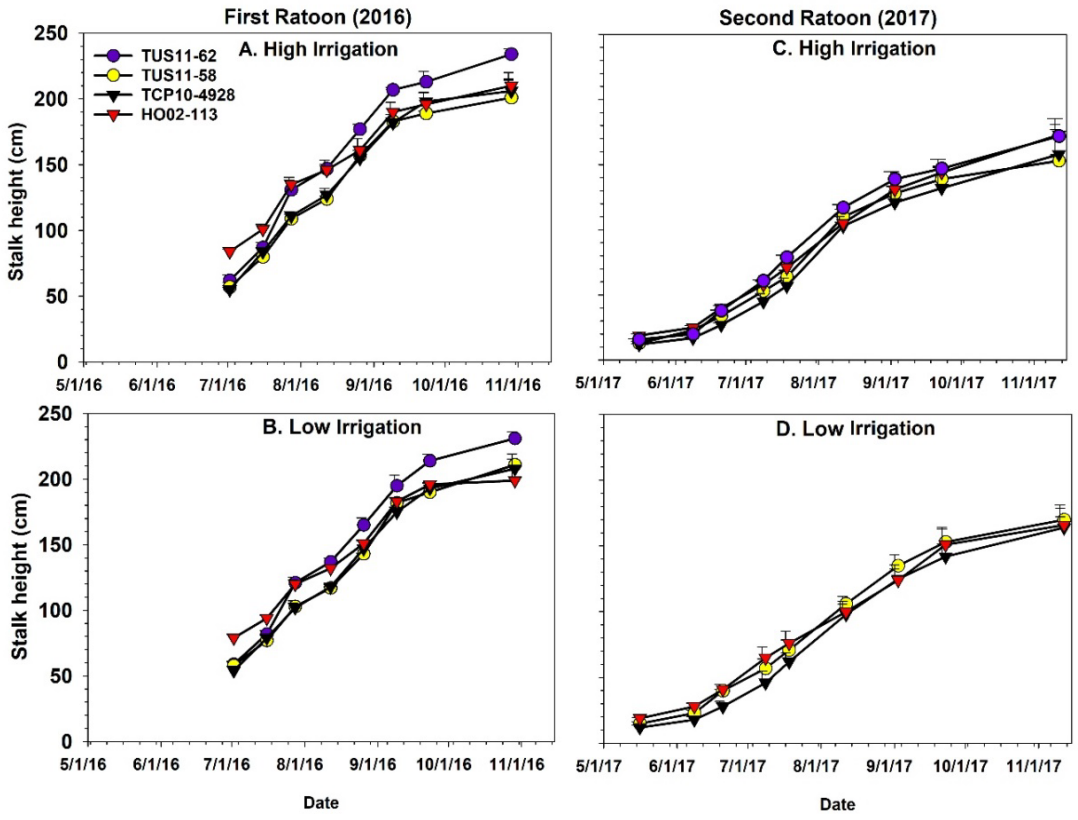

Figure 2.3 Stalk height of energy cane genotypes during first ratoon in 2016 at high and low irrigation treatments (A and B) and second ratoon in 2017 at high and low irrigation treatments (C and D). Error bars are the standard error of the mean.

Leaf Area Index

Figure 2.4 presents the LAI of plant cane in 2016 and the ANOVA results are presented in Table 2.2. Leaf area index showed a significant difference among genotypes ($p<0.01$). In general, the LAI development showed a sigmoid growth pattern (Figure 2.4). It increased at a slower rate in the first two months after planting (mid-May to July), increased at an increasing rate from August to September, and continued to increase at a slower rate until harvest in late October (Figure 2.4). The LAI at final sampling (Oct 28) was the highest for the genotype TCP10-4928 (4.86±0.5), which also

had the highest stalk density. Genotype TUS11-62 had the lowest LAI at the final sampling date (3.32±0.2) which also was the tallest genotype, but had the lowest stalk density compared to other genotypes in the study.

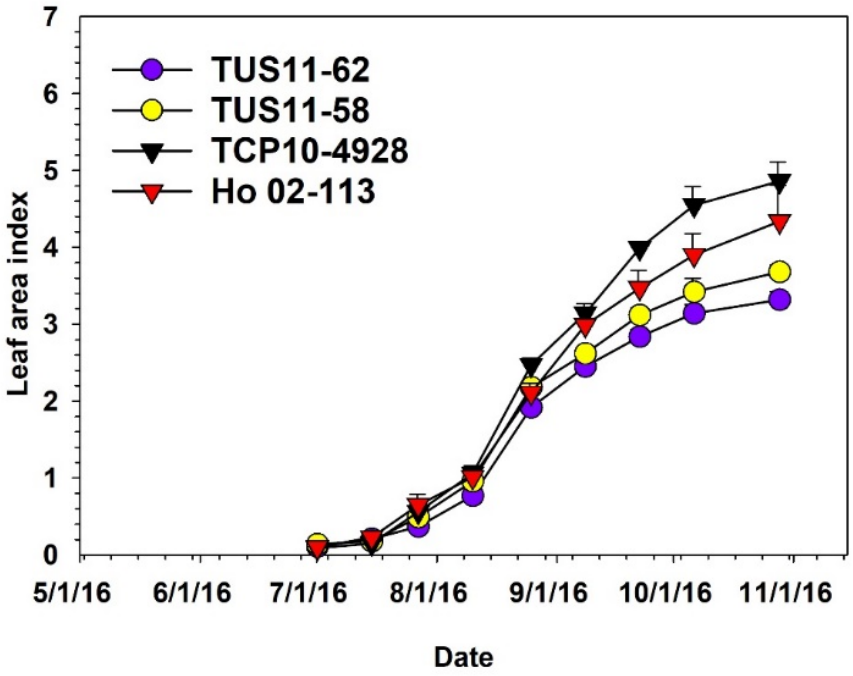

Figure 2.4 Leaf area index (LAI) of energy cane genotypes during plant cane growing season (May to October) in 2016 at high irrigation treatment. Error bars are the standard error or the mean.

Figure 2.5A-D present LAI during the first and second ratoon phases in high and low irrigation treatments. Two distinctive LAI progression with crop growth stage was observed in the high irrigation treatment in the first ratoon phase. Genotypes TCP10-4928 and Ho 02-113 had similar LAI development that peaked in the third week of September (Figure 2.5A). The maximum LAI of TCP10-4928 and Ho 02-113 were 5.84±0.10 and 5.57±0.09 respectively. Genotypes TUS11-58 and TUS11-62 had lower LAI compared to TCP10-4928 and Ho 02-113. Both these genotypes followed similar

LAI development which peaked around the last week of August. In the low irrigation treatment, genotype TCP10-4928 had the highest LAI and showed similar LAI development as in the high irrigation treatment. However, genotype Ho 02-113 showed a slight decline in LAI development. Similar to high irrigation, TUS11-58 and TUS11-62 had similar LAI development and the lowest LAI (Figure 2.5B).

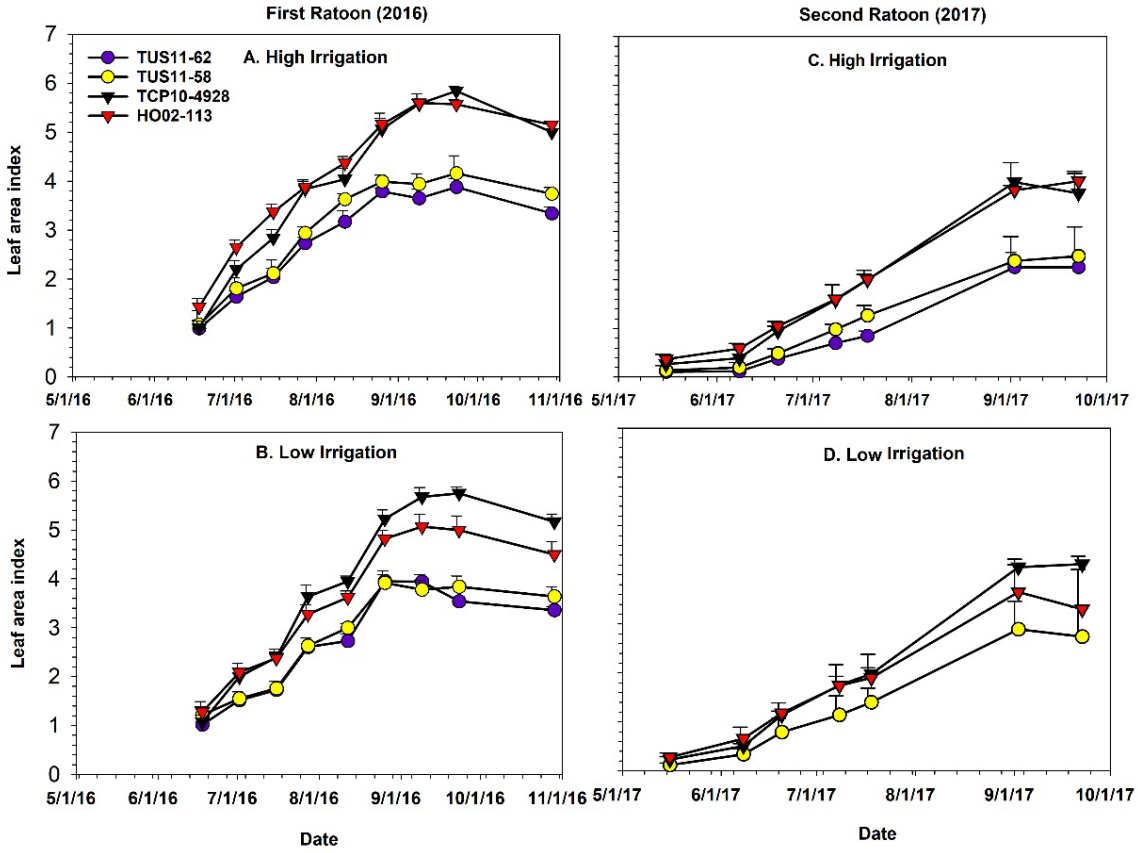

Figure 2.5 Leaf area index (LAI) of energy cane genotypes during first ratoon in 2016 at high and low irrigation treatments (A and B) and second ratoon in 2017 at high and low irrigation treatments (C and D). Error bars are the standard error of the mean.

As discussed previously, growth and development of all genotypes were affected in the second ratoon phase. The LAI of all genotypes followed similar development pattern as in the first ratoon phase, but the LAI was significantly lower. Similar to first

ratoon, genotypes TCP10-4928 and Ho 02-113 had higher LAI and TUS11-58 and TUS11-62 had lower LAI. All genotypes reached their peak LAI in the first week of September. The highest LAI of genotype TCP10-4928 and Ho 02-113 were 4.0± 0.41 and 3.84±0.15 respectively whereas, TUS11-58 and TUS11-62 had 2.39±0.53 and 1.99±0.30 respectively. In low irrigation treatment, genotype TUS11-62 did not survive the hard freezing during winter. Genotype TCP10-4928 had the highest LAI (4.1±0.16) in the low irrigation treatment which was recorded in early September.

Comparable LAI values (3 – 5) were reported in plant cane and ratoons in Georgia (Chiluwal et al., 2018) and in Florida (Na et al., 2015). Among all genotypes, TCP10-4928 and Ho 02-113 had consistently higher LAI during the plant cane and the two ratoon cycles compared to TUS11-58 and TUS11-62. The observed feedstock differences in LAI may be related to slight differences in leaf/canopy architectures. For instance, TCP10-4928 tends to have wider leaf blades similar to sugarcane compared to the other genotypes with narrower leaf blades reminiscent of their *S. spontaneum* parent (Matsuoka et al., 2014). Field observation showed that genotypes TCP10-4928 and Ho 02-113 had comparatively wider leaves than TUS11-58 and TUS11-62, which had narrower and more erect leaves (Pokhrel et al., 2017). In addition, relatively higher stalk density of TCP10-4928 and Ho 02-113 may have also contributed to higher LAI.

Table 2.2. Analysis of variance for canopy growth parameters of energy cane affected by genotype, irrigation, and growth stage. Results are presented for plant cane (2016), first ratoon (2016) and second ratoon (2017).

Source	LAI
Plant cane (2016)	
Genotype	**
Growth stage	**
Genotype x Growth Stage	**
First ratoon (2016)	
Irrigation	*
Genotype	**
Irrigation x Genotype	NS
Growth Stage	**
Genotype x Growth Stage	**
Irrigation x Genotype x Growth Stage	NS
Second Ratoon (2017)	
Irrigation	NS
Genotype	**
Irrigation x Genotype	NS
Growth Stage	**
Genotype x Growth Stage	NS
Irrigation x Genotype x Growth Stage	NS

* significant at $p< 0.05$, ** significant at $p<0.01$, and NS: non-significant at $p = 0.05$

Normalized Difference Vegetation Index and Leaf Area Index

There was a strong relationship between LAI and NDVI (Figure 2.6), which was similar to the relationship observed for other field (Attia and Rajan, 2016; Shafian et al., 2018). For many row crops, NDVI become invariant to changes in leaf development as LAI increases above 3.0 (Ko et al., 2005; Viña et al., 2011). When LAI is 3.0 or above, most row crops have 80% or more ground cover and NDVI peaks at this stage (Shafian et al., 2018). Hence, further increase in LAI does not cause significant changes in NDVI. The result from our study showed that the empirical relationship between LAI and NDVI of energy cane genotypes could be useful to predict canopy growth and development up

to a certain stage. Further studies are needed to determine the applications of this method, which was beyond the scope of this current study.

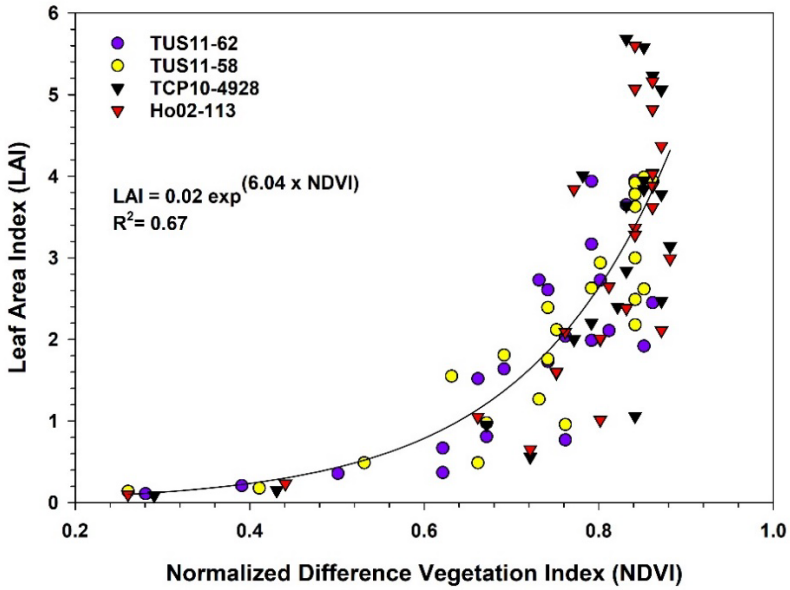

Figure 2.6 Relationship between leaf area index (LAI) and normalized difference vegetation index (NDVI) of energy cane genotypes. Data include plant cane, first ratoon and second ratoon phases.

Aboveground Dry Biomass Yield

Average aboveground dry biomass yields are presented in Figure 2.7. There was no significant difference in biomass yield of first ratoons in high and low irrigation treatments. The average biomass yield doubled in the first ratoon phase (40.37 t ha^{-1}) compared to plant cane phase (20.16 t ha^{-1}). Although many studies have reported similar biomass yield in energy cane first and second ratoons (Chiluwal et al., 2018; Knoll et al., 2013; Yang et al., 2018), yield declined in the second ratoon phase at our site due to severe winter freezing. The average biomass yield (26.4 t ha^{-1}) in the second ratoon phase was similar among genotypes and irrigation treatments, and comparable to

the biomass yield (20 t ha^{-1}) reported by Chiluwal et al. (2018) under marginal production conditions in Georgia. Higher biomass yield of plant cane was reported by Yang et al. (2018) in the coastal region of the Texas. In a study in Florida, Leon et al. (2015) reported a dry biomass yield of 26 t ha^{-1} in both plant cane and first ratoon. Energy cane showed higher biomass yield in the regions with higher annual temperature and precipitation and were affected by genotype characteristics and management practices (Leon et al., 2015; Yang et al., 2018; Zhao et al., 2017).

Our results indicate that the severity of winter was a major driver in determining the biomass yield of energy cane genotypes (discussed earlier). In addition, the longer growing period of ratoon (~8 months) increased the biomass production compared to the plant cane phase which had a shorter growing period (~ 5.5 months) in the Texas Rolling Plains. Although in-season data showed variations in stalk density, stalk height, and LAI of energy cane genotypes, final biomass yields were not significantly different. For example, genotype TCP10-4928 had the highest stalk density and genotype TUS11-58 had the lowest stalk density in the first ratoon phase. However, both genotypes had similar biomass yield. This may be due to the fact that the genotype TCP10-4928 had thinner stalks (mean stalk diameter 16.76 mm) compared to the genotype TUS11-58, which had thicker stalks (mean stalk diameter 18.07 mm). Reduced irrigation water input did not significantly impact biomass yields indicating that limited irrigation would be an economic option for biomass production in the Texas Rolling Plains especially in years with more than average precipitation.

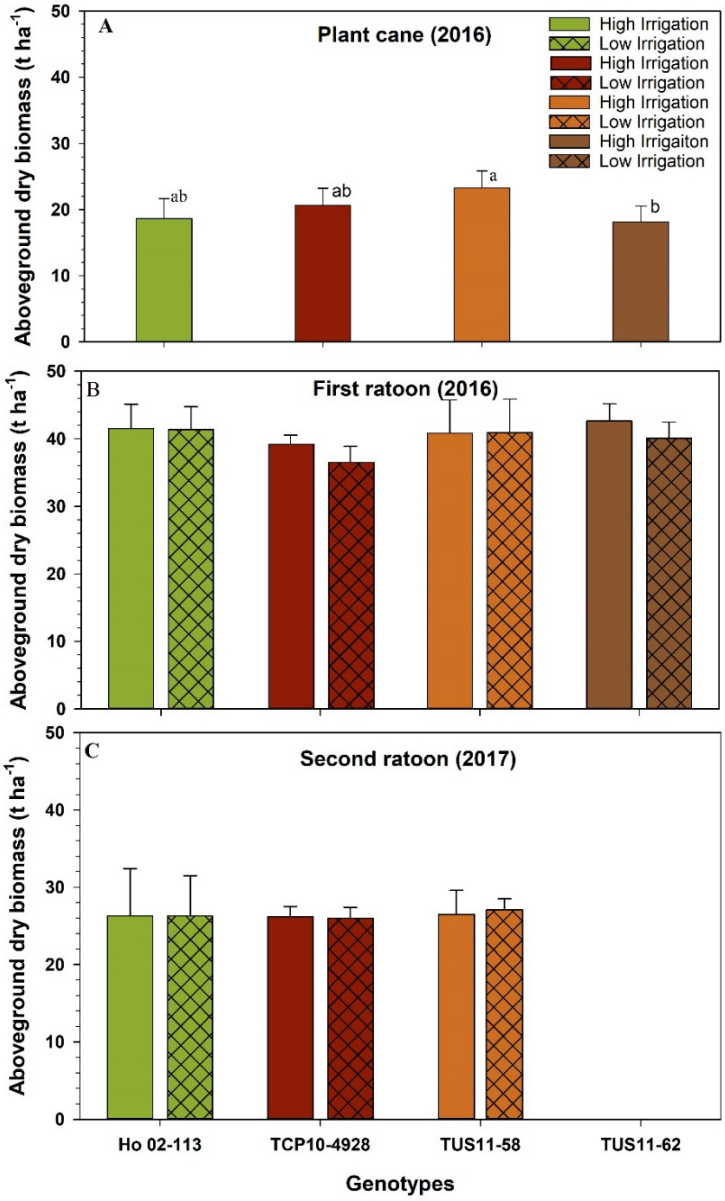

Figure 2.7 Aboveground dry biomass yield of energy cane genotypes of (a) plant cane (2016) (b) first ratoon (2016) and (c) second ratoon (2017). Error bars in the bar graph are the standard error of the mean.

Biomass Composition

The chemical composition of lignocellulosic materials plays an important role in optimizing strategies for ethanol production. The chemical composition can vary

depending on the type of plant, age, growing environment, and management. In addition, the methods used in compositional analysis can also influence the tissue fractions (Canilha et al., 2012; Hatfield and Fukushima, 2005). Table 2.3 summarizes the tissue composition of energy cane stems and leaves collected at final harvest of plant cane, first ratoon, and second ratoon. The lignin content of stems and leaves ranged from 17-20% which was similar to the lignin content reported for energy canes (da Silva, 2017; Fedenko et al., 2013; Kim and Day, 2011; Na et al., 2016a). Cellulose content in stems and leaves were similar (35-36%), but was slightly lower in stems (30-31%) in second ratoon phase. Hemi-cellulose content in stems and leaves ranged from 16-19% and 19-20% respectively. Tissue cellulose and hemicellulose content observed in our study were lower than the values reported in other studies. Kim and Day (2017) reported 43% and 23% cellulose and hemicellulsoe contents respectively in energycane. Thammasittirong et al (2017) reported 43% cellulose and 28% hemicellulose in energy cane growing in Thailand. da Silva (2017) reported 22-30% cellulose and 29 -35% hemicellulose and on TUS11 clones. In our study, TUS11-62 had slightly higher cellulose content (35%) but significantly lower hemicellulose content (18%). In general, the lignin, cellulose and hemicellulose contents reported in this study were similar to reported values for the lignocellulosic biofuel crop *Miscanthus* × *giganteus* (Ussiri and Lal, 2015).

Extractives are non-structural materials in biomass which include sucrose, chlorophyll, waxes, and other soluble solids. Free ash consists of mainly minerals and inorganic component that does not contributes to the energy production. Higher amount of extractives and ash content could reduce the conversion efficiency of lignocellulosic

materials (Na et al., 2016b). The extractives in stem tissues varied from 14-18% whereas leaves had significantly lower total extractives (1-4%). Extractives content in our study were slightly lower than the value (23.22%) reported by de Carvalho and Tannous (2017) in other energy cane varieties. Average ash contents were 6-8% in stem and 6-11% in leaves. These values were also higher than those reported in leaf tissue (3-4%) by Na et al (2016a and b).

Table 2.3. Stem and green leaf tissue composition of energy cane genotypes grown in Chillicothe Texas during 2016- 2017. Results are presented for plant cane (2016), first ratoon (2016) and second ratoon (2017). The values are presented as means ± standard deviation.

	Stem					Green leaf				
	Lignin (%)	Cellulose (%)	Hemi-cellulose (%)	Extractive (%)	Extractive free ash (%)	Lignin (%)	Cellulose (%)	Hemi-cellulose (%)	Extractive (%)	Extractive free ash (%)
Plant cane										
Ho 02-113	18.0±0.4	35.0±0.2	18.8±0.4	17.5±1.9	7.7±0.6	21.0±0.2	35.9±0.3	18.9±0.4	3.5±0.9	9.7±0.5
TCP10-4928	18.3±0.2	35.2±0.3	18.7±0.7	14.4±2.6	8.3±0.7	20.8±0.4	36.0±0.1	18.8±0.5	1.5±1.1	10.2±0.8
TUS11-58	17.1±0.4	35.1±0.1	18.0±0.1	15.8±0.8	7.9±0.2	20.2±0.7	36.3±0.3	18.9±0.3	2.0±1.4	9.7±0.5
TUS11-62	18.0±0.4	35.3±0.2	18.6±0.4	14.6±1.3	8.4±0.2	19.8±0.5	36.1±0.2	18.3±0.3	3.9±1.0	11.0±0.3
First ratoon										
Ho 02-113	19.3±0.6	35.4±0.4	19.3±1.3	18.2±2.1	6.9±0.6	20.6±0.7	36.0±0.3	19.5±0.3	2.8±0.8	9.9±0.5
TCP10-4928	18.9±0.6	35.3±0.2	18.8±1.0	16.7±2.2	7.3±0.8	20.6±0.4	36.0±0.2	19.3±0.6	2.3±0.7	9.6±0.4
TUS11-58	18.8±0.8	35.4±0.2	18.2±0.6	15.4±1.8	7.4±0.8	19.9±0.7	36.3±0.2	18.8±0.2	1.9±0.9	9.7±0.3
TUS11-62	19.1±0.5	35.5±0.2	18.6±0.3	16.0±1.8	7.2±0.5	19.4±0.9	36.1±0.1	18.3±0.4	4.4±0.9	10.3±0.3
Second Ratoon										
Ho 02-113	17.6±1.4	29.9±0.9	16.9±1.1	-	6.2±0.9	21.1±1.8	36.9±0.4	19.6±0.4	-	6.9±0.2
TCP10-4928	20.1±1.3	31.5±0.9	18.0±0.8	-	7.5±0.6	20.1±1.1	37.1±0.4	20.7±0.4	-	7.8±0.6
TUS11-58	19.4±2.3	30.9±0.5	18.2±0.5	-	6.8±0.9	21.2±3.5	37.5±0.8	21.0±0.3	-	7.7±0.2

CONCLUSIONS

Energy cane genotypes were evaluated for their yield performance and quality in the semi-arid Texas Rolling Plains. Length of the growing season and severity of the winter affected biomass yield. Biomass yield of first ratoon was significantly higher than plant cane and second ratoon. Higher stalk density, taller and thicker stalk during the first ratoon cycle contributed to the higher biomass yield. Extreme low temperature (-14°C to -16°C) during the winter prior to the second ratoon emergence reduced plant vigor and biomass yield among all genotypes in the subsequent second ratoon season. Genotype TUS11-62 showed higher sensitivity towards low temperature and did not have regrowth in low irrigation treatment during the second ratoon cycle. Dry biomass yield was similar in high and low irrigation treatments. Thus, low irrigation could be an economic option for biomass production in the Texas Rolling Plains particularly in years with more than average precipitation. However, further studies with more irrigation levels are required to estimate optimum irrigation water requirement for biomass production in the study site

CHAPTER III

MODELING THE GROWTH AND BIOMASS YIELD OF ENERGY CANE (*Saccharum spp.* Hybrid) USING DSSAT-CANEGRO SUGARCANE MODEL

INTRODUCTION

Simulation models are widely used in many aspects of crop improvement due to their capability to integrate the response of genotype, growing environment, management practices, and their interactions on predicting crop development (White, 1998). Although conducting agronomic trials help to identify suitable crop management practices under real-world conditions, it requires significant time and resource investments. Simulation models work as tools to integrate information from past agronomic experiments and facilitate prediction of varying spatial (e.g. land), temporal (e.g. weather), and management (e.g. irrigation, fertilizer, tillage) factors on crop growth and yield (Attia et al., 2016a; Chavez et al., 2018; Jones et al., 2003) yield. Models are powerful tools that can be used to optimize inputs and management practices in an agricultural production system (Boote et al., 2001; Thorp et al., 2014). Researchers have been widely using this tool for the last few decades in various aspects of crop improvement such as yield prediction, determination of optimal management practices, precision agriculture, and in many other aspects of agronomic and plant breeding activities around the globe (Adhikari et al., 2016; Attia et al., 2016a; Marin et al., 2012; Sannagoudar et al., 2019; Sonkar et al., 2019).

Simulation models often use the same generic codes that address the relationship between crop, environment, and management practices to predict the growth characteristics of multiple crops that have similar growth characteristics (Boote et al., 2002; Singh et al., 2016). The unique differences among the cultivar characteristics and environment are addressed in a specific crop model (Boote et al., 2001). Due to the ability of simulation models to address general relationships, they can be modified and adapted to simulate the growth and development of a new crop. The CANEGRO model is a sugarcane crop simulation model developed by Inman-Bamber (1991) at the South African Research Institute. This model was further refined by Singels and Bezuidenhout (2002) and Singels et al. (2008). CANEGRO model is now included in the Decision Support System Agrotechnology Transfer DSSAT software (Hoogenboom et al., 2019). The DSSAT software is a computer application that simulates crop growth, development, and yield by using soil, weather, management, and cultivar input data (Jones et al., 2003). The DSSAT-CANEGRO model has been successfully used for simulating sugarcane production and yield around the globe. CANEGRO model is widely used in parameterization and evaluation of sugarcane cultivars (Marin et al., 2011; Sonkar et al., 2019), predicting the impact of climate change on sugarcane production (Jones and Singels, 2018; Singels et al., 2014; Sonkar et al., 2019) and predicting genotypic difference in sugarcane (Hoffman et al., 2018).

The objective of this study was to evaluate the use of DSSAT-CANEGRO-Sugarcane model for simulating energy cane (*Saccharum spp.* hybrid) biofuel feedstock production in the Texas Rolling Plains. Energy cane is a biomass crop developed by

crossing sugarcane (*Saccharum spp*.) with a wild sugarcane relative (*S. spontaneum*) in late 19th century (Leon et al., 2015). The growing interest in energy cane for its biomass for fuel ethanol production has led to the development of several high yielding genotypes in the last decade (Waclawovsky et al., 2010). There are two types of energy canes available for growing as biofuel feedstocks. Type I energy canes, which are similar to conventional sugarcane cultivars but have lower sugar (10-14%) and higher fiber (14-20%) contents, can be cultivated for biomass in addition to sugar production (Knoll et al., 2013). Type II energy canes have low sugar (<10%) and high fiber (>20%) contents and are used primarily for lignocellulosic biomass production. The extensive research and breeding efforts also increased disease resistance, adaptability, and biomass yield of energy canes that ultimately made them highly suitable for biomass production for a wide range of production regions.

Growth and biomass yield of energy cane is highly dependent on the type of genotype, soil conditions, and nutrient supply (Leon et al., 2015; Zhao et al., 2017). Severity and duration of winter also play a crucial role in limiting feedstock yield (Na et al., 2014). Current studies on energy cane are limited to subtropical and humid tropical regions. Only limited information is available about the performance of newly developed second-generation feedstocks in the semi-arid regions where low precipitation, high evapotranspiration, and dry freezing events are the dominant climatic characteristics. These climatic factors may have a prominent effect on the growth and development of the feedstocks that were developed predominantly for the tropical and subtropical environment (Silva et al., 2008).

In this study, we used the DSSAT-CANEGRO model for simulating the growth and biomass yield performance of newly developed Type II genotypes in the semi-arid climatic conditions of the Texas Rolling Plains. Although this is a sugarcane model, our goal was to test the feasibility of using the DSSAT-CANEGRO model for simulating energy cane production in the Texas Rolling Plains. Genetic coefficients were adjusted using crop phenology data collected from agronomic trials in the Texas Rolling Plains. After adjusting the genetic coefficients, performance of the model was tested using field data from Type II genotypes.

MATERIALS AND METHODS

DSSAT-CANEGRO-Sugarcane Model

The DSSAT Version 4.7 was used in the present study. CANEGRO is a modular component of the DSSAT software program. The CANEGRO- sugarcane model in DSSAT simulates the growth and development of sugarcane by combining the effects of crop genotype, weather, soil characteristics, and management practices (Singels et al., 2008). This model is a process-based growth and development model that includes phenology, canopy development, biomass accumulation and partitioning, root growth, water stress, and lodging (Marin et al., 2011; Singels et al., 2008). The model uses daily solar radiation, precipitation, maximum and minimum temperature, and irrigation (Attia et al., 2016b). The soil module in DSSAT simulates soil water balance, which is modeled based on the amounts of precipitation and irrigation (input data) and estimated values of evapotranspiration, soil water drainage, infiltration, and surface runoff. Water holding characteristics of the soil profile is calculated based on a specified drained upper

limit (DUL) lower limit (LL), and saturated water capacity (SAT). The assumption is that unsaturated upward flow in the soil profile occurs when a layer has a water content between LL and DUL, and saturated downward flow occurs when a layer has a water content higher than DUL. As the excess water accumulates in the lower soil profile, it is considered as drained water (not available for plants). Evapotranspiration is modeled using the FAO-65 method. The model assumes adequate nutrients present in the soil profile.

The DSSAT-CANEGRO model simulates sugarcane leaf area, stalk and root biomass, plant phenology, and other variables (Marin et al., 2011). The model estimates canopy level daily gross photosynthesis using a radiation use efficiency approach as described by Inman-Bamber (1991) and Singels et al. (2008) The model estimates seasonal growth by simulating individual plant parts such as leaves and tillers, and scale up the growth by multiplying the number of plant parts to unit area (Marin et al., 2011). Phenological phases are calculated based on the thermal time period, which describes emergence of the primary tiller, leaf emergence, leaf elongation, stalk elongation, maximum tillering, and senescence. Partitioning of assimilates is based on source strength and regulated by sink. Root growth is expressed in terms of the extension of the rooting depth and length in each soil layer. Water stress in the model is simulated based on the ratio of transpiration rate to root water uptake.

The DSSAT crop simulation model also includes the genetic parameters of a crop (Jones et al., 2011). Genetic parameters are further divided into species, ecotype, and cultivar. Species in the model describe the broader and characteristics of plant

species such as photosynthesis, respiration, partitioning, root growth, and plant response to water stress. Ecotype parameters are more specific than a species and can be similar for more than one cultivar. Cultivar parameters are highly specific to a genotype which determines biomass partitioning, canopy (leaf and tiller) development, and phenological stages (Marin et al., 2011).

Field Experiment

Field studies were conducted for three years at the Texas A&M AgriLife Research station in Chillicothe, Texas [34° 11' 46.99" N & 99° 31' 51.83" W, 437 m elevation]. This part of Texas has a rolling topography (thus called the Texas Rolling Plains) and semi-arid climate. The average annual precipitation is approximately 560 mm (Attia et al., 2015). Two-third of the annual precipitation occurs during the crop growing season (May – October) and dry freezing events are common from December to February.

Energy cane plots were established in 2015, and data collection was continued in 2016 and 2017 from the ratoons. The plots were laid out in a split-plot design with two levels of irrigation (high and low) as main plot factors and four energy cane genotypes (TUS11-62, TUS11-58, TCP10-4928, and Ho 02-113) as sub-plot factors. The first three genotypes were derived from crosses and selections as part of the Texas A&M AgriLife sugarcane breeding program in Weslaco, Texas, and are intended for biomass production in the U.S. Gulf Coast region (Landivar et al., 2016). Ho 02-113 was developed and released by the USDA-ARS Sugarcane Research Unit in Houma, Louisiana, for use as a feedstock for biofuel production (Hale et al., 2013). The experiment was replicated four

times. The site was plowed to a depth of 25 cm depth using a chisel plow four weeks before planting in 2015, and ridges and furrows were created at a meter spacing. Individual plots of 6 x 4m size were established, and cane billets were planted manually at 32 cm spacing in each row. Plots were irrigated using furrow irrigation method. This experiment was maintained with irrigation to minimize water stress. Approximately 33% less water was supplied to low irrigation plots during the entire crop growing season. Nitrogen fertilizer (urea, 46-0-0) was applied at 67 kg ha^{-1} once during the crop growing season, and weed and pest management were done whenever required. Details of the irrigation and management activities are listed in Table 3.1. A second set of plots were planted in 2016 next to the previously established study. Plots were laid out in a randomized complete block design (RCBD) using the same energy cane genotypes as in 2015 and replicated four times. Only the high irrigation treatment was used in this test.

Energy cane goes through a dormant phase during winter. During dormancy, aboveground plant parts senesce, but underground rhizomes remain alive. Rhizomes usually start producing tillers in late February to mid-March when soil temperature gradually increases above freezing point as a ratoon. However, severe freezing soil temperatures could kill rhizomes and prevent the energy cane from ratooning in successive years. Energy cane was successfully established in 2015 and data collection continued until 2017. However, the energy cane planted in 2016 did not survive the freezing temperatures during the 2016-17 winter period. As such, only one year of data from 2016 is available from this experiment.

Table 3.1. Details of major crop management activities in the field study

Activities	Year		
	2015	2016	2017
Planting	May 22	First ratoon	Second ratoon
Fertilizer application	May 5	Aug 13	Jun 22
Biomass harvest	Oct 29	Oct 28	Nov 10
Planting	-	May 18	No regrowth
Fertilizer application	-	Aug 13	-
Biomass harvest	-	Oct 28	-
Irrigation (high)	601 mm	420 mm	358 mm
(low)	359 mm	265 mm	245 mm

Crop Phenology Data

Field data collected include stalk height, stalk density, leaf area, biomass, and absorbed photosynthetically active radiation (APAR). Plant height was measured by randomly selecting 12 plants per plots. Height was measured from soil surface to the visible collar of the uppermost leaf. Stalk density was measured by counting tillers per meter of crop rows. Leaf area index (LAI) was measured non-destructively using a plant canopy analyzer (Model LI-COR 2200C; LI-COR Biosciences, Lincoln, NE). Absorbed photosynthetically active radiation (APAR) was measured using a ceptometer (Model ACCUPAR LP-80; Meter Environment, Pullman, WA). Data were collected at biweekly intervals during the plant growing season. In season biomass samples were taken using a $0.3m^2$ quadrant every 30 days from the designated plots. Plant parts (stalk and leaf) were separated, samples were oven-dried at 60°C, and dry weight was recorded.

Model Input Data: Weather

Crop growth simulation in DSSAT is driven by daily weather data that was collected from a weather station on site. Air temperature and relative humidity were collected using a temperature/RH sensor (Model HMP50, Campbell Scientific Inc.,

Logan, UT, USA). Solar irradiance was measured using a pyranometer (Model LI-190SB, LI-COR Biosciences, Lincoln, NE, USA), and precipitation was measured using a tipping bucket rain gauge (Model TE525, Campbell Scientific Inc., Logan, UT, USA). Wind speed and direction were measured using a wind sentry set (Model 03002-L, Campbell Scientific Inc., Logan, UT, USA). All data were collected at 10-second intervals using a CR1000 datalogger (Campbell Scientific Inc., Logan, UT, USA), which was used for hourly calculations. Using hourly data, daily values were obtained for maximum air temperature, minimum air temperature, relative humidity, cumulative solar radiation, cumulative precipitation, and average wind speed (Figure 3.1).

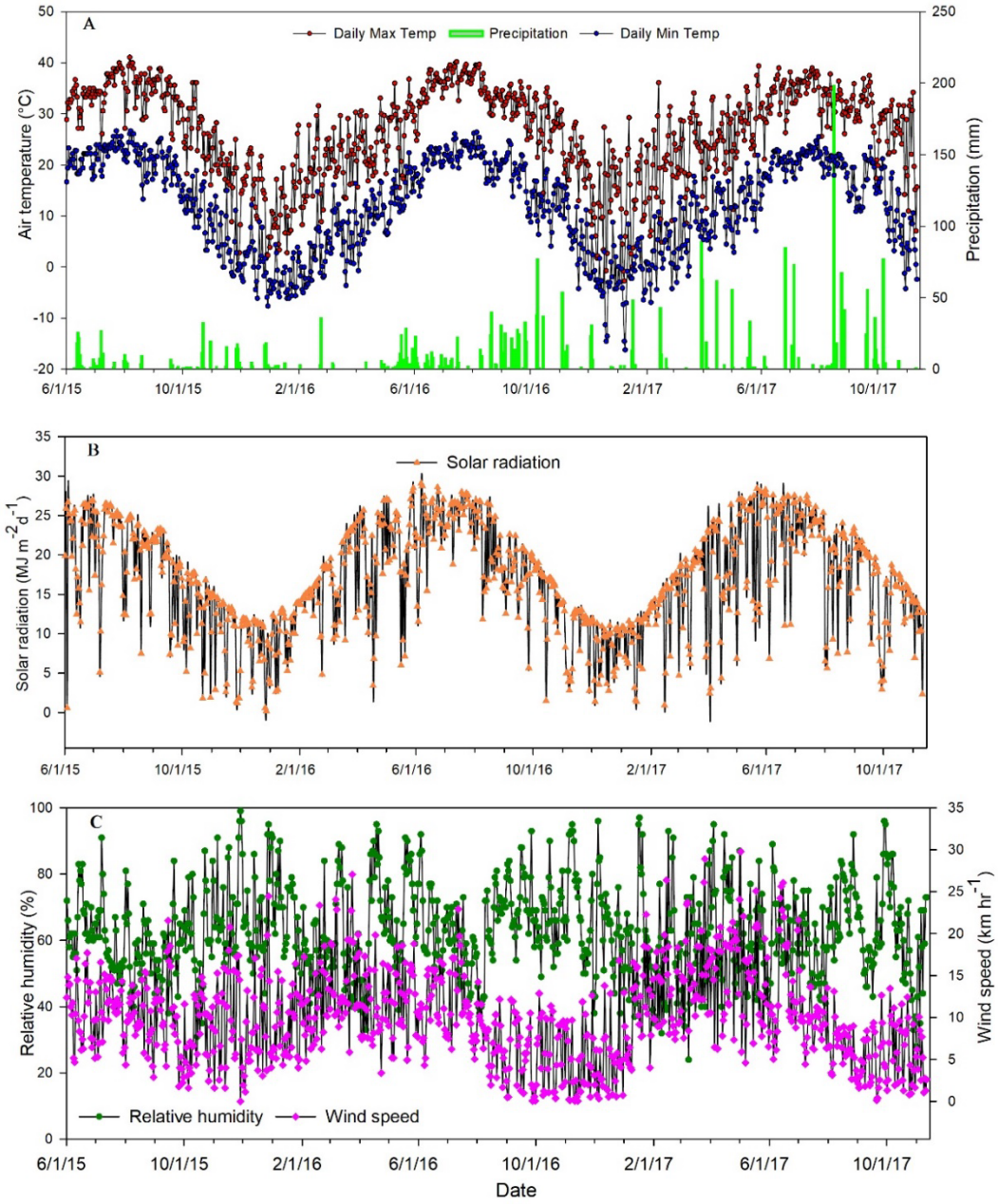

Figure 3.1. Meteorological data collected during the experiment from May 2015 until November 2017 (A) Growing season daily maximum and minimum temperature and daily cumulative precipitation; (B) Daily cumulative solar radiation; (C) Daily average relative humidity and wind speed in 2015 – 2017.

Model Input Data: Soil Profile

The soil profile for the Abilene clay loam (Fine, mixed, superactive, thermic Pachic Argiustolls with 0-1% slope) at the experiment site was divided into six layers based on data from previous studies conducted at the same research station (Modala et al., 2015) and from soil samples collected as part of this study (Table 3.2).

Table 3.2. Soil physical, chemical, and hydrological properties used in DSSAT simulation

Depth cm	SLCL (%)	SLSI (%)	SLOC (%)	SLHW	CEC (cmol kg^{-1})	SLNI (%)	LL (cm cm^{-1})	DUL (cm cm^{-1})	SSAT (cm cm^{-1})	SBDM (g cm^{-1})	SSKS (cm h^{-1})	SRGF
5	40	26	0.77	7.3	20	0.1	0.335	0.319	0.47	1.32	1.32	1
15	40	26	0.66	7.3	20	0.1	0.335	0.319	0.47	1.32	1.32	1
30	28	32	0.67	7.7	20.3	0.07	0.184	0.313	0.44	1.40	0.23	0.63
45	34	27	0.64	7.6	21.4	0.07	0.213	0.335	0.44	1.41	0.23	0.47
60	32	34	0.48	7.9	23.5	0.05	0.199	0.33	0.44	1.39	0.23	0.35
160	32	34	0.31	7.9	23.5	0.04	0.194	0.321	0.43	1.41	0.23	0.11

SLCL = clay content, SLSI = silt content, SLOC = organic carbon, SLHW = pH in water, CEC = cation exchange capacity, SLNI = total nitrogen concentration, LL = lower limit, DUL = drained upper limit, SSAT = saturation, SBDM = bulk density, SSKS = saturated hydraulic conductivity, and SRGF = soil root growth factor

Model Evaluation

The sugarcane cultivar HYP_HF in CANEGRO was used as the default genotype for modeling, as it is a cultivar with high fiber content. A number of default cultivar-specific parameter coefficients were modified to simulate the growth and yield observations collected during the field experiment. As data from two independent field experiments was available, data from the 2016 trial for genotype Ho 02-113 at high irrigation was used for adjusting cultivar-specific parameters. After adjusting cultivar parameters, performance of the model was evaluated using data for the same genotype collected from the 2015 field experiment that was established in 2015. The model performance was further investigated to test its suitability for simulating phenology and

biomass of other energy cane genotypes TUS11-62, TUS11-58, and TCP10-4928 using the 2016-17 data.

Model Performance Indicators

The model performance was evaluated using several statistical indices. Percent error (PE) was used to assess the performance of the model for simulation of stalk height and aboveground biomass (Equation 3.1). This is a good index to determine if the model simulations are over (positive) or under (negative) estimates when compared with the observed data (Yang et al., 2014).

$$PE = \frac{(SSimulated - Obsereved)}{Observed} * 100 \qquad \text{[Equation 3.1]}$$

D index is a measure of agreement between observed and simulated data based on dispersion (Willmott, 1981). The value of D index ranges from 0 - 1, where 1 indicates the perfect agreement of simulation and observed data (i.e. $Y_i = \hat{Y}_i$), and 0 indicates no agreement between observed and simulated data. When D index value is zero, it indicates all model simulated values are identical and equal to the average of experimental data i.e. $\hat{Y}_i = \overline{Y}$ (Equation 3.2)

$$\text{D index} = 1 - \frac{\sum_{i=1}^{N}(Y_i - \hat{Y}_i)^2}{\sum_{i=1}^{N}(|\hat{Y}_i - \bar{Y}| + |Yi - \bar{Y}|)^2} \qquad \text{[Equation 3.2]}$$

RESULTS AND DISCUSSION

Model Performance Before and After Adjusting Cultivar Coefficients

Simulations were performed using the default cultivar HYP_HF in DSSAT-CANEGRO using model input data for 2016 (weather, soil, and management) without adjusting cultivar coefficients. Simulation results of aboveground biomass yield and stalk height were then compared against observed data from the field experiment for the energy cane genotype Ho 02-113 planted in 2016. Results showed that the CANEGRO model overestimated final aboveground biomass by 85% and final stalk height by 51% when default cultivar parameters were used (Table 3.3). As using default cultivar parameters significantly overestimated the growth characteristics of Ho 02-113, several cultivar coefficients were adjusted using observed field data of this genotype (Table 3.4).

Table 3.3. Comparison of observed and simulated stalk height and aboveground biomass at different dates before and after adjusting the genetic coefficients. PE is percent error which is an index to determine if the model simulations are over or under estimates when compared with the observed data. Over estimations are shown as positive numbers and under estimations are shown as negative numbers.

			Simulated value			
Growth Parameters	Date	Observed value	Before adjusting genetic coefficients	PE	After adjusting genetic coefficients	PE
Stalk height (cm)	08/10	39	61	+65	48	+23
	08/25	65	108	+66	70	+7
	09/08	92	148	+60	93	+1
	9/22	110	174	+58	114	-3
	10/28	128	194	+51	140	+10
Aboveground biomass (t ha^{-1})	08/10	2.02	10.49	+419	5.41	+167
	09/08	7.91	21.99	+178	11.71	+48
	10/08	12.52	31.74	-153	17.16	+37
	10/28	18.64	34.59	+85	19.71	+5.7

A prominent characteristic that differs energy cane from sugarcane is that energy cane allocates a significant portion of photosynthates to underground rhizomes

compared to sugarcane (Matsuoka et al., 2014). Although rhizomatousness is an important trait that determines regrowth and ratooning of sugarcane and perennial bioenergy crops, studies on biomass potential generally do not consider the allocation of total dry biomass to belowground parts. Thus, limited information is available on the total dry weight of the belowground parts of any Saccharum species, including energy cane (García et al., 2011; Matsuoka et al., 2014). A study conducted by Carvalho et al. (2013) reported that 35% of the total sugarcane dry matter was allocated into the belowground part, and the allocation was declined to 25% in the second ratoon. In our study, a sensitivity analysis for the parametrization of cultivar coefficients resulted in an APFMAX value of 0.60, which is the maximum fraction of dry mass increments that can be allocated to aerial dry mass. Coelho et al. (2020) reported APFMAX values ranging from 0.68 to 0.72 for sugarcane varieties. As we expect similar or more dry matter allocation to belowground parts of energy cane compared to sugarcane, an APFMAX value of 0.60 was considered acceptable (Table 3.4).

Cultivar parameters governing leaf and canopy development were also adjusted based on observed trends in crop development (Table 3.4). Studies had shown that sugarcane LAI range from 4-8 and is affected by cultivar type, soil characteristics, and growing season water supply (Marin et al., 2011; Teruel et al., 1997). In our study, LAI of energy cane genotypes varied from 3-5 (unpublished data). Similar LAI values were also observed by Chiluwal et al. (2018) for energy cane in a study conducted in Georgia. Energy cane has narrower leaves compared to sugarcane, but stalk density is higher for energy cane (Matsuoka et al., 2014). Three genetic coefficients related to canopy

development were adjusted to capture differences between sugarcane and energy cane development. The maximum leaf elongation rate (LER_0) was adjusted to 0.2 to simulate slower leaf area development of energy cane. As leaves develop, the rate of expansion of leaves increases as subsequent leaves form and reach a maximum allowable blade area (MXLFAREA). After forming a specific number of leaves (MXLFARNO), the maximum leaf area remains at a constant value for the rest of leaves (Inman-Bamber and Kiker, 1997; Singels et al., 2008). In the present study, MXLFARNO was adjusted to 230 from its default value 382, and MXLFARNO was adjusted to 13 from its default value 23 (Table 3.4).

Our field data showed that primary tillers emerged earlier than the model predicted dates in the second and third year (ratoon). Tiller emergence in CANEGRO is simulated after a specified period of thermal time has accumulated from the beginning of ratooning (TTRATNEM). As the thermal time requirement for tiller emergence was low for energy cane, TTRATNEM value was adjusted from 10 to 5. Stalk elongation begins after a cultivar-specific thermal time has elapsed since the emergence of the primary tiller (CHUPIBASE in Table 3.3). For energy cane, the CHUPIBASE value was adjusted from 1000 to 700 to indicate earlier stalk growth. The number of tillers produced by energy cane genotypes is higher than its commercial sugarcane parent (Fageria et al., 2013; Leon et al., 2015). In our study, the cultivar-specific parameter related to tiller appearance rate (TAR_0) was adjusted to 0.03, which resulted in a higher tiller population.

Field data showed that the average stalk density was approximately 30 (stalks m^{-2}) for all genotypes during the late vegetative growth stage, which was higher than sugarcane stalk density observed in different field experiments (Bell and Garside, 2005; Carter et al., 1985; de Silva and de Costa, 2004; Marin et al., 2011). As stalk density was higher for the energy cane genotypes in our study, a cultivar-specific parameter related to this (POPTT16) was increased from 15 to 30 in the cultivar file used in DSSAT version 7.4.5. The maximum tiller elongation rate (SER_0) was adjusted to 0.18 to simulate the observed stalk growth rate during the field experiment (unpublished data).

Table 3.4. Genetic coefficients for the sugarcane high fiber cultivar HYP_HF in the DSSAT-CANEGRO-Sugarcane module (version 4.7.5). Coefficients that are adjusted based on field data are highlighted in bold italics.

Parameter	Description	Units	Default Value	Calibrated Value
	Biomass accumulation and partition			
MaxPARCE	Maximum (no stress) radiation conversion efficiency expressed as assimilate produced before respiration, per unit PAR.	g MJ^{-1}	6.9	6.9
APFMX	***Maximum fraction of dry mass increments that can be allocated to aerial dry mass***	***t t^{-1}***	***0.88***	***0.60***
STKPFMAX	Fraction of daily aerial dry mass increments partitioned to stalk at high temperatures in a mature crop (on dry mass basis)	t t^{-1}	0.60	0.60
	Sucrose accumulation			
SUCA	Sucrose partitioning parameter: Maximum sucrose contents in the base of stalk	t t^{-1}	0.30	0.30
TBFT	Sucrose partitioning: Temperature at which partitioning of unstressed stalk mass increments to sucrose is 50% of the maximum value	°C	25.0	25.0
	Canopy - leaves			
LFMAX	Maximum number of green leaves a healthy, adequately- watered plant will have after it is old enough to lose some leaves.	Leaf number	13.0	13.0
MXLFAREA	***Max leaf area assigned to all leaves above leaf number MXLFARNO***	***cm^{-1}***	***382.0***	***230.0***
MXLFARNO	***Leaf number above which leaf area is limited to MXLFAREA***	***leaf***	***23.0***	***13.0***
LER0	***Max. leaf elongation rate***	***cm $°Cd^{-1}$***	***0.30***	***0.20***

Table 3.4 Continued

Parameter	Description	Units	Default values	Calibrated values
	Leaf Phenology			
PI1	Phyllocron interval 1 (for leaf numbers below Pswitch,	°C d	69.00	69.0
PI2	Phyllocron interval 2 (for leaf numbers above Pswitch,	°C d	117.0	117.0
PSWITCH	Leaf number at which the Phyllocron changes.	leaf	12.0	12.0
	Tiller Phenology			
TDELAY	Delay between primary shoot appearance & appearance of first secondary shoot		50.0	50.0
TAR0	***Maximum tiller appearance rate, per primary shoot***	***shoot $^{-1}$ °Cd^{-1}***	***0.02***	***0.03***
POPTT16	***Stalk population at/after 1600-degree days***	***Stalks m^{-2}***	***15.0***	***30.0***
	Phenology			
TTPLNTEM	Thermal time to emergence for a plant crop	°Cd	150.0	150.0
TTRATNEM	***Thermal time to emergence for a ratoon crop***	***°Cd***	***10.0***	***05.0***
CHUPIBASE	***Thermal time from emergence to start of stalk growth***	***°Cd***	***1000.0***	***700.0***
SER0	***Max. stalk elongation rate***	***cm °Cd^{-1}***	***0.300***	***0.18***
TT_POP GROWTH	Thermal time to peak tiller population	°C d	600.0	600.0
	Lodging			
LG_ AMBASE	Aerial mass (fresh mass of stalks, leaves, and water attached to them)	t ha^{-1}	220	220

Figure 3.2 presents the stalk height and aboveground biomass simulation results after adjusting the genetic coefficients discussed above. Results showed that the model was able to simulate stalk height with high accuracy. However, the model over-predicted aboveground biomass early in the growing season compared to observed values (Table 3.3). *Saccharum spontaneum* growing in harsh environments are known to develop underground rhizomes early in the season as an adaptation strategy to withstand environmental stresses (Matsuoka et al. (2014) and Matsuoka and Franco-Garcia (2011). This adaptation strategy could have led to the accumulation of less aboveground biomass during the initial months of growth of energy cane billets, as observed in our field data.

Adjusting genetic coefficients related to root growth in CANEGRO could result in the allocation of more biomass to belowground parts and better simulation of early-season biomass growth. However, adjusting root growth, specific coefficients require additional data related to biomass partitioning in energy cane which was beyond the scope of the current study. The model predicted final aboveground biomass with less than 6% PE, which was considered satisfactory in this study.

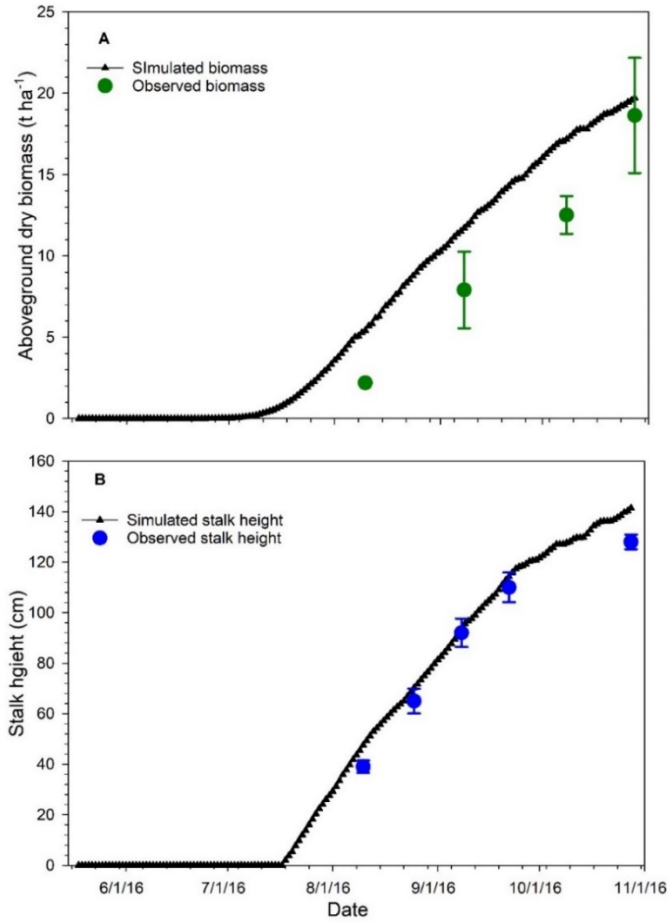

Figure 3.2. Daily simulated dry aboveground biomass and stalk height of Ho 02-113 after adjusting genetic coefficients using field experiment data from 2016 (plant cane). Simulations are performed using weather, soil and management data for 2016. Observed field data are shown as closed circles. Error bars are the standard error of the mean.

Model Evaluation of Ratoons: Genotype Ho 02-113

The performance of the DSSAT-CANEGRO sugarcane model with adjusted genetic coefficients for energy cane genotype Ho 02-113 was further evaluated using observed data from ratoon cycles for the same genotype (Figure 3.3A and 3.3B). The model underestimated stalk height in early growth stages in both irrigation treatments. As the season progressed, the difference between simulated and observed values was decreased considerably. Final stalk height was slightly overpredicted by the model in both high (+13%) and low (+10%) irrigation treatments. The D-index value for stalk height in 2016 was 0.93 for both irrigation treatments, which indicated excellent model prediction for plant height. Final aboveground biomass for high irrigation treatment was predicted with greater accuracy (Table 3.5) but aboveground biomass was underestimated in low irrigation treatment with a PE of -11.3% (Table 3.5).

In the second ratoon cycle (2017), the model significantly overestimated both stalk height and final aboveground biomass (Figure 3.4A and 3.4B). Final aboveground biomass for both irrigation treatments were overestimated by 32%. Similarly, stalk height was overestimated by 46% in high irrigation treatment and 50% in low irrigation treatment. The D-index value decreased to 0.89 and 0.80 in high irrigation treatment and low irrigation treatments respectively.

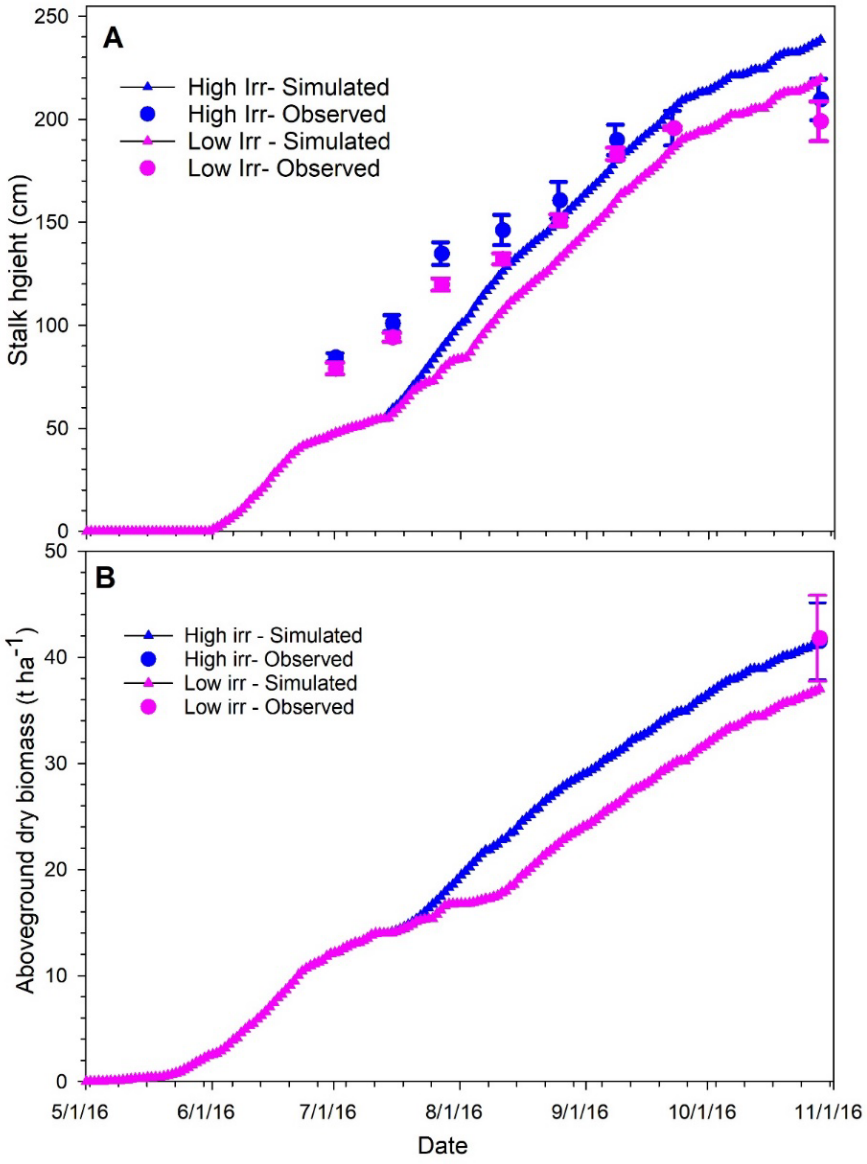

Figure 3.3. Daily simulated dry aboveground biomass and stalk height of Ho 02-113 in the first ratoon cycle (2016). Simulations are performed for both high and low irrigation treatments. Observed field data are shown as closed circles. Error bars are the standard error of the mean.

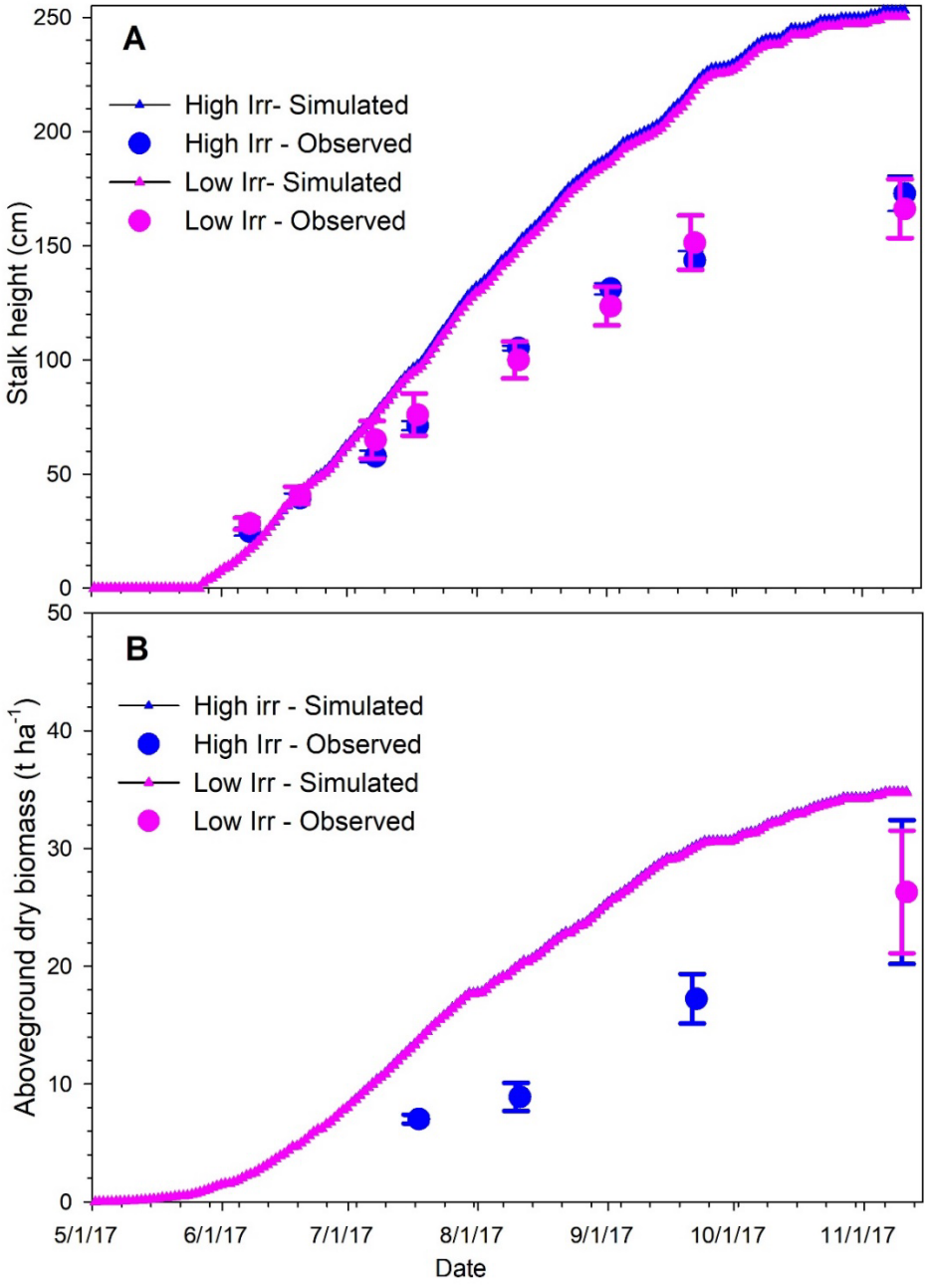

Figure 3.4. Daily simulated dry aboveground biomass and stalk height of Ho 02-113 in the second ratoon cycle (2017). Simulations are performed for both high and low irrigation treatments. Observed field data are shown as closed circles. Error bars are the standard error of the mean.

Table 3.5. Comparison of observed and simulated stalk height and aboveground biomass at harvest for Ho 02-113. PE is percent error which is an index. Over estimations are shown as positive numbers and under estimations are shown as negative numbers. D index shows how simulated model fits with the observed data. D index value of 1 indicates perfect agreement of simulated and observed data and 0 indicated no agreement.

Growth Parameters	**High Irrigation**				**Low Irrigation**			
First ratoon (2016)	**Sim**	**Obs**	**PE**	**D index**	**Sim**	**Obs**	**PE**	**D index**
Aboveground biomass (t ha^{-1})	41.49	41.9	-1	-	37.03	41.78	-11.3	-
Final stalk height (cm)	239	210	+13	0.93	220	199	+10	0.93
Second ratoon (2017)	**Sim**	**Obs**	**PE**	**D index**	**Sim**	**Obs**	**PE**	**D index**
aboveground biomass (t ha^{-1})	34.8	26.3	+32	0.72	34.7	26.3	+32	-
Final stalk height (cm)	253	172	+46	0.89	250	166	+50	0.80

Similar to plant cane simulations discussed earlier, the DSSTA-CANEGRO model performed satisfactorily in simulating energy cane growth in the first ratoon cycle. However, the model overestimated energy cane growth in the second ratoon cycle. In the case of conventional sugarcane, biomass yield usually declines from plant cane to older ratoons. In case of energy cane, several studies had reported higher biomass production in the ratoon cycle lasting up to eight years than in the first year of plant cane (Bischoff et al., 2008; Giamalva et al., 1985; Matsuoka et al., 2014; Matsuoka and Stolf, 2012). However, the majority of these reports on energy cane production are from humid subtropical and tropical areas with higher rainfall. In a recent study conducted by Boschiero et al. (2019) in northeastern Brazil, similar trends in biomass production were observed for energy cane genotypes. In their study, cumulative rainfall in the plant cane year was 1416 mm, and in the first ratoon year was 1093 mm. Although the rainfall was low in the ratoon cycle, most energy cane genotypes had higher dry biomass production

that year compared to plant cane year. Field data herein for dry biomass yield and stalk height of all energy cane genotypes were higher in the first ratoon cycle (40.4 ± 1.14 t ha^{-1} and 212 ± 3.4 cm) than the plant cane cycle. Then in the second ratoon cycle (2017), biomass and stalk height declined (24.3 ± 1.3 t ha^{-1} and 168 ± 4.8 cm) although the precipitation was higher and well distributed over the growing season compared to the first ratoon cycle (Figure 3.1A). A possible reason for this decline could be the extreme low-temperatures days (air temperature as low as -16°C; Figure 3.1) that occurred at the beginning of the second ratoon year. This might have resulted in rhizome death and reduced growth in 2017. This hypothesis was further strengthened by the loss of the 2016 planted energy cane (second field experiment) which failed to produce any regrowth in 2017. Peixoto et al. (2015) reported that Miscanthus rhizomes tolerated temperatures as low as –6.5 °C, however, the rhizome mortality rate was as high as 50% for some genotypes. Fonteyne et al. (2016) reported that up to 50% of miscanthus rhizomes were killed at sub-zero temperatures in an experiment with 95 different genotypes.

Results indicate that the model failed to recognize the decline in growth in the second ratoon cycle. The current version of DSSAT-CANEGRO simulates crop growth on an annual basis. There is an option in the model to specify if the crop that is simulated is plant cane or ratoon. However, the model doesn't distinguish between the first ratoon or the second ratoon. As management was similar between first and second ratoon cycles, we assume that the decline in biomass yield of energy cane genotypes in the second year could have been due to the severe freezing temperatures. However, the

model is not set up to account for rhizome mortality associated with severe winter freezing. Model also does not address subsequent yield loss in ratoon cycles due to nutrient loss, disease, weed, and/ or pests. The model prediction mainly relies on inputs such as ratoon appearance date, tiller number per unit area, weather, and management inputs.

Model Evaluation of Ratoons: Genotypes TUS11-62, TUS11-58, and TCP10-4928

The performance of the CANEGRO sugarcane model with adjusted genetic coefficients for Ho 02-113 was further evaluated for its suitability in simulating the growth of other energy cane genotypes in the experiment (TUS11-62, TUS11-58, and TCP10-4928). Both high irrigation and low irrigation treatments were compared. Figures 3.5A and 3.5B show observed stalk height of the energy cane genotypes and model-simulated stalk height in the first ratoon cycle (2016). Figure 3.6A and 3.6B shows simulated and observed aboveground dry biomass yield in the same year. In the first ratoon, PE for stalk height estimation was between ± 5 % in low irrigation treatments for all three genotypes (Table 3.6). Stalk height was overestimated by 18% for TUS11-62 and +15% for TCP10-928rrigation treatment. PE for biomass yield estimation was between ± 9% for all three genotypes (Table 3.6).

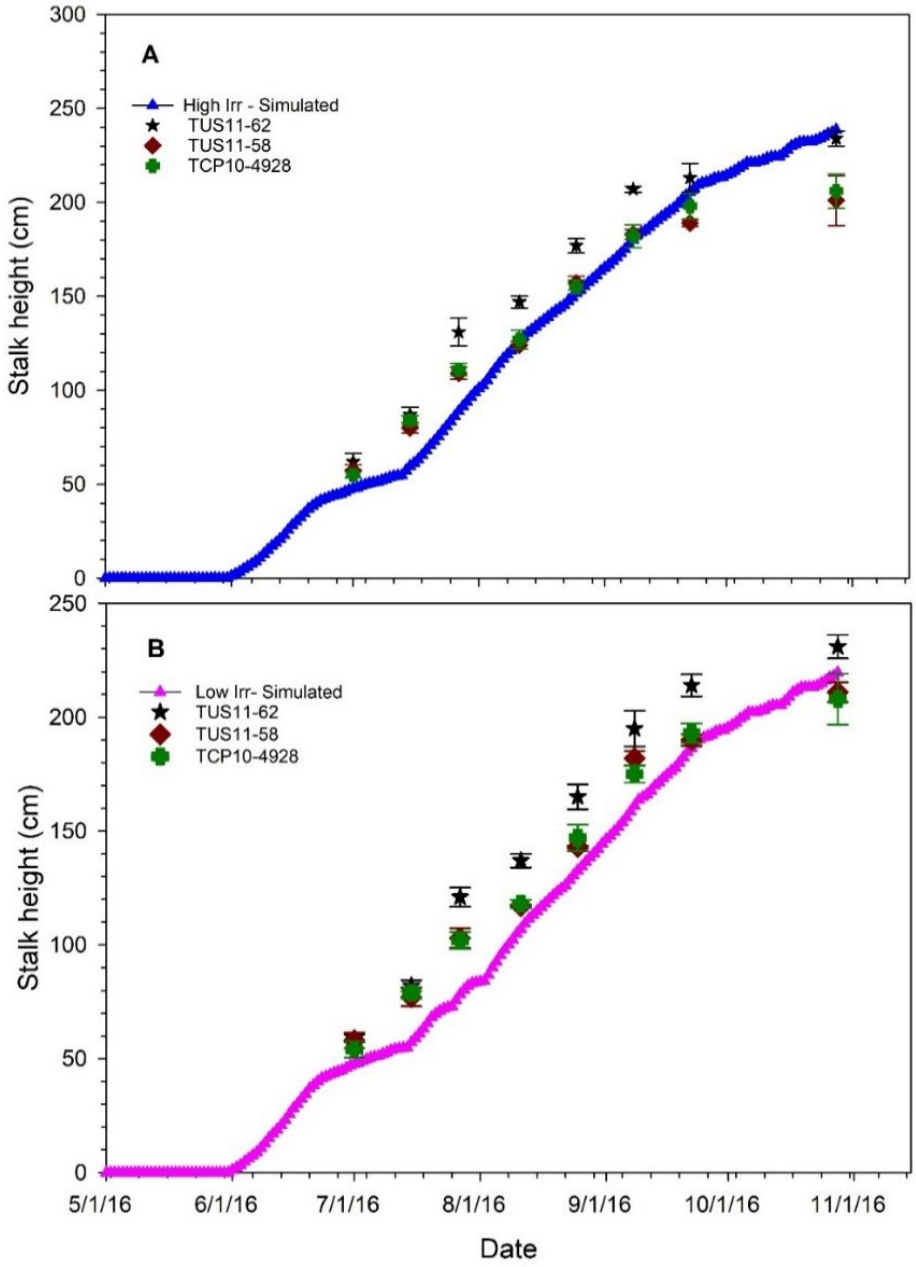

Figure 3.5. Daily simulated stalk height of energy cane genotypes TUS11-62, TUS11-58, TCP10-4928 in the first ratoon cycle (2016). Simulations are performed for both high (A) and low irrigation treatments (B). Observed field data for different genotypes are shown with different symbols. Error bars in the symbols are the standard error of the mean.

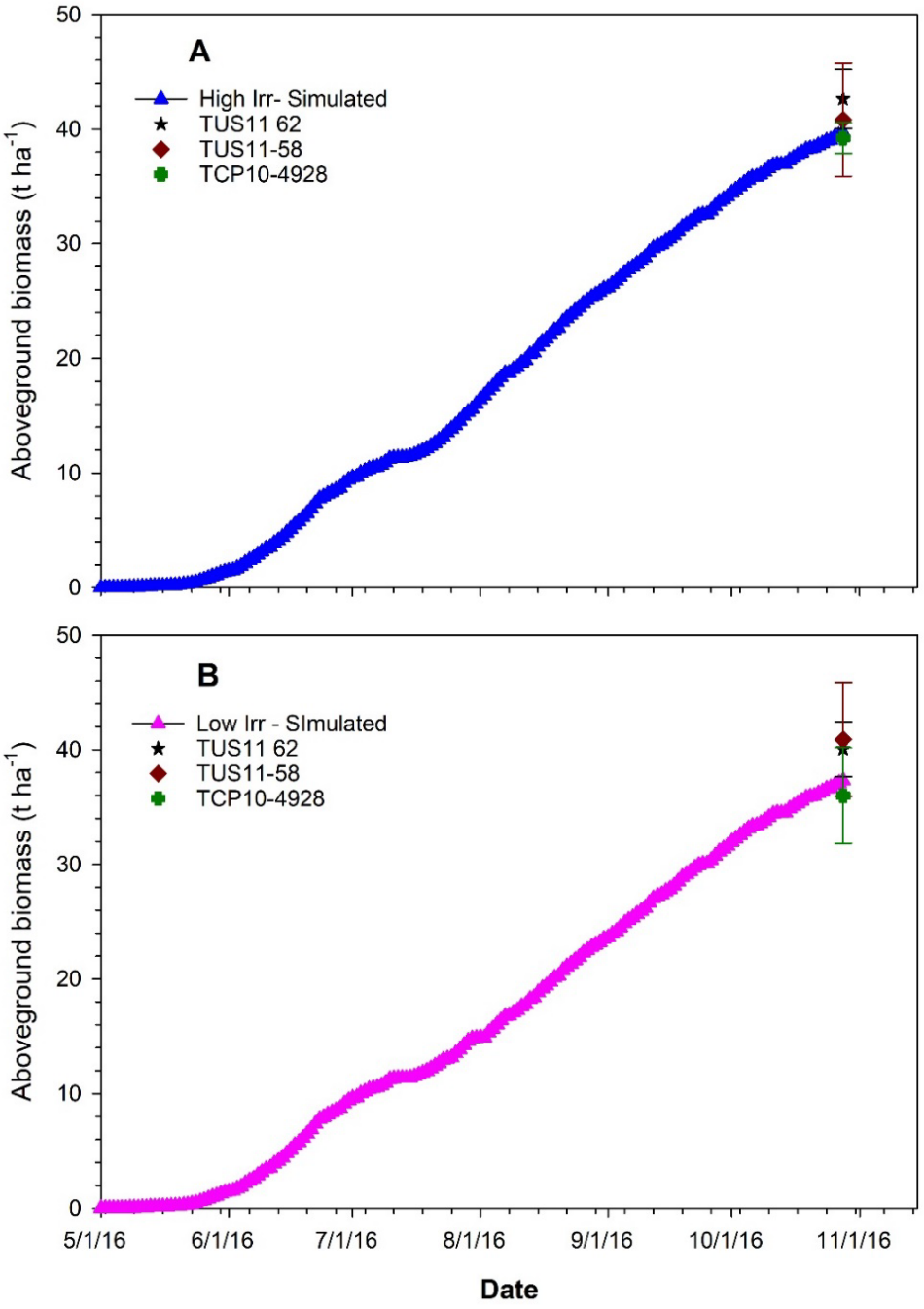

Figure 3.6. Daily simulated aboveground dry biomass of energy cane genotypes TUS11-62, TUS11-58, TCP10-4928 in the first ratoon cycle (2016). Simulations are performed for both high (A) and low irrigation (B) treatments. Observed field data for different genotypes are shown with different symbols. Error bars in the symbols are the standard error of the mean.

Table 3.6. Comparison of observed and simulated stalk height and aboveground biomass at harvest for TUS11-62, TUS11-58 and TCP10-4928 in 2016 and 2017. PE is percent error which is an index. Over estimations are shown as positive numbers and under estimations are shown as negative numbers. D index value of 1 indicates perfect agreement of simulated and observed data and 0 indicated no agreement.

	Biomass			Stalk height		
Genotype	**Obs**	**Sim**	**PE**	**Obs**	**Sim**	**PE**
First ratoon (2016)						
High Irrigation						
TUS11-62	42.63	39.7	- 6.9	233	238	+2
TUS11-58	40.82	39.7	- 2.7	201	238	+18
TCP10-4928	39.23	39.7	+ 1.2	206	238	+15
Low Irrigation						
TUS11-62	40.05	37.32	- 6.9	230	219	- 4.8
TUS11-58	40.89	37.32	- 2.7	211	219	+3.8
TCP10-4928	36.00	37.32	+ 1.2	208	219	+5.2
Second Ratoon (2017)						
High Irrigation						
TUS11-62	18.4	34.86	+ 89.4	172	252	+46.5
TUS11-58	26.5	34.86	+ 31.5	152	252	+65.7
TCP10-4928	26.5	34.86	+ 31.5	158	252	+59.4
Low Irrigation						
TUS11-58	27.5	34.72	+26.2	166	250	+50.0
TCP10-4928	26.0	34.72	+ 33.4	164	250	+52.4

Similar to Ho 02-113, the model greatly overestimated both stalk height and biomass yield for all genotypes in the second ratoon cycle (Figures 3.7 and 3.8). Percent error for stalk height estimation ranged from 45 to 66% (Table 3.6). The highest PE for biomass yield estimation was +89.4% for the genotype TUS11-62 in high irrigation treatment. For other genotypes, simulated yield was overestimated between 31 to 34% in both irrigation treatments. Observed field data showed some phenological differences among the energy cane genotypes. Genotypes Ho 02-113, TUS11-58, and TCP10-4928 had similar stalk height (~205 cm). However, TUS11-62 was significantly taller (233 cm). Overwintering rhizomes of TUS11-62 showed 100% mortality during the second

ratoon cycle in low irrigation plots. In high irrigation plots, regrowth of TUS11-62 was observed, but the aboveground biomass production was the lowest compared to other genotypes. Overall, TUS11-62 appeared to be a cold-sensitive genotype compared to other genotypes tested in the study.

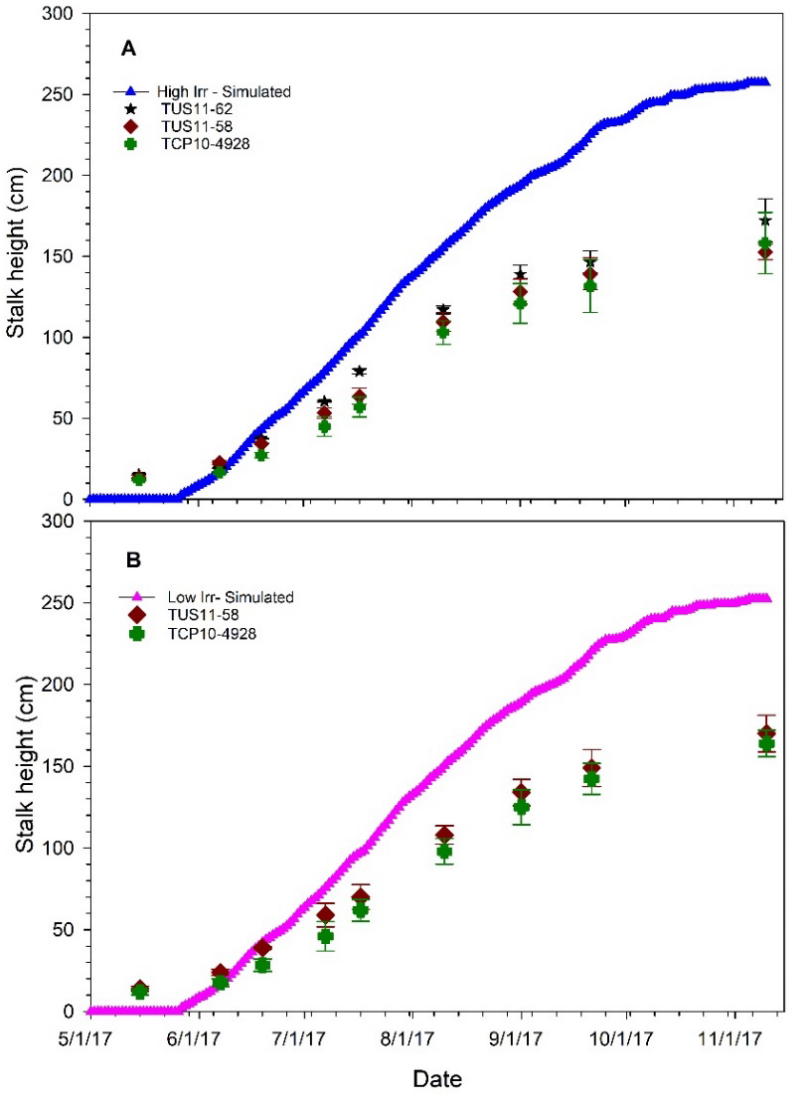

Figure 3.7. Daily simulated stalk height of energy cane genotypes TUS11-62, TUS11-58, TCP10-4928 in the second ratoon cycle (2017). Simulations are performed for both high (A) and low irrigation treatments (B). Observed field data for different genotypes are shown with different symbols. Error bars in the symbols are the standard error of the mean.

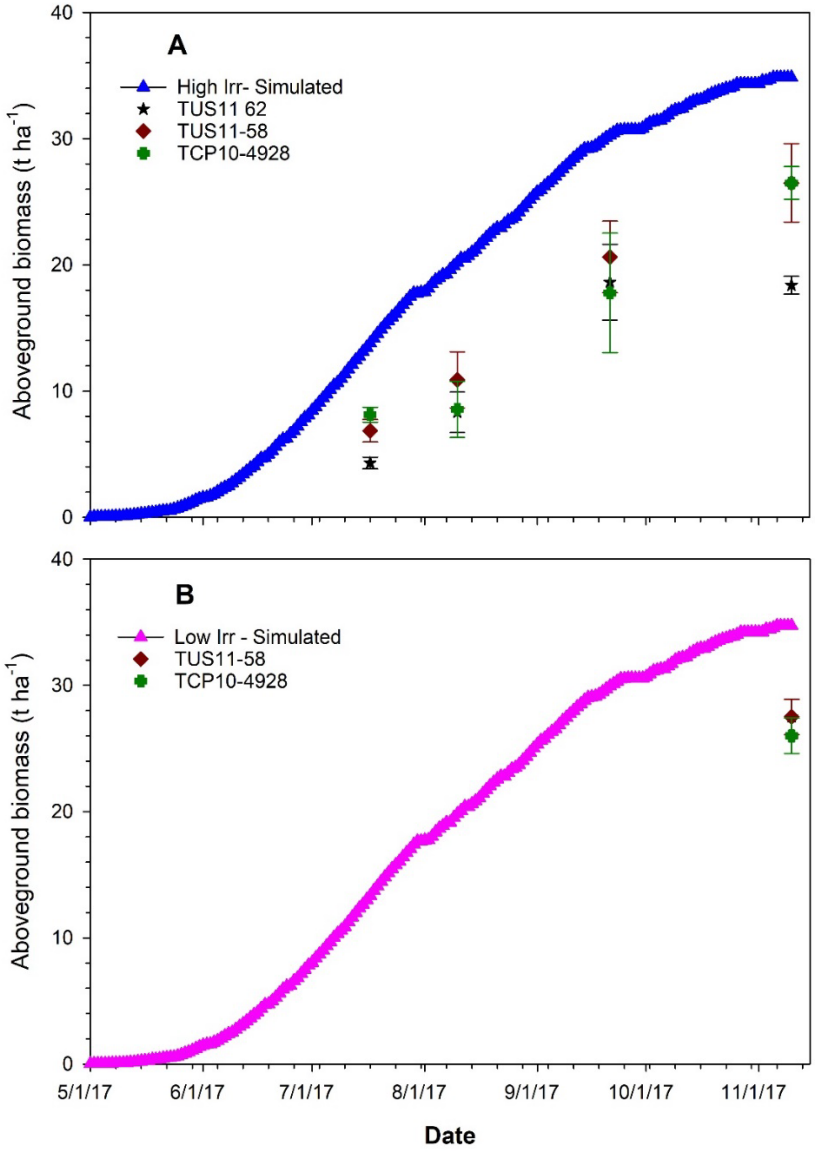

Figure 3.8. Daily simulated aboveground dry biomass of energy cane genotypes TUS11-62, TUS11-58, TCP10-4928 in the second ratoon cycle (2017). Simulations are performed for both high (A) and low irrigation (B) treatments. Observed field data for different genotypes are shown with different symbols. Error bars in the symbols are the standard error of the mean.

Our results showed that DSSAT-CANEGRO satisfactorily simulated stalk height and biomass yield for all the three genotypes (TUS11-62, TUS11-58, and TCP10-4928) in the first ratoon cycle although the model was calibrated for genetic coefficients using

data from Ho 02-113. Similar to Ho 02-113, the model significantly overestimated stalk height and biomass yield in the second ratoon cycle. Overestimation was as high as 90% for cold-sensitive genotype TUS11-62 as the model failed to account for rhizome mortality associated with severe winter freezing in the Texas Rolling Plains

CONCLUSIONS

The DSSAT-CANEGRO model was adapted to simulate energy cane growth and development by optimizing the genotypic traits for biomass accumulation and partitioning, canopy-leaf, and tiller phenology characteristics. After adjusting the genetic coefficients, the model satisfactorily simulated the stalk height and aboveground biomass of energy cane in the plant cane (2015) and first ratoon cycle (2016) with PE less than ±10 for most genotypes. Low temperatures during the overwintering period reduced the regrowth and aboveground biomass production of all energy cane genotypes in the second ratoon cycle (2017). Significant overestimation of stalk height and aboveground biomass (PE ranging from +30 to +90%) in the second ratoon cycle showed that the model failed to recognize the decline in growth due to rhizome mortality associated with severe winter freezing. To the best of our knowledge, our study is one of the first attempts in adapting the DSSAT-CANEGRO sugarcane model for simulating energy cane production. Although the results are promising, further improvement is necessary for considering the effects of sub-zero temperatures on rhizome mortality when the model is used for testing the performance of energy cane in regions where such conditions exist during the overwintering period.

CHAPTER IV

EVALUATING THE IMPACT OF CLIMATE CHANGE VARIABILITY ON BIOMASS PRODUCTION OF ENERGY CANE USING DSSAT-CANEGRO IN THE TEXAS ROLLING PLAINS

INTRODUCTION

Energy cane (*Saccharum* spp. hybrid) is an interspecific hybrid of commercial sugarcane (*Saccharum officinarum*) and *S. spontaneum*, a grassy wild species growing naturally in Africa, Southeast Asia and Pacific islands (Matsuoka et al., 2014). Due to its evolution in diverse environments, *S. spontaneum* is resistant to many diseases that attack commercially grown sugarcane, a characteristic that was passed on to energy cane. Energy cane hybrids are also known for higher biomass productivity due to its prolific tillering ability (Leon et al., 2015). Several high yielding energy cane genotypes were developed in the last decade as an alternative of feed-based fuel ethanol production (Valentine et al., 2012; Waclawovsky et al., 2010). Two types of energy canes (Type I and II) are available for growing as biofuel feedstocks. Type I energy canes are similar to conventional sugarcane cultivars but have lower sugar (10-14%) and higher fiber (14-20%) contents. Type II energy canes have low sugar (<10%) and high fiber (>20%) contents and are used primarily for lignocellulosic biomass production (Knoll et al., 2013; Leon et al., 2015). The extensive research and breeding efforts in the past few decades resulted in development of several high yielding energy cane genotypes with disease and pest resistances and high biomass (Fageria et al., 2013; Fouad et al., 2015; Matsuoka et al., 2009). To ensure the production of dedicated energy crops, these

second-generation lignocellulosic feedstocks are designed for production in agriculturally degraded and marginal lands instead of prime farm lands (Chiluwal et al., 2019; Matsuoka et al., 2014). While grown on marginal lands, high yield is still need to maintain economic viability.

The Texas Rolling Plains located in northern Texas is an ecological region characterized by marginal production conditions. High solar radiation, low precipitation and strong winds are the characteristics of weather in this region. Average annual precipitation in the region from west to east ranges from 460 to 760 mm (Modala, 2014). Increasing crop water demand, frequent droughts, warmer summer temperatures, and decreasing precipitation are affecting crop production and economic revenues in this semi-arid region. As farmers in this region seek alternate crop options, high-biomass producing biofuel feedstocks may emerge as a viable opportunity in the future. However, only limited information is available about the performance of newly developed energy cane hybrids in semi-arid regions such as the Texas Rolling Plains.

Climatic conditions in semi-arid regions may have a prominent effect on the growth and development of energy cane feedstocks as they were predominantly developed for tropical and subtropical environments. Although conducting agronomic trials help to identify suitable crop management practices under real-world conditions, it require significant time and resource investments. In such conditions, crop simulation models can work as tools to integrate information from past agronomic experiments and facilitate prediction of biomass yield under varying spatial (e.g. land), temporal (e.g. weather) and management (e.g. irrigation, fertilizer, tillage) conditions (Attia et al.,

2016a; Jones et al., 2003). The Decision support system for Agrotechnology Transfer (DSSAT) is a computer software application developed to simulate crop growth, development, and yield by using soil, weather, management, and cultivar input data (Jones et al., 2003). The DSSAT includes a collection of cropping systems simulation models (Jones et al., 2003). The CANEGRO model within DSSAT is a sugarcane crop simulation model developed by Inman-Bamber (1991). This model was further refined by Singels and Bezuidenhout (2002) and Singels et al. (2008). The CANEGRO model has been successfully used for simulating sugarcane production and yield around the globe (Marin et al., 2011; Sonkar et al., 2019).

Process-based crop simulation models such as DSSAT-CANEGRO are powerful tools for studying the effect of crop management regimes, soil types and genotypic differences in broader climatic zones. Calibrated and validated models can also be used to study crop performance under various future climate change scenarios (Asseng et al., 2015). Studies have shown that the effect of climate change is highly prominent in semi-arid regions (Huang et al., 2016; Huang et al., 2012). Reduced precipitation and warmer temperatures in semi-arid regions lead to more evaporation and extended drought events (Huang et al., 2016). Stewart et al. (2018) and Shrestha et al. (2020) reported that the temperature and precipitation variability in the U.S. Great Plains is increasing, which is causing declining crop performance. These shifting climatic trends may affect biomass production in various ways. Increasing temperature favors early growth and development but increase evapotranspiration (ET) and crop water requirement during the crop growing season. However, elevated CO_2 in the atmosphere may offset the impact of

water stress by reducing mid-day leaf gas exchange (Stokes et al., 2016; Vu and Allen, 2009). A properly calibrated and validated crop growth model is a valuable tool for investigating the effect of climate change on crop production. The objective of the current study was to use a version of DSSAT-CANEGRO that was calibrated and validated for simulating energy cane production in the Texas Rolling Plains to assess the biomass production using long-term climate data from the region. A second objective was to conduct a climate change impact assessment on energy cane production using the long-term weather data.

MATERIALS AND METHODS

CANEGRO – Sugarcane Model

The DSSAT-CANEGRO sugarcane crop model was used in this study. CANEGRO is a modular component of the DSSAT software program. It combines the effect of weather, soil characteristics, management practices, and crop genotype to simulate the growth and development of sugarcane (Singels et al., 2008). This model uses meteorological inputs such as cumulative solar radiation, precipitation, and maximum and minimum temperatures on daily basis and simulate the growth and development processes. Model simulation includes phenology, canopy development, biomass accumulation and partitioning, root growth, water stress, and lodging (Marin et al., 2011; Singels et al., 2008). The soil water balance in the DSSAT's soil module is based on the amounts of precipitation and irrigation and estimated values of ET, soil water drainage, infiltration and surface runoff. Water holding characteristics of the soil

profile is calculated based on a specified drained upper limit (DUL) lower limit (LL), and saturated water capacity (SAT). The model assumes that the water moves to the upper layers as unsaturated flow when a layer has a water content between LL and DUL. The downward water flow occurs when a layer has a water content greater than DUL. Water in the lower soil profile is considered as the drained water, which does not play a role in plant growth and development. The soil profile at the study location was Abilene clay loam (Fine, mixed, superactive, thermic Pachic Argiustolls with 0-1% slope). For model simulations, soil profile was set up with 6 layers based on available data from previous studies that were conducted at the same research station (Modala et al., 2015) and from soil samples that were collected as part of this study. The details of the soil profile set up in DSSAT are listed in Table 4.1.

Table 4.1. Physical, chemical, and hydrological properties of soil profile used in DSSAT simulation modeling

Depth cm	SLCL (%)	SLSI (%)	SLOC (%)	SLHW	CEC (cmol kg^{-1})	SLNI (%)	LL (cm cm^{-1})	DUL (cm cm^{-1})	SSAT (cm cm^{-1})	SBDM (g cm^{-1})	SSKS (cm h^{-1})	SRGF
5	40	26	0.77	7.3	20	0.1	0.335	0.319	0.47	1.32	1.32	0.95
15	40	26	0.66	7.3	20	0.1	0.335	0.319	0.47	1.32	1.32	0.95
30	28	32	0.67	7.7	20.3	0.07	0.184	0.313	0.44	1.40	0.23	0.63
45	34	27	0.64	7.6	21.4	0.07	0.213	0.335	0.44	1.41	0.23	0.47
60	32	34	0.48	7.9	23.5	0.05	0.199	0.330	0.44	1.39	0.23	0.35
160	32	34	0.31	7.9	23.5	0.04	0.194	0.321	0.43	1.41	0.23	0.11

SLCL = clay content, SLSI = silt content, SLOC = organic carbon, SLHW = pH in water, CEC = cation exchange capacity, SLNI = total nitrogen concentration, LL = lower limit, DUL = drained upper limit, SSAT = saturation, SBDM = bulk density, SSKS = saturated hydraulic conductivity, and SRGF = soil root growth factor

Adapting DSSAT-CANEGRO for Energy Cane Simulations

DSSAT's crop simulation models use genetic parameters of a crop to simulate its specific growth (Jones et al., 2011; Li et al., 2018). In DSAT, the genetic parameters are divided into species, ecotype, and cultivar. Species in the model describes the broader characteristics of a plant species such as photosynthesis, respiration, root growth, and

plant response to water stress. Ecotype parameters are more specific than a species but can be similar for more than one cultivar. Cultivar parameters are highly specific to a genotype which determines biomass partitioning, canopy (leaf and tiller) development, and phenological stages (Marin et al., 2011)

We adapted the DSSAT-CANEGRO for simulating energy cane using data from a field experiment at the Texas A&M AgriLife Research Station located near Chillicothe (34°15′ N, 99°30′ W; 431 m above mean sea level) in the Texas Rolling Plains. Energy cane plots were established in 2015 and allowed to ratoon in 2016 and 2017. A second experiment was established in 2016 at the same site, but severe winter freezing during 2016-2017 caused 100% rhizome mortality, resulting in limited regrowth in 2017 (Pokhrel et al., 2019). Both field experiments were set up to evaluate the performance of four energy cane genotypes, TUS11-62, TUS11-58, TCP10-4928, and Ho 02-113. The first three genotypes were derived from crosses and selections as part of the Texas A&M AgriLife sugarcane breeding program in Weslaco, Texas, and are intended for biomass production in the U.S. Gulf Coast region (Landivar et al., 2016). Genotype Ho 02-113 was developed and released by the USDA-ARS Sugarcane Research Unit in Houma, Louisiana for use as a feedstock for biofuel production (Hale et al., 2013). The experiment was replicated four times. Two levels of irrigation (high and low) were applied in the study that was established in 2015. Approximately 33% less water was supplied in low irrigation plots. The 2016-planted experiment was maintained with high irrigation. Details of these studies can be found in Pokhrel et al., (2020).

Crop data collected during the growing season include stalk height, stalk density, leaf area, and biomass. Growth data of energy cane genotype Ho 02-113 was used in model calibration. HYP_HF was the default cultivar selected for model simulations due to its high fiber content. Several cultivar coefficients were adjusted during model calibration. The default and adjusted crop growth parameters are presented in table 4.2. A prominent characteristic of energy cane compared to sugarcane is its highly rhizomatousness nature. Energy cane allocates a significant portion of photosynthates to underground rhizomes (Matsuoka et al., 2014). To account for this, the APFMX parameter (the maximum fraction of dry mass increments) was adjusted to 0.60 Mg Mg^{-1}. Coelho et al. (2020) reported APFMX value of 0.68 to 0.72 Mg Mg^{-1} for the different sugarcane cultivars. Cultivar parameters that govern the leaf and canopy development were adjusted based on our field observed data. During our field study, LAI value of energy cane genotypes varied from 3-5. Due to slower leaf area development of energy cane compared to sugarcane, the maximum leaf elongation rate (LER_0) was adjusted to 0.2 cm/^oCd. As the growing season progresses, the rate of expansion of leaves gradually increases and reach a maximum allowable blade area (MXLFAREA). After the plant produces a specific number of leaves (MXLFARNO), the maximum leaf area remains at a constant value for the rest of leaves that are developing (Inman-Bamber and Kiker, 1997; Singels et al., 2008). In the present study, MXLFArea was adjusted to 230 cm^2 and MXLFArno was adjusted to 13 leaves. Our field observation showed the tillers appeared earlier than the model simulated date in the ratoon phase. To simulate earlier tiller regrowth, degree days for ratoon cane emergence (TTRATNEM) was adjusted to 5

GD. Stalk elongation begins when a cultivar-specific thermal time period is reached. In case of energy cane, stalk growth happens earlier than sugarcane. The genetic coefficient, CHUPIBASE, was adjusted to 700 GD to indicate earlier stalk growth. Stalk density in energy cane is higher than the existing sugarcane cultivars which was reported in several previous studies (Chiluwal et al., 2018; da Silveira et al., 2015; Leon et al., 2015). To capture high tillering characteristic of energy cane, the cultivar-specific parameter related to tiller appearance rate (TAR_0) was adjusted to 0.03 shoots/^oCd. Due to its high tillering nature, stalk density of energy cane is also higher. Our field data showed that the average stalk density of energy cane was 30 stalk m^{-1}. The genetic coefficient SER_0 (maximum tiller elongation rate) was adjusted to 0.18 cm/^oCd and the POPTT16 value, which is stalk population at/after 1600-degree days was adjusted to 30 stalks m^{-2}.

Table 4.2. The default genetic coefficients for the sugarcane high fiber cultivar HYP_HF cultivar in the DSSAT- CANEGRO-Sugarcane module (version 4.7.5) and calibrated genetic coefficients for energy cane genotype. Only adjusted parameters in the module and their default values are presented in the table.

Parameter	Description	Unit	Default Value	Calibrated Value
	Biomass accumulation and partition			
APFMX	Maximum fraction of dry mass increments that can be allocated to aerial dry mass	$t\ t^{-1}$	0.88	0.60
	Canopy - leaves			
MXLFAREA	Max leaf area assigned to all leaves above leaf number MXLFARNO	cm^{-1}	382.00	230.0
MXLFARNO	Leaf number above which leaf area is limited to MXLFAREA	leaf	23.00	13.00
LER_0	Max. leaf elongation rate,	$cm\ °Cd^{-1}$	0.30	0.20
	Tiller Phenology			
TAR_0	Maximum tiller appearance rate	$shoot^{-1}\ °Cd^{-1}$	0.02	0.03
POPTT16	Stalk population at/after 1600-degree days	$Stalks\ m^{-2}$	15.00	30.0
	Phenology			
TTRATNEM	Thermal time to emergence for a ratoon crop	°Cd	10.00	05.00
CHUPIBASE	Thermal time from emergence to start of stalk growth	°Cd	1000.00	700.0
SER0	Max. stalk elongation rate, per °Cd	$cm\ °Cd^{-1}$	0.300	0.18

Model Evaluation

After adjusting the genetic coefficients and setting up the soil profile and management conditions, model was simulated using daily weather data from a weather station near the field experiment site. The weather data collected at this site include the daily maximum and minimum air temperatures, daily cumulative solar radiation, and daily average wind speed. Model performance in simulating late season stalk height and final above-ground biomass was evaluated using data from plant cane (planted in 2016) and first ratoon cycle (planted in 2015). In total, 15 biomass and 44 stalk height data points were available for model performance evaluation. Simulated final stalk height and

aboveground biomass were compared with corresponding observed data. The overall accuracy of the model simulations was determined using ordinary least squares regression analysis. The slope and intercept of the linear regression line was tested against the 1:1 line (slope =1 and intercept = 0) using the Student's t test. No significant difference would indicate a satisfactory performance of the model for simulating energy cane stalk height and final biomass in the Texas Rolling Plains. The root mean square of error (RMSE) was calculated as an additional test for the accuracy model simulations.

Historic Weather Data

Historical weather data for the Texas Rolling Plains was collected from 1984 - 2017. The temperature and precipitation data were obtained from the integrated Agricultural Information and Management System (iAIMS). Daily cumulative solar radiation and windspeed were obtained from the National Aeronautics and Space Administration – Prediction of Worldwide Energy Resources (NASA-POWER) website (NASA-POWER, 2020) The average annual precipitation during 1984 - 2017 period was 688 mm. Yearly weather data was categorized into three classes based on the annual precipitation amount. The years with precipitation amount in the first quartile was grouped as dry years and years with annual perception above third quartile was grouped as wet years. Among all years, 1995 had unusually high precipitation was not used in model simulation. Based on this classification scheme, the years with average annual precipitation less than 535 mm was categorized as dry, 536-784 mm as normal, and 785 and above was categorized as wet years (Figure 4.1). In total, all 31 years during the

1984-2017 period were classified into three groups of 8 dry, 7 wet, and 16 normal years for the Texas Rolling Plains.

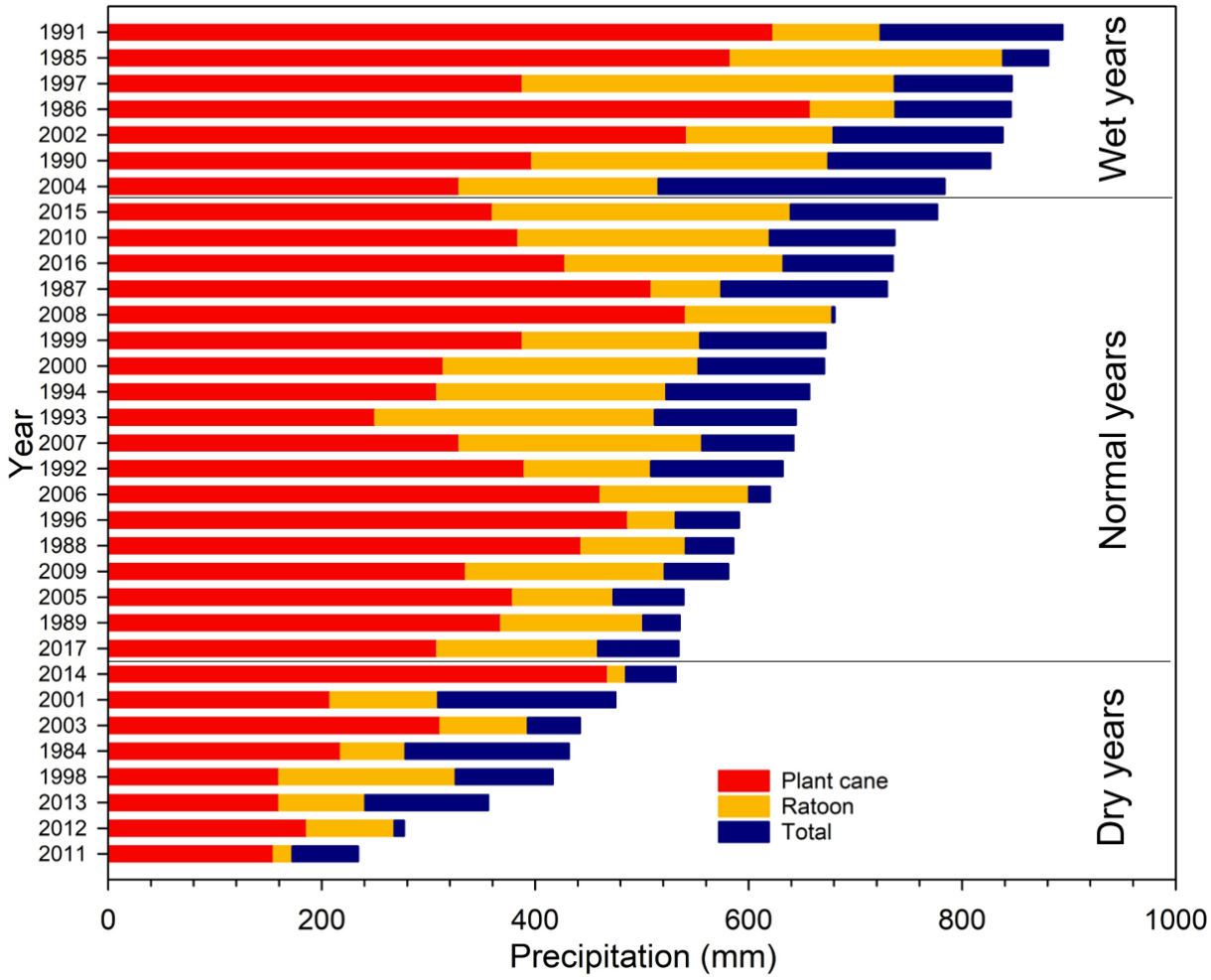

Figure 4.1. Annual precipitation in the Texas Rolling Plains. Red bar indicates the precipitation during plant cane growing season (May – Oct), yellow bar indicates the additional precipitation during ratoon growing season (Feb – Oct), and blue bar indicates remaining precipitation (Nov – Jan). The years are categorized into three classes based on annual precipitation. Dry years had precipitation <535 mm, normal years had precipitation from 536 to 784 mm and wet years had precipitation >785 mm.

Cultural and Management Inputs

Table 4.3 shows the details cultural and management inputs used in model simulation using historical weather data. Simulations were done for both irrigated and rainfed biomass production. Irrigation was applied as a minimum input to support the growth and development. Irrigation events were scheduled in June, July, and August at an interval of 15 days to minimize the effect of high temperature during the vegetative growth phase. 50 mm water was applied in each application for six times providing a total of 300 mm irrigation water for overall crop growing season. The model was set to start simulation 15 days before the target cane planting date (May 15). For ratoon cropping years, the model simulations started on 1 February which was 15 days prior to the observed regrowth time in the field study. A total of four simulations were performed each year; plant cane-irrigated, plant cane-rainfed, ratoon-irrigated, and ratoon-rainfed.

Table 4.3. Field activities inputs for simulating the biomass yield for plant and ratoon

Activities	Plant cane	Ratoon
Planting	May 15 (using cane billets)	Regrowth (Feb 15)
Model simulation start date	May 1	February 1
Irrigation	300 mm (6 applications)	300 mm (6 applications)
Biomass harvesting	~170 DAP (Oct 31)	~260 DAP (Oct 31)

Climate Change Impact Assessment

The potential impact of a change in climatic variables on biomass yield of energy cane feedstock in semi-arid, rolling plains of the Texas was model for the years 1984-2017. The simulation experiments focused on changes in air temperature and precipitation amounts and estimated aboveground biomass for both plant cane and first

year ratoon. The first simulation gradually increased maximum and minimum daily temperatures by 0.5, 1 and 2ºC. A second simulation decreased the precipitation amount by 5%, 10%, 15% and 20% during the crop growing season without changing the temperatures. Finally, a third set of simulations was a combination of increasing temperatures and decreasing precipitation (Table 4.4).

Table 4.4. Hypothetical levels of changing temperature and precipitation for model simulation.

Conditions	Weather variables	Number of simulations
Baseline (1984- 2017)	Daily weather data: maximum and minimum temperature, solar radiation, and precipitation.	33 plant cane and 33 ratoons for irrigated and rainfed conditions
Change in temperature	+0.5ºC +1ºC, +2ºC	99 plant cane and 99 ratoons for irrigated and rainfed conditions
Change in precipitation	- 5%, -10%, -15%, -20%	132 plant cane and 132 ratoons for irrigated and rainfed conditions
Combined change in temperature and precipitation	+0.5ºC and all level of precipitation +1ºC and all level of precipitation +2ºC and all level of precipitation	396 plant cane and 396 ratoons for irrigated and rainfed conditions

RESULTS AND DISCUSSION

Model Performance Evaluation

Figure 4.2 presents observed biomass yield plotted against simulated data for plant cane and first ratoon (N = 15). The linear regression fit to these points explained 96% of the total variance indicating a good agreement between the observed and simulated biomass data. The results of the Student's t test showed the slope of the regression line was not significantly different from 1 ($p = 0.09$) and the intercept was not significantly different from zero ($p = 0.09$). The RMSE was 2.91 t ha^{-1} or ~ 10% of the

average observed aboveground biomass yield. The performance of DSSAT-CANEGRO for simulating energy cane stalk height was also tested (Figure 4.2). The linear regression fit to simulated versus observed data explained 85% of the total variance indicating a good agreement between the observed and simulated stalk height data. The results of the Student's t test showed the slope of the regression line was not significantly different from 1 ($p = 0.07$) and the intercept was not significantly different from zero ($p = 0.06$). The RMSE was 16 cm or ~ 9.9% of the average observed stalk height. The t test, high R^2 and the low RMSE demonstrated that the DSSAT-CANEGRO model can be used to simulate energy cane aboveground biomass and stalk height in the Texas Rolling Plains.

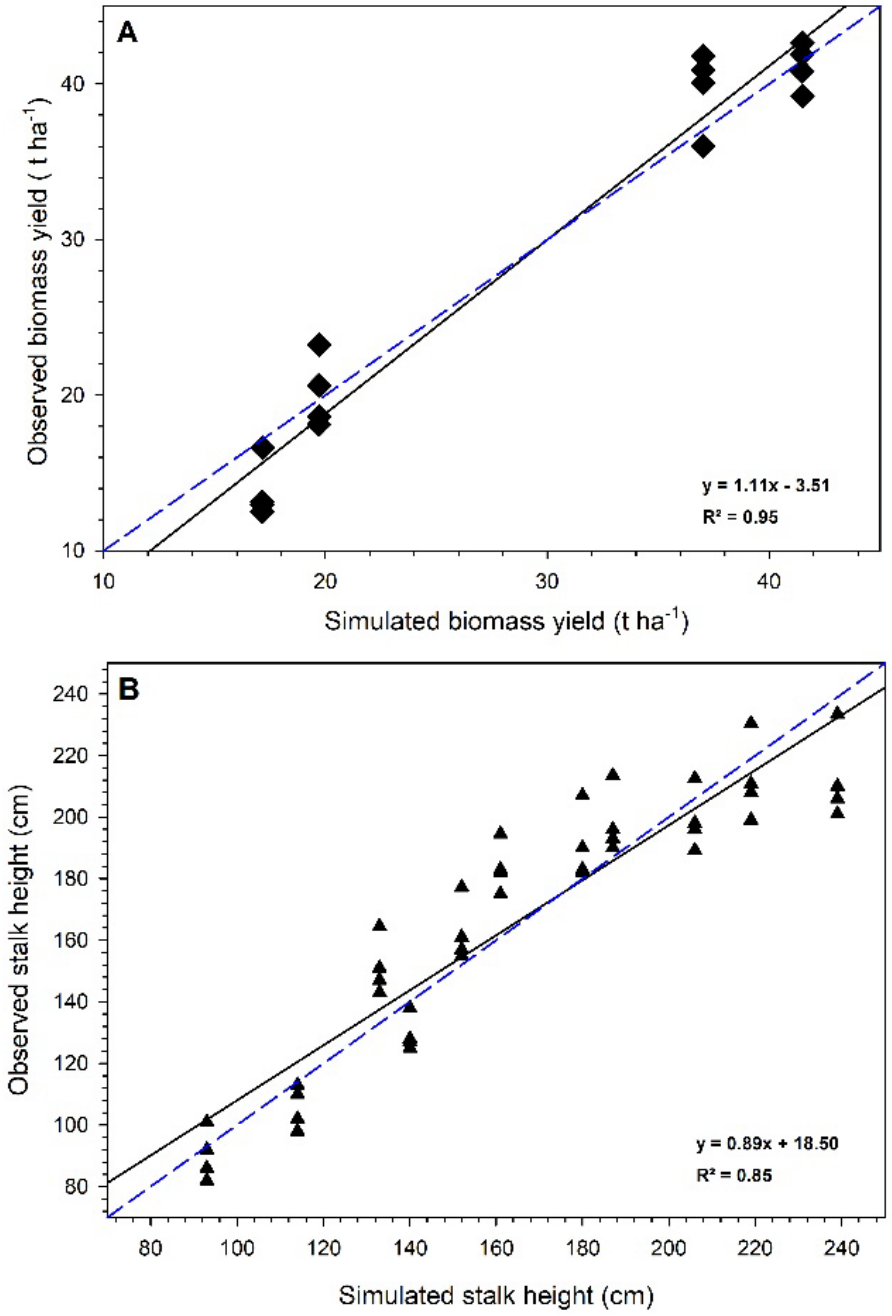

Figure 4.2. (A) Average observed biomass yield from the field experiment plotted against simulated biomass for plant cane and first ratoon (N = 15). (B) Average stalk height after DOY (200) plotted against simulated stalk height for plant cane and first ratoon (N = 44) from the field experiment. In both graphs, solid line is a linear regression line and dashed line is a 1:1 line. The results of the Student's t test showed that the regression lines were not significantly different from the 1:1 line ($p>0.05$).

Effect of Growing Season Precipitation on Biomass Yield

Figures 4.3A-4.3D present the average aboveground biomass yields of plant cane and ratoon during the 33-year simulation period (1984-2017) plotted against the amount of precipitation received from July - September for plant cane and May - September for ratoon. Under irrigated condition, both plant cane and ratoon crops received an additional 300 mm of water from June to August. Growing season precipitation from July to September explained 66% of total variability in final biomass yield of plant cane under both irrigated and rainfed conditions (Figure 4.3A and B). In the case of ratoon, growing season precipitation from May to September explained 72% and 62% of total variability of final biomass yield under irrigated and rainfed conditions respectively.

The number and survival of tillers are key factors determining the biomass accumulation in energy cane. Moisture stress during the maximum vegetative growth stage of energy cane (July – September in plant cane and May to September in ratoon) have similar effect on growth and biomass yield as observed in sugarcane studies. In this simulation, 62-72% yield variation in plant cane and ratoon was explained by the amount of precipitation received during the maximum vegetative growth stage.

The remaining variation in the final biomass yield may have been caused by the timing of precipitation and other management practices. Irrigation reduced the high temperature stress and supported normal tiller growth and development of energy cane in our field study at the same location (Pokhrel et al., 2017). Energy cane planted in May reached peak tillering in July which was critical to determine the biomass yield. Peak tillering in ratoon occurred during April and started accumulating significant biomass

from May to September. Hence irrigation during June to September significantly increased biomass of both plant cane and ratoon.

The average aboveground biomass yield was the highest (38.1±0.7 t ha^{-1}) for the ratoon crop in wet years (precipitation > 785 mm). Without irrigation, average yield was declined by 45% to 20.8±1.5 t ha^{-1}. In normal years (536-784 mm precipitation), average yield of the ratoon crop was 34.8±1.1 t ha^{-1}. The yield reduction was 48% without irrigation during those years (16.7±0.9 t ha^{-1}). In dry years, irrigated ratoon crop had an average yield of 23.6±3.5 t ha^{-1}. Under rainfed condition, yield was declined to 9.4 ±2.1 t ha^{-1} in dry years, which was approximately 60% reduction in yield compared to irrigated ratoon. Similar to ratoon, plant cane yield was the highest in wet years with irrigation (14.2±1.0 t ha^{-1}). Without irrigation, yield was declined to 9.0±0.7 t ha^{-1} (37% reduction). In normal years, plant cane yield was 13.1±0.8 t ha^{-1} with irrigation and 7.5±0.7 t ha^{-1} without irrigation (43% reduction). Dry conditions severely affected plant cane yield without irrigation. Average simulated yield in dry years was 4.4±0.9 t ha^{-1}. With an addition 300 mm irrigation, biomass yield was improved to 10.5±1.0 t ha^{-1}.

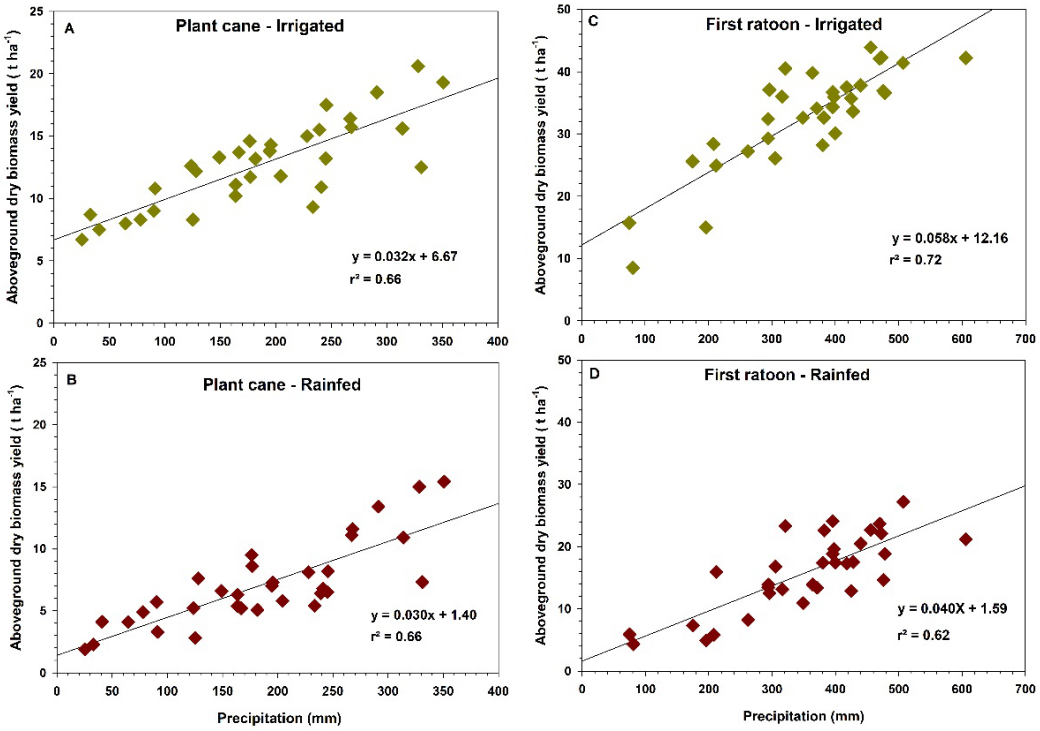

Figure 4.3. Simulated aboveground dry biomass yield regressed against the growing season precipitation during vegetative growth phase of plant cane at (A) irrigated and (B) rainfed and first ratoon at (C) irrigated and (D) rainfed.

In semi-arid regions, water is a major limiting factor for plant growth (Rajan et al., 2015; Steiner, 1986). Studies have shown that growing season precipitation and biomass yield of grass species are positively correlated (Fike et al., 2006; Muir et al., 2001; Sanderson et al., 1999). In general, plant cane yield is lower compared to ratoon because of shorter growing season. Chiluwal et al. (2018) reported an average plant cane biomass yield of 19.6 t ha^{-1} when the growing season precipitation was 843 mm. Knoll et al. (2012) reported energy cane biomass yield of ~28 t ha^{-1} for plant cane in Georgia when growing season precipitation was about 960 mm. Yang et al. (2018) reported plant cane biomass yield of ~25 t ha^{-1} in Beaumont, Texas when growing season precipitation

was ~ 1400 mm. In all these studies, energy cane was planted in October and harvested after 12 months. Simulated biomass yield in our study site under rainfed condition was significantly lower compared to plant cane biomass yield in other studies reported above. Texas Rolling Plains region has a shorter growing season when energy cane is planted using cane billets in May. This is a significant contributor to lower plant cane biomass yield in the region. However, the simulated biomass yield of ratoon is comparable to the energy cane biomass yield reported in Georgia by (Chiluwal et al., 2018). Our simulation results showed that significantly longer growing season doubled the biomass production of ratoon crop than plant cane in the Texas Rolling Plains under both irrigated and rainfed conditions.

Limited information is available regarding biomass yield of newly developed lignocellulose biomass crops such as energy cane in the semi-arid regions of the US. However, several studies have reported biomass yield of other dedicated biofuel feedstock crops in the semi-arid Southern Great Plains region of the US. Biomass sorghum (*Sorghum bicolor* L. Moench), a high yielding biomass feedstock crop, had yield ranging from 13 t ha^{-1} (Tamang et al. (2011) to 32 t ha^{-1} (Rooney et al. (2007) in the Texas High Plains under irrigated condition. Switchgrass (*Panicum virgatum* L) is another perennial grass for biomass production. Biomass yield of switchgrass was 6.25 t ha^{-1} in Oklahoma in a study reported by Wagle and Kakani (2014). Another switchgrass study reported a biomass yield of ~10 t ha^{-1} in Dallas and 16 t ha^{-1} in Stephenville, Texas (Sanderson et al., 1999). However, rainfall in Dallas and Stephenville average 1000 mm and 900 mm, respectively, which is significantly higher than the rainfall in the Texas

Rolling Plains. Our simulation results showed that energy cane produced less biomass than biomass sorghum and comparable biomass to switchgrass in the first year. However, ratoon crop produced similar biomass under rainfed growing condition in years with average annual precipitation over 536 mm (classified as normal and wet years). Biomass yield of energy cane ratoon was higher than biomass sorghum with 300 mm irrigation in both normal and wet years.

Crop water use efficiency (WUE) of energy cane, defined as the kg of aboveground dry biomass produced per hectare per mm of rainfall, was about 31 kg ha^{-1} mm^{-1} in both irrigated and rainfed conditions (Figure 4.3A and B). Similarly, WUE of irrigated ratoon was 58 kg ha^{-1} mm^{-1} (Figure 4.3C) and rainfed ratoon was 40 kg ha^{-1} mm^{-1} (Figure 4.3D). WUE in our study is comparable to WUE of bioenergy sorghum by Hao et al. (2014) in the Texas High Plains. In their study, WUE of biomass sorghum was 45.5 kg ha^{-1} mm^{-1} under limited irrigation and 55 kg ha^{-1} mm^{-1} under rainfed condition.

Shorter growing season for plant cane resulted lower biomass yield than ratoon which ultimately lowered WUE in plant cane. However, similar WUE of ratoon to the existing energy sorghum shows that energycane could be a competitive biomass feedstock in the Texas Rolling plains. Our study indicates that energycane genotypes have the potential of biomass production in the semi-arid Texas Rolling Plains.

Effect of Increasing Daily Temperature on Biomass Yield

Figure 4.4 presents the average simulated aboveground biomass yield of plant cane under irrigated and rainfed conditions when daily maximum and minimum temperature increased by 0.5°C, 1°C, and 2°C from the baseline air temperature recorded during the 1984-2017 study period. Simulation results showed a gradual decrease in biomass yield under these warming scenarios although the differences were not statistically significant. In dry years, 0.5ºC, 1°C, and 2°C increases in daily air temperature resulted in an average rainfed plant cane yield decline of 4%, 8% and 17% respectively compared to the baseline with no increase in temperatures. In years with normal precipitation, the average decline in rainfed plant cane yield was 4%, 8% and 14% when air temperatures were increased by 0.5ºC, 1°C, and 2°C respectively. In years with higher precipitation, the average decline in rainfed plant cane yield was 3%, 5%, and 14% when air temperatures were increased by 0.5ºC, 1°C, and 2°C respectively. Similarly, in dry years, 0.5º C, 1°C, and 2°C increases in daily air temperature resulted in an average irrigated plant cane biomass yield decline by 3%, 5%, and 10%. The biomass yields also decreased in normal years by 1%, 3%, and 8% when air temperature increased by 0.5° C, 1°C, and 2°C in irrigated plant cane. Biomass yield was unchanged in irrigated plant cane in wet years when air temperature increased by 0.5°C and 1°C. However, biomass yield decreased by 2% when air temperature increased by 2°C.

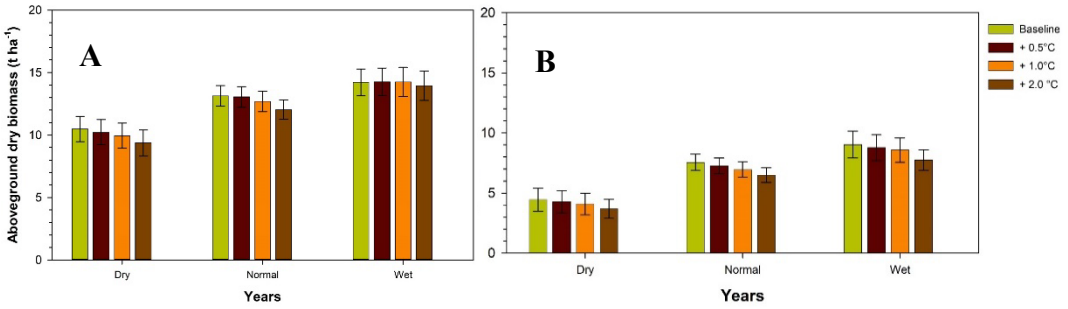

Figure 4.4. Effect of increasing daily maximum and minimum air temperature on biomass yield of plant cane in (A) irrigated and (B) rainfed growing conditions during dry, normal, and wet years. Daily maximum and minimum temperature were increased by 0.5°C, 1°C, and 2°C from the baseline temperature during simulation experiment.

Figure 4.5 presents the simulated aboveground biomass yield of first ratoon under irrigated and rainfed conditions when daily maximum and minimum temperature increased from 0.5°C, 1°C, and 2°C from the baseline temperature recorded during 1984-2017. Simulation experiment showed mixed results in biomass yield under different temperature regimes. Differences in biomass yields were not statistically significant. In dry years, increase in daily air temperature by 0.5°C, 1°C, and 2°C from the baseline resulted an average decrease in biomass yield of rainfed ratoon by 2% when temperature increased by 2°C, however, yield did not change when temperature increased by 0.5°C and 1°C. In normal years, when air temperature increased by 0.5°C, 1°C, and 2°C from the baseline the biomass yield of rainfed ratoon increased by 2%, 2%, and 3%. Similarly, in wet years when the air temperature increased by 0.5°C, 1°C, and 2°C from the baseline, biomass yield of rainfed ratoon increased by 2.1%, 5%, and 7%. Biomass yield of irrigated ratoon also showed mixed result on biomass yield due to change in daily maximum and minimum temperatures. In dry years, biomass yield of

irrigated ratoon decreased by 3%, 7%, and 23% when air temperature increased by 0.5°C, 1°C, and 2°C from the baseline. In normal years, biomass yield of irrigated ratoon increased by 1% when temperature increased by 0.5°C. Biomass yield decreased by 1% and 4% when daily maximum and minimum temperature increased by 1°C and 2°C. In wet years, biomass yield of irrigated ratoon increased by 1%, 2%, and 3% when daily maximum and minimum temperature increased by 0.5°C, 1°C, and 2°C from the baseline.

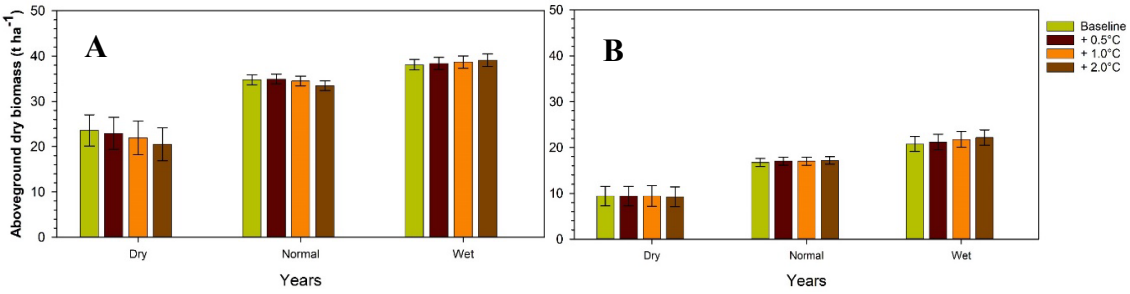

Figure 4.5. Effect of increasing daily maximum and minimum air temperature on biomass yield of first ratoon in (A) irrigated and (B) rainfed growing conditions during dry, normal, and wet years. Daily maximum and minimum temperature were increased by 0.5°C, 1°C, and 2°C from the baseline temperature during simulation experiment.

Photosynthetic rate increases with increase in temperature and accelerates early canopy development and biomass accumulation in sugarcane species (Singels et al., 2014). Higher light interception in early growth stages help to accumulate biomass at higher rate when growing season soil moisture is not limited (de Carvalho et al., 2015). In our study, cane billets were planted in May, when maximum daily maximum temperature was about 30°C. The temperature is optimum for tiller growth and development. As the season progress, higher daily temperature increased rate of

evapotranspiration (ET) in plants. If water availability is limited and does not fulfill the ET requirement, it reduce the biomass yield (de Carvalho et al., 2015). A study in sugarcane, Sonkar et al. (2019) reported 14% yield loss in sugarcane fresh stalk mass in rainfed production system when temperature increase by 4°C. Comparable results were found in our study, where biomass yield was reduced ~ 8% when daily maximum and minimum temperature was increased by 2°C. Our simulation study findings were also similar to the de Carvalho et al. (2015) where a decrease in sugarcane in yield in Brazil (during 2040- 2060) was associated with an increase in temperature. These observations support the findings herein where reductions in biomass yield were higher in rainfed than in irrigated conditions and in dry years compared to wet years.

Tillering in sugarcane species is temperature dependent (Inman-Bamber, 1994). In simulation, increased temperature resulted in earlier tiller growth (~7-12 days) in ratoon crops. Ratoon crop biomass yield increased in normal and wet years as daily maximum and minimum temperatures were increased. Similar observation was reported in sugarcane study, where Begum and Islam (2012) reported high tiller mortality in dry years. In wet years, high precipitation during tiller formation and vegetative growth enhanced the survival of tillers resulting higher biomass yield accumulation over the growing season.

Effect of Decreasing Daily Precipitation on Biomass Yield

Simulation results showed gradual decrease in biomass yield under reduced precipitation scenarios (Figure 4.6), but the yield reduction was significant in only normal years with daily precipitation decrease of 20%. In the dry years, 5%, 10%, 15%, and 20% decrease in daily precipitation decreased the average biomass yield of rainfed plant cane by 4%, 9%, 13%, and 16% respectively compared to the baseline precipitation. In years with normal precipitation, decrease in precipitation by 5%, 10%, 15%, and 20% from the baseline on daily basis decreased the average biomass yield of rainfed plant cane by 3%, 8%, 12%, and 17%. In the years with high precipitation, decrease in daily precipitation by 5%, 10%, 15%, and 20% decreased the average biomass yield of rainfed plant cane by 4%, 8 %, 12%, and 18%.

In the dry years, 5%, 10%, 15%, and 20% decrease in daily precipitation decreased the biomass yield of irrigated plant cane by 1%, 3%, 4%, and 5% respectively compared to the baseline precipitation. In normal years, the average biomass yield of irrigated plant cane decreased by 2%, 3%, 5%, and 7% when the daily precipitation decreased by 5%, 10%, 15%, and 20% from the baseline. Similarly, average biomass yield of irrigated plant cane decreased when the by 1%, 2%, 4%, and 5% when daily precipitation decreased by 5%, 10%, 15%, and 20% from the baseline in wet years.

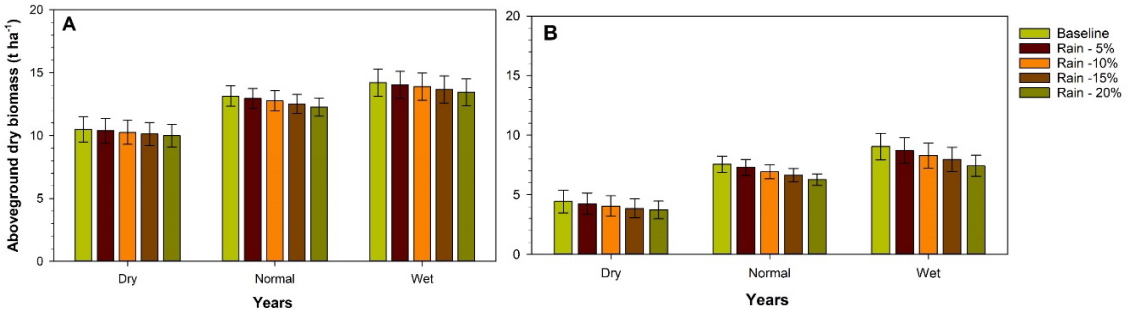

Figure 4.6. Effect of decreasing daily precipitation on biomass yield of plant cane in (A) irrigated and (B) rainfed growing conditions during dry, normal, and wet years. Daily precipitation amount was decreased by 5%, 10%, 15%, and 20% from the baseline precipitation during simulation experiment.

Similar to the plant cane, average biomass yield decreases in the ratoon as precipitation was reduced (Figure 4.7). Yield reduction was significant in normal and wet years when daily precipitation decreased by 15% and 20% in normal years and 20% in wet years. In dry years, 5%, 10%, 15%, and 20% decrease in daily precipitation decreased the average biomass yield of rainfed ratoon by 5%, 9%, 13%, and 17% respectively compared to the baseline precipitation. In years with normal precipitation, decrease in precipitation by 5%, 10%, 15%, and 20% from the baseline on daily basis decreased the average biomass yield of rainfed ratoon by 4%, 10%, 16%, and 21%. In the years with high precipitation, decrease in daily precipitation by 5%, 10%, 15%, and 20% decreased the average biomass yield of rainfed ratoons by 4%, 8 %, 13%, and 17%. Similarly, in the dry years, 5%, 10%, 15%, and 20% decrease in daily precipitation decreased the biomass yield of irrigated ratoon by 2%, 5%, 7%, and 9% respectively compared to the baseline precipitation. Biomass yield of irrigated ratoon decreased by 2%, 4%, 6%, and 8% when daily precipitation from the baseline decreased by 5%, 10%,

15%, and 20% in normal years. The average biomass yield of irrigated ratoon decreased by 1%, 2%, 3%, and 4% in wet years when daily precipitation decreased by 5%, 10%, 15%, and 20% from the baseline.

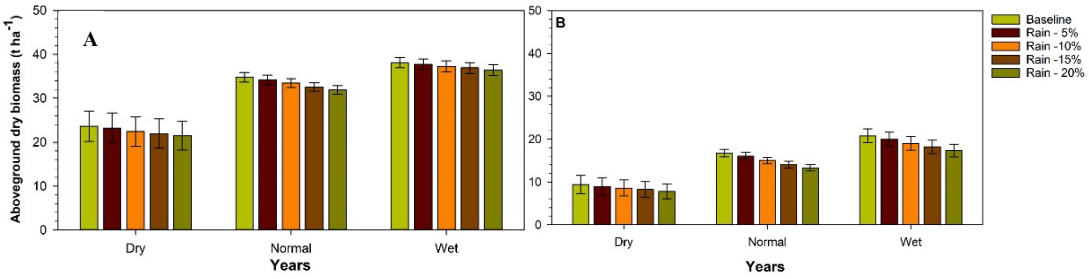

Figure 4.7. Effect of decreasing daily precipitation on biomass yield of first ratoon in (A) irrigated and (B) rainfed growing conditions during dry, normal, and wet years. Daily precipitation amount was decreased by 5%, 10%, 15%, and 20% from the baseline precipitation during simulation experiment.

Reduction in precipitation had significant negative effect on biomass yield of sugarcane (de Carvalho et al., 2015; Sonkar et al., 2019). Results from the simulated experiment showed reduced precipitation had significantly reduced yield in both plant cane and ratoon during normal years. Biomass yields were already low and not different due to decease in precipitation in dry years due to higher stress level.

Combined Effect Change in Temperature and Precipitation on Biomass Yield

Simulation results showed gradual decrease in biomass yield under combined effect of a gradual increase in temperature and decrease in precipitation (Figure 4.8). When daily maximum and minimum air temperature increased by 0.5°C and precipitation decreased by 5%, 10%, 15%, and 20%, average biomass yield of rainfed

plant cane decreased by 8%, 13%, 19%, and 21% respectively in dry years, 8%, 11%, 15%, and 22% in normal years, and 6%, 11% 15%, and 20% in wet years. When daily maximum and minimum air temperature increased by 1°C and precipitation decreased by 5%, 10%, 15%, and 20%, average biomass yield of rainfed plant cane decreased by 12%, 18%, 22%, and 25% in dry years, 12%, 15%, 20% and 26% in normal years, and 10%, 16%, 19%, and 23% in wet years. When daily maximum and minimum air temperature increased by 2°C and precipitation decreased by 5%, 10%, 15%, and 20%, average biomass yield of rainfed plant cane decreased by 21%, 26%, 27%, and 31% in dry years, 18%, 23%, 28% and 31% in normal years, and 19%, 22%, 26%, and 28% in wet years.

Similarly, when daily maximum and minimum air temperature increased by 0.5°C and precipitation decreased by 5%, 10%, 15%, and 20%, average biomass yield of irrigated plant cane decreased by 4%, 5%, 6%, and 8% respectively in dry years, 2%, 5%, 7%, and 9% in normal years, and 1%, 3%, 4% and 20% in wet years. When daily maximum and minimum air temperature increased by 1°C and precipitation decreased by 5%, 10%, 15%, and 20%, average biomass yield of irrigated plant cane decreased by 6%, 8%, 9%, and 10% dry years, 5%, 7%, 9% and 11% in normal years, and 1%, 3%, 5%, and 6% in wet years. When daily maximum and minimum air temperature increased by 2°C and precipitation decreased by 5%, 10%, 15%, and 20%, average biomass yield of irrigated plant cane decreased by 12%, 14%, 16%, and 18% dry years, 10%, 12%, 14% and 16% in normal years, and 3%, 5%, 7%, and 9% in wet years.

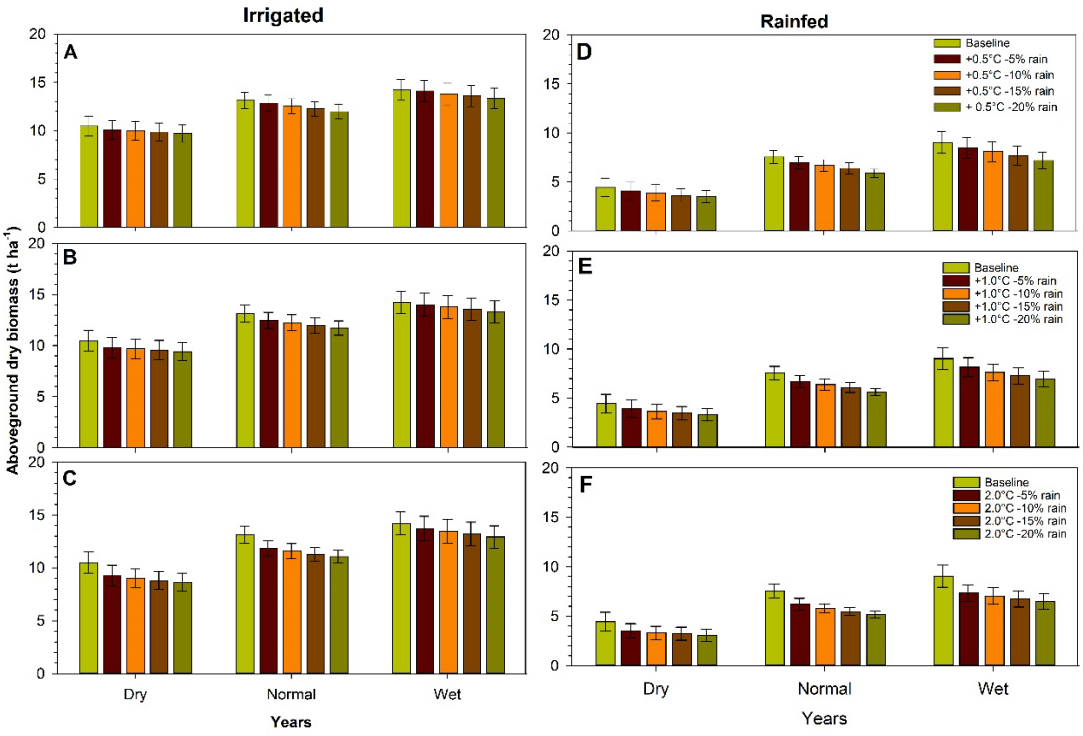

Figure 4.8. Effect of increasing daily maximum and minimum temperatures and decreasing daily precipitation on biomass yield of plant cane in irrigated and rainfed condition during dry, normal, and wet years. Daily maximum and minimum temperature were increased by 0.5°C, 1°C, and 2°C from the baseline temperature and precipitation amount was decreased by 5%, 10%, 15%, and 20% from baseline precipitation during simulation experiment.

Figure 4.9 presents the simulated average aboveground biomass yield of ratoon under irrigated and rainfed conditions when daily maximum and minimum air temperature increased by 0.5°C, 1°C, and 2°C and daily precipitation decreased by 5%, 10%, 15%, and 20% from the weather baseline data during 1984-2017. Overall, simulation results showed gradual decrease in biomass yield under combined effect of gradual increase in temperature and decrease in precipitation. When daily maximum and minimum air temperature increased by 0.5°C and precipitation decreased by 5%, 10%, 15%, and 20%, average biomass yield of rainfed ratoon decreased by 5%, 8%, 12%, and

19% respectively in dry years, 3%, 9%, 15%, and 20% in normal years, and 3%, 6% 10%, and 14% in wet years. When daily maximum and minimum air temperature increased by 1°C and precipitation decreased by 5%, 10%, 15%, and 20%, average biomass yield of rainfed ratoon decreased by 4%, 10%, 14%, and 18% in dry years, 4%, 9%, 15% and 20% in normal years, and 0%, 4%, 8%, and 13% in wet years. When daily maximum and minimum air temperature increased by 2°C and precipitation decreased by 5%, 10%, 15%, and 20%, average biomass yield of rainfed ratoon decreased by 7%, 11%, 15%, and 18% in dry years, 3%, 7%, 12% and 17% in normal years, and 3% (increase), 1%, 8%, and 13% in wet years.

Similarly, when daily maximum and minimum air temperature increased by 0.5°C and precipitation decreased by 5%, 10%, 15%, and 20%, average biomass yield of irrigated ratoon 6%, 7%, 9%, and 12% respectively in dry years, 2%, 4%, 6%, and 9% in normal years, and 0%, 3%, 1% and 3% in wet years. When daily maximum and minimum air temperature increased by 1°C and precipitation decreased by 5%, 10%, 15%, and 20%, average biomass yield of rainfed ratoon decreased by 9%, 11%, 14%, and 16% in dry years, 3%, 6%, 7% and 10% in normal years, and 1% (increase), 0%, 2%, and 3% in wet years. When daily maximum and minimum air temperature increased by 2°C and precipitation decreased by 5%, 10%, 15%, and 20%, average biomass yield of rainfed ratoon decreased by 16%, 19%, 22%, and 24% in dry years, 10%, 12%, 14% and 16% in normal years, and 1% (increase), 2%, 3%, and 5% in wet years.

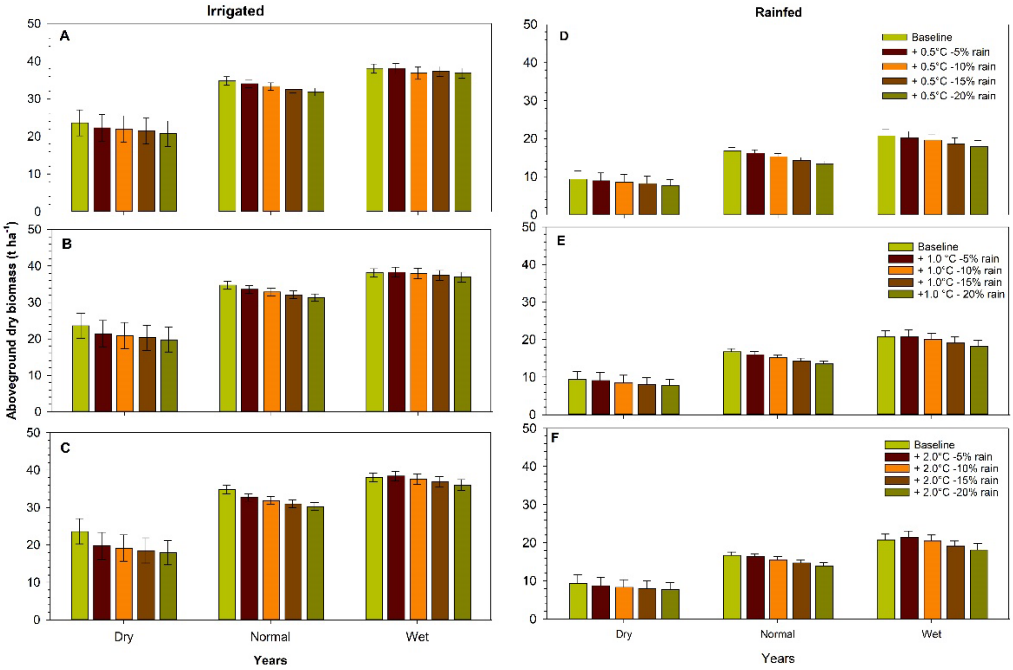

Figure 4.9. Effect of increasing daily maximum and minimum temperatures and decreasing daily precipitation on biomass yield of first ratoon in irrigated and rainfed condition during dry, normal, and wet years. Daily maximum and minimum temperature were increased by 0.5°C, 1°C, and 2°C from the baseline temperature and precipitation amount was decreased by 5%, 10%, 15%, and 20% from baseline precipitation during simulation experiment.

Studies have shown the potential of biomass yield reduction of sugarcane under future climate change scenario of increasing temperature and decreasing precipitation in different agroclimatic regions (de Carvalho et al., 2015; Knox et al., 2010; Sonkar et al., 2019). Increasing temperature and decreasing precipitation creates need for more water to fulfill higher evapotranspiration demand (Singels et al., 2014). However, in the Texas Rolling Plains, where water supply is limited and crop yield mainly depends on precipitation, warmer summer and less rainfall events resulted significant reduction in the biomass yield reduction. Higher yield loss was observed when temperature increased by 2°C and precipitation decrease by 20% in rainfed plant cane (31% yield loss) and

ratoon (19% yield loss) in dry years. Increase in air temperature positively affected ratoon emergence and biomass accumulation in early stage after overwintering. Early canopy development led to more ET and moisture stress in normal and dry years (Singels et al., 2014)**.** The effect of high temperature and moisture stress was reduced in wet years and irrigated growing condition resulting lower percent of yield loss.

CONCLUSIONS

The evaluated CANEGRO Sugarcane model was used to estimate the impact of changing climate on energy cane biomass production in the Texas Rolling Plains. Effect of increase in daily maximum and minimum air temperatures, decrease in daily precipitation and interaction between increasing temperature and decreasing precipitation were simulated from the baseline weather data during 1984-2017. Precipitation during peak vegetative growth stage explained 66% variability of biomass yield of plant cane in both irrigated and rainfed conditions. Similarly, precipitation during peak vegetative growth stage of ratoon explained the variability in biomass yield by 62% in rainfed and 72% in irrigated conditions. Simulation results showed aboveground biomass of plant cane ranged from 11- 14 t ha^{-1} in irrigated and 4-9 t ha^{-1} in rainfed conditions and ratoon ranged from 24 - 38 t ha^{-1} in irrigated and 10 – 21 t ha^{-1} in rainfed conditions respectively. The magnitude of yield loss varied at different combinations of the weather variables. Yield loss was higher daily maximum and minimum temperature increased by 2°C and daily precipitation decreased by 20%. Maximum biomass yield loss ranged from 18% -24% of ratoon and 18% - 31% of plant

cane in dry years. Current simulation models provide a guide of how changing temperature and precipitation affects biomass yield of energycane in the semi-arid regions of Texas. Growing season water management is a key factor determining the biomass yield in biomass production, optimizing the irrigation scheduling helps to maximize the biomass yield.

CHAPTER V

AGRONOMIC PERFORMANCE OF ENERGY SORGHUM (*Sorghum bicolor* L. Moench) HYBRIDS IN THE SEMI-ARID TEXAS ROLLING PLAINS

INTRODUCTION

The lignocellulosic biofuels are projected to become a major contributor to the renewable energy sector around the globe as the technologies become more cost-effective (Langholtz et al., 2016). These second-generation biofuels are expected to have greater environmental benefits compared to first-generation starch and sugar-based biofuels. Because of the benefits associated with better environmental stewardship, the U.S. Renewable Fuel Standard Program (US-RFS) mandates blending a significant amount of second-generation lignocellulosic biofuels with conventional transportation fuels (DOE, 2019b; Sharma et al., 2019). In 2019, the cellulosic biofuel mandate was 32 billion liters, however the target was later reduced to 1.6 billion liters due to inadequate production (EPA, 2018b). Production of cellulosic biofuels has increased gradually over the years; however, current situation shows a huge gap between targeted and produced volumes. To achieve the targeted volumes mandated by the US-RSF, biofuel production from cellulosic sources requires significant advancements in the processing sector. Another major challenge is production of high yielding cellulosic feedstocks without affecting the national and global food security (Sohl et al., 2012). To achieve this and to be economically viable, cellulosic biomass feedstocks must be produced in underutilized

marginal lands with less management inputs. This requires development of high biomass yielding feedstocks that are adapted to growing in marginal conditions.

Sorghum (*Sorghum bicolor* L. Moench) is a multipurpose C4 cereal crop adapted to grow in dry hot conditions. The crop was originated in the arid part of northeastern Africa and was brought to the U.S. in the 1700's (Rooney et al., 2007). Although sorghum is a staple food crop in many regions of Africa and India, it is used as an animal feed (grain and forage) in the U.S. In 2018, the U.S. produced about 9.2 million tons of grain, the largest in the world (FAO, 2019). In recent years, as much as one-third of the U.S. grain sorghum is used for starch-based ethanol production (Sorghum-Checkoff, 2020). As the demand for feeds for livestock production is rapidly increasing nationally and globally, the use of sorghum grains for fuel ethanol production competes with its need in the livestock sector (Propheter et al., 2010). Thus, alternative sources of biofuels that does not compete with the existing food and feed supply chains are important to ensure the future of clean energy.

Energy sorghums are specifically bred for lingo-cellulosic biofuel production (Shoemaker and Bransby, 2010). These are similar to forage sorghums used for grazing and silage and are specifically selected for biomass yield rather than nutritional quality (Staggenborg, 2019). Energy sorghums are drought tolerant, high water use efficient, requires relatively low inputs, and can be grown in a wide range of environments (Rooney et al., 2007; Sharma et al., 2017; Wight et al., 2012). Some hybrids are photo-period sensitive which also is an advantage as it extends the vegetative growth period and, therefore accumulate higher biomass yield and offers flexible harvesting options

(Hao et al., 2014; Rooney et al., 2007). Past and current research have shown the potential for genetic improvement for better adaptability of energy sorghums under marginal growing conditions (Rooney et al., 2007).

To be sustainable, the production of lignocellulosic feedstocks such as energy sorghums must utilize agriculturally degraded and marginal lands instead of prime farmlands (Chiluwal et al., 2019; Matsuoka et al., 2014). High biomass yield potential under marginal conditions is a necessary prerequisite to ensure economic and environmental sustainability of the expanding biofuels and bioproducts economy. In this study, we conducted an agronomic trial of energy sorghum hybrids in the Texas Rolling Plains, a semi-arid region in the northern part of Texas which has marginal production conditions. This region is characterized by limited precipitation, high windspeed, hot and dry summer, and freezing winter. Average annual precipitation varies from 460 in the west to 760 mm in the east (Modala, 2014). Increasing summer temperature, frequent droughts, and uneven precipitation distribution during the growing season are some of the major challenges for crop production in this semi-arid region. The major crops in the region include winter wheat (*Triticum aestivum*), cotton (*Gossypium hirsutum*), and grain sorghum. As the demand for cellulosic biomass is expected to increase in the future, energy sorghums have the potential to be incorporated into the existing crop rotation systems. Studies have shown that energy sorghum has the potential to accumulate high biomass in a short growing cycle of 60-90 days (Rooney et al., 2007). If the main crop is lost due to unforeseen weather factors, such as frost, hail or drought conditions at planting, biomass sorghum could be a promising alternate crop. Although

the commercial production of energy sorghums for cellulosic ethanol requires development of cost-effective processing facilities in the region, scientific information is lacking on the agronomic performance of this potential feedstock crop in the Texas Rolling Plains.

The overall objective of this study was to evaluate the growth and biomass yield of two biomass sorghum cultivars (ES 5140 and ES 5240) from the Texas A&M biomass sorghum breeding program in the Texas Rolling Plains. Additionally, we investigated the light interception characteristics of the two hybrids as light utilization is a major characteristic for improving the photosynthetic activity of plants (Bai et al., 2016; Rajan et al., 2013).

MATERIALS AND METHODS

Field Experiment

The study was conducted at the Texas A&M AgriLife Research Station near Chillicothe, Texas [34° 11' 46.99" N & 99° 31' 51.83" W, 437 m elevation]. The soil type at the study site was Abilene clay loam (Fine, mixed, thermic Pachic Argiustolls). Two energy sorghum cultivars ES 5140 and ES 5200 were evaluated during the study. The experimental design was a randomized complete block with a split plot arrangement and four replications. The main plots consisted of two irrigation treatments (high and low) and subplots consisted of two energy sorghum cultivars. Individual plots were 6 m long and 4 m wide with 4 rows and 1 m inter-row spacing. Plots were maintained with 1.5 m alleys between individual plots and 3 m alleys between blocks. Ridges and

furrows were created a week before planting. Nitrogen fertilizer (urea 46-0-0) was applied at 67 kg N ha^{-1} a day before planting. Sorghum was planted on ridges using a plot planter at a seeding rate of 165,000 seeds ha^{-1} on 24 May in 2015 and 30 May in 2017. Irrigation water was applied using the furrow method. In 2015, irrigation water was applied ten times in high irrigation plots and six times in low irrigation plots from June to August. High irrigation plots received a total of 601 mm irrigation water and low irrigation plots receive a total of 359 mm irrigation water. An additional 257 mm precipitation was received during the plant growing season from May to October. In 2017, irrigation water was applied four times in high irrigation plots and three times in low irrigation plots respectively. High irrigation plots received a total of 358 mm irrigation water and low irrigation plots received a total of 245 mm irrigation water from June to August. An additional 775 mm precipitation was received by the crop during June to November. Sugarcane aphid (*Melanaphis sacchari*) infestation was observed about 60 days after planting in 2017. SIVANTO prime (Bayer Crop Science) was sprayed at 750 ml ha^{-1} on August 10 using a tractor mounted sprayer to manage sugarcane aphids. Weed infestation was also observed in 2017, which was managed manually whenever required.

Weather Data

A weather station was established near the plots during the experimental years. The weather parameters recorded included air temperature, precipitation, and solar radiation. Air temperature was measured using a temperature/relative humidity sensor (Model HMP50, Campbell Scientific Inc., Logan, UT, USA). Precipitation was

measured using a tipping bucket rain gauge (Model TE525, Campbell Scientific Inc., Logan, UT, USA), and solar irradiance was measured using a pyranometer (Model LI-190SB, LI-COR Biosciences, Lincoln, NE, USA). A CR1000 datalogger (Campbell Scientific Inc., Logan, UT, USA) was used to collect data at an interval of 10 second interval, which was used to calculate the values on hourly basis. Hourly data was used to calculate daily values for maximum and minimum air temperature, cumulative precipitation, and cumulative solar radiation. Historical temperature and precipitation data for the Texas Rolling Plains (1984 -2017) were obtained from the integrated Agricultural Information and Management System (iAIMS)(iAIMS, 2020). The daily weather data obtained from the iAIMS was used to calculate long term monthly averages for the Texas Rolling Plains. The year 2011 was excluded from the long-term average calculation as it was considered a mega drought year in the region (Long et al., 2013; Rajan et al., 2015).

Within-Season Data

With-in season growth measurements were taken at 15-20 days interval in 2015. However, in 2017, limited growth measurement data were recorded due to aphid infestation that started nearly two months after planting in the field. Plant height and leaf area index (LAI) measurements were collected from the energy sorghum plots during both growing seasons. All measurements were made from middle two rows of individual plots. Plant height was recorded by randomly selecting 12 plants per plot and measuring their height from soil surface to the arch of the completely open top leaf. A hand-held plant canopy analyzer (Model LI-COR 2200C; LI-COR Biosciences, Lincoln, NE) was

used for making non-destructive LAI measurements. This sensor measures the attenuation of diffuse sky radiation and by making measurements above and below the canopy, light transmittance is measured which is then used to calculate LAI. One above canopy and four below canopy measurements per plot were taken in early morning (7:00 am ± 30 min) when sun was low in the horizon as per the instrument guidelines. In 2017, stalk or tiller number per meter of crop row was counted to calculate stalk or tiller density at harvest.

Canopy light interception was measured using a ceptometer (Model ACCUPAR LP-80; Meter Environment, Pullman, WA) in both years. Prior to taking measurements from each plot, total incoming photosynthetically active radiation (PAR_{Top}) was measured by holding the sensor above the canopy (when plants were small) or outside the plot. Measurements were taken by avoiding any shading to the probe. Above canopy measurements were followed by four measurements below the canopy (PAR_{Bottom}) by placing the sensor in a horizontal position across the plant rows about 15 cm above the soil surface. These measurements were taken during ±1 hour of solar noon on days with no cloud cover. The fraction of intercepted photosynthetically active radiation (*f*IPAR) was calculated using the following equation.

$$f\text{IPAR} = \frac{PAR_{Top} - PAR_{Botton}}{PAR_{Top}} \qquad \text{[Equation 5.1]}$$

The relationship between canopy light interception and leaf area development was explored by plotting *f*IPAR against LAI. The light extinction coefficient (k) which is a measure of the decrease in light intensity as light passes through the plant canopy was calculated using a modified form of the Beer-Lambert Law (Vose et al., 1995). The

natural logarithm of the relative light intensity (ratio of PAR_{Bottom} to PAR_{Top}) was regressed against LAI to estimate k as follows (Equation 5.2):

$$ln\left[\frac{PAR_{Bottom}}{PAR_{Top}}\right] = k\ (LAI) \qquad \text{[Equation 5.2]}$$

Spectral reflectance characteristics of the energy sorghum canopy was studied by calculating the normalized difference vegetation index (NDVI) using measurements made using a multispectral radiometer (Model MSR5; CROPSCAN Inc, Rochester, MN). Similar to PAR measurements, two measurements per lots were taken during solar noon (±1 hour) on cloud-free days. The radiometer was mounted on top of a stand and faced vertically down. Approximately 1 m distance was maintained between sensor and the canopy during measurements. Spectral reflectance in the red (670 mm) and near-infrared (830 mm) wavelengths were used to calculate the normalized difference vegetation index (NDVI) using the following equation (Attia and Rajan, 2016).

$$NDVI = \frac{NIR-Red}{NIR+Red} \qquad \text{[Equation 5.3]}$$

Biomass and Quality

Final aboveground biomass measurements were made on October 29 in 2015 and November 11 in 2017. Five stalks were selected randomly from each plot and harvested manually. Stalk number per two-meter crop row was counted from middle two rows at harvest. Fresh weight was recorded immediately after harvesting and stem and leaves were separated. Stalk diameter was measured using a Vernier caliper (only in 2017). Measurements were taken at10 cm above the bottom end, middle of the stalk, and 10 cm below the top end. These three numbers were averaged to calculate the stalk diameter for

individual stalks. Stem and leaves were oven dried at 60°C until biomass weight remained unchanged. Final dry biomass was calculated on area basis by multiplying dry sample weight by number of stalks per unit area.

Plant tissue samples (stem and leaves) were analyzed to estimate lignin, cellulose, and hemicellulose contents in 2017. Oven dried stem samples were first passed through a woodchipper to break down stem into smaller chip size (about 3-5 cm). Stem chips and leaves were then ground separately using a Wiley Mill (Thomas Scientific, NJ) and passed through a 1 mm screen. A Near-infrared spectroscopy (NIRs) analyzer (SpectraStar analyzer, Model 2500X RTW, Unity Scientific, Inc., Purcellville, VA) was used to estimate cellulose, hemicellulose, and lignin content in the tissue samples. Before analyzing the energy sorghum tissue content, NIR method was optimized to analyze the tissue components of bioenergy feedstocks (sugarcane, energy cane, and miscanthus).

Statistical Analysis

Statistical analysis was done using SAS v 9.4 (SAS, 2016). The mixed model procedure in SAS was used for statistical analysis. Repeated measures were analyzed by analysis of variance (ANOVA). Replication was considered a random variable, and irrigation and genotypes were considered as fixed effects. Treatment means were separated by the Tukey method at $p \leq 0.05$ significance level.

RESULTS AND DISCUSSION

Growing Season Weather

Figure 5.1A and 5.1B present the monthly average maximum and minimum air temperatures and cumulative precipitation during the crop growing season (May-November) in 2015 and 2017. The long-term monthly averages of temperature and precipitation from 1984-2017 (33 years excluding 2011) are presented in Figure 5.1C. Cumulative precipitation from crop planting to harvest (May 24 to Oct 29) was 257 mm in 2015, which was 25% less than the long-term precipitation during the same period (343 mm). However, cumulative precipitation during the 2017 crop growing season (May 30 to Nov 11) was three times higher (775 mm) than 2015 and 2.3 times higher than the long-term average. Precipitation distribution also varied in the two growing seasons. In 2015 growing season, the wettest month was May with a total precipitation of 213 mm (2.4 times higher than long-term average of 86 mm) and the driest month was September with a total precipitation of only 13 mm (about one fifth of long-term average). In 2017, monthly cumulative precipitation was higher than the long-term average except May. Approximately 45% of the total precipitation occurred during the 2017 crop growing season was received in August alone. About 200 mm precipitation occurred within 24 hours on August 14. Maximum and minimum air temperatures followed similar trends as in the case of long-term average during both crop growing seasons. However, maximum air temperature during August 2017 was approximately 2°C lower than 2015 as well as the long-term average. Frequent cloud cover and rainfall

events along with high precipitation during the month of August may have played a role in lowering the air temperature.

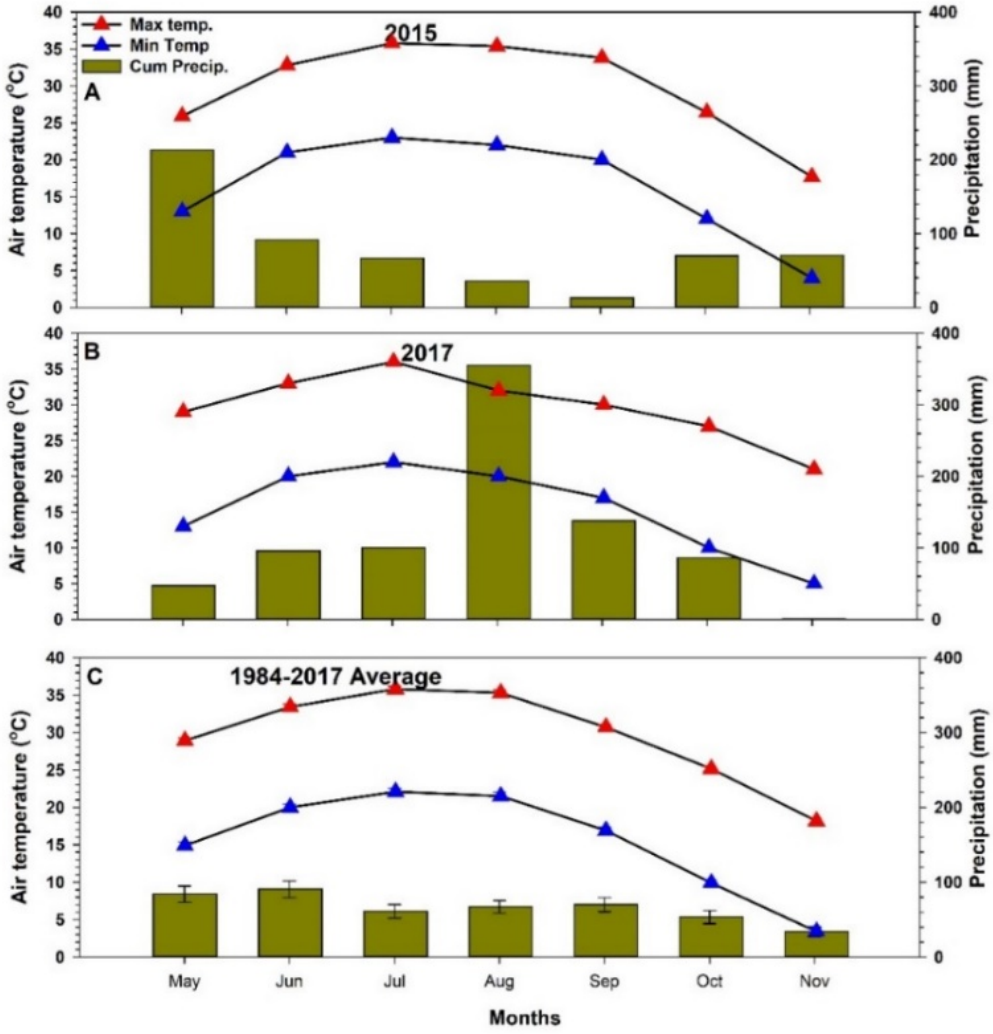

Figure 5.1. Average monthly maximum air temperature, monthly minimum air temperature, and cumulative precipitation for (A) 2015 (B) 2017 and (D) 1984-2017 (2011 was excluded). Error bars are the standard error of the mean.

Stalk Density and Diameter

In 2017, with-in season stalk density and stalk diameter at harvest were not affected by irrigation, crop genotype, and their interaction. The average stalk diameter of

at harvest was 15.3 ± 0.49 mm. Average stalk density was 17 stalks m^{-2} a month after planting. However, it decreased to 14.5 stalks m^{-2} (~14% less) after 50 days of planting and final stalk density was ~13.5 stalks m^{-2}. This reduction in tiller numbers may have been due to self-thinning of the weaker tillers during the early vegetative growth period. A study conducted in Pecos, an arid region of Texas, reported stem diameter of 34 mm and 36 mm for ES 5140 and ES 5200 respectively in irrigated growing condition (Enciso et al., 2019). The same genotypes in our experiment produced thinner stalks which may be due to higher tiller density at our study site than in Pecos (6.4 stalks m^{-2}). Reduced stem diameter was reported by Snider et al., (2012) in Alabama when seeding rate of biomass sorghum was increased. The stem diameter reported in their study (16-24 mm) was comparable to the stalk diameter observed in our study. Plant available soil moisture can significantly affect stalk density in semi-arid growing conditions (Berenguer and Faci, 2001; Tang et al., 2018). In 2017, irrigation and above-average precipitation provided adequate soil moisture at our study site. However, the sugarcane aphid infestation might have influenced stalk growth and development. The studies cited above did not report any major pest infestation.

Table 5.1. Analysis of variance for crop growth parameters of energy sorghum affected by genotype, irrigation, and growth stage. Results are presented for plant growing season 2015 and 2017

Source	Stalk density	Plant height	Leaf area index
2015			
Irrigation	-	**	**
Genotype	-	NS	NS
Irrigation x Genotype	-	NS	NS
Growth Stage	-	**	**
Genotype x Growth Stage	-	NS	NS
Irrigation x Genotype x Growth Stage	-	NS	NS
2017			
Irrigation	NS	NS	NS
Genotype	NS	NS	*
Irrigation x Genotype	NS	NS	NS
Growth Stage	**	**	**
Genotype x Growth Stage	NS	NS	NS
Irrigation x Genotype x Growth Stage	NS	NS	NS

* significant at $p < 0.05$, ** significant at $p<0.01$, and NS: non-significant at $p = 0.05$

Plant Height and Leaf Area Index

In 2015, plant height and leaf area development of both hybrids were similar early in the growing season in both irrigation treatments except ES 5140 which had slightly lower LAI (Figure 5.2A and B). As the season progressed, irrigation treatment significantly affected both plant height and LAI development ($p \leq 0.01$) (Table 5.1). Plant height reached its peak in early October in both low and high irrigation treatments. Final average plant height at harvest was 242 ± 1.6 cm in high irrigation treatment and 186 ± 1.9 cm in low irrigation treatment. In low irrigation treatment, LAI reached a maximum value of ~3 during the first week of August and did not increase for the remaining growing season. In high irrigation treatment, LAI continued to increase until

late September. An average LAI of 4.5 ± 0.1 was recorded on 25 September in high irrigation plots.

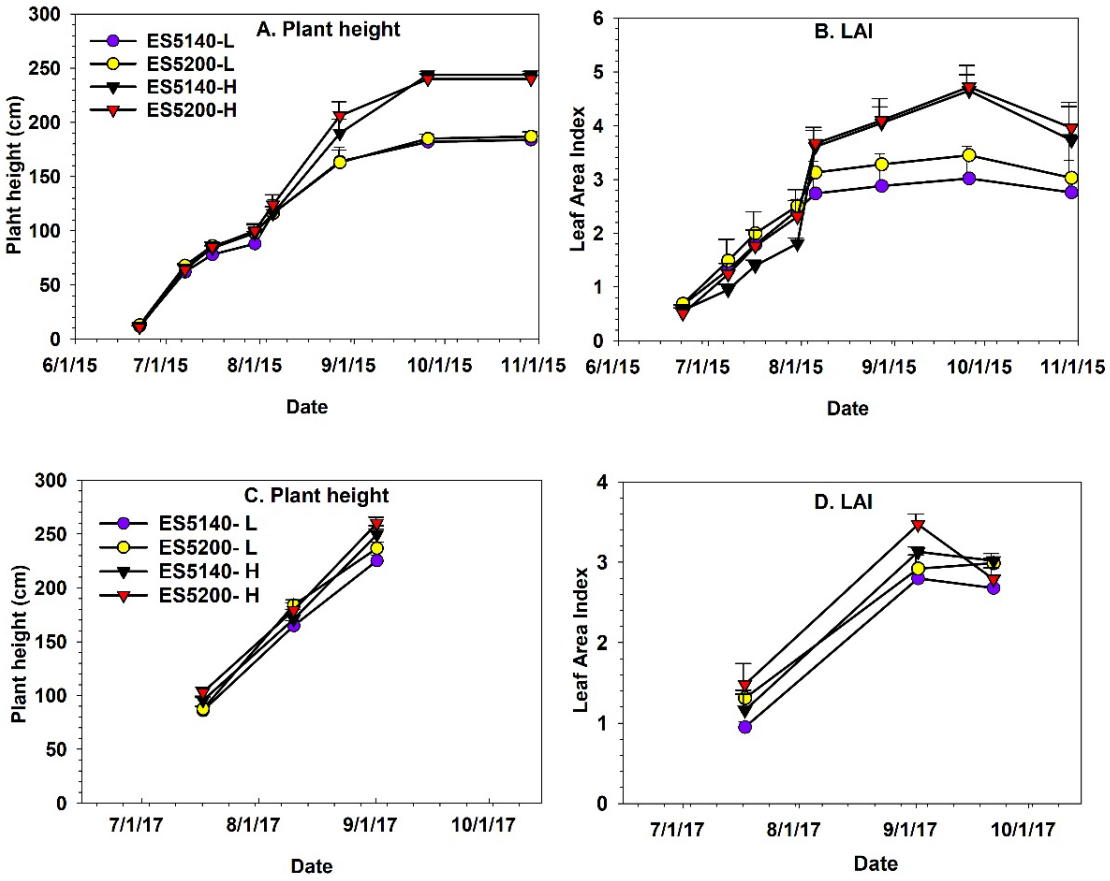

Figure 5.2. Plant growth characteristics (plant height and leaf area index) of energy sorghum hybrids in 2015 (A and B) and 2017 (C and D). Error bars are the standard error or the mean. L and H indicates low and high irrigation treatments respectively.

In 2017, plant height and LAI measurements were taken only three times during the crop growing season. Unlike 2015, final LAI recorded on 21 September in 2017 was similar in both irrigation treatments (2.9 ± 0.1 in high irrigation and 2.8 ± 0.1 in low irrigation). Plants were significantly taller in 2017 compared to 2015. For example, the plant height recorded on 1 September 2017 in high irrigation treatment was 254 ± 5.73

cm. Around the same time in 2015 (27 August), average plant height was 198 ± 5.79 cm. Similarly, average plant height was 231 ± 4.63 cm in low irrigation treatment on 1 September 2017 and 164 ± 5.6 cm on 27 August 2015.

Among the experimental years, 2017 was a wet year (Fig 5.1). Adequate moisture and added irrigation resulted in similar crop growth and development in high and low irrigation treatments in 2017. However, sugarcane aphid infestation caused leaf chlorosis and necrosis of lower leaves which reduced the overall green leaf area. Sugary substances on the leaves led to black mold growth on leaves which limited light absorption needed for photosynthesis. In addition, a hail storm during mid-October also damaged the remaining green leaves. Plant height values in our study compares well with other studies using biomass sorghum hybrids. A study using ES 5140 and ES 5200 reported an average plant height of 2.35 m in Weslaco, Texas and 1.35 m in Pecos, Texas (Enciso et al., 2019). Plants were shorter in the drier Pecos climate. Snider et al., (2012) reported plant height of biomass sorghum varying from 3 to 4.5 m in Alabama.

Figure 5.3 presents plant height plotted against corresponding LAI in 2015 and 2017. A strong linear relationship was observed between plant height and LAI (R^2 = 0.82). This empirical relationship between height and LAI showed that plant height could be used as an indirect method to estimate LAI. Little information is available in the literature about plant height-LAI relationship in energy sorghum. We recommend further studies with additional hybrids, row spacing and planting densities to test the relation between plant height and LAI of energy sorghum.

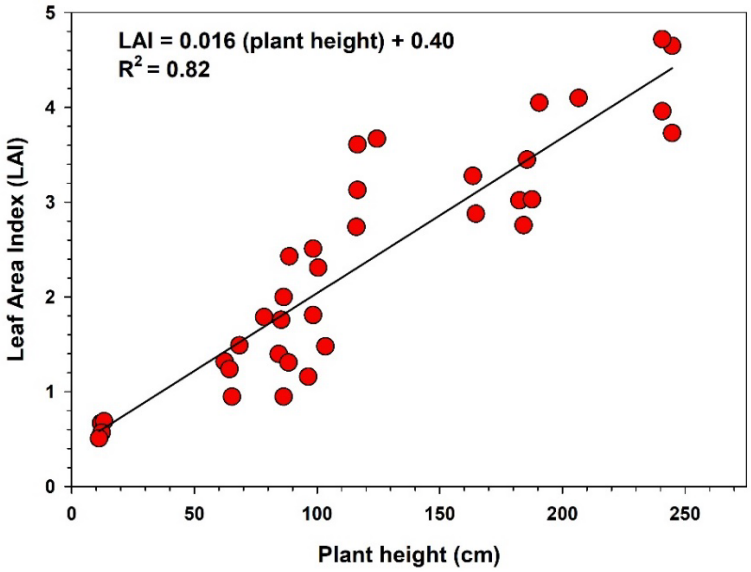

Figure 5.3. Relationship between leaf area index (LAI) and plant height of energy sorghum hybrids.

Normalized Difference Vegetation Index

Figure 5.4 presents NDVI plotted against corresponding LAI in 2015 and 2017. The relationship between NDVI and LAI was exponential in nature with an R^2 of 0.82. The NDVI increased as canopy developed, but remained unchanged after LAI was ≥ 2.5. For majority of crops, absorption of red-light peaks above 95% and reflectance becomes less than 5% as LAI is 2.5 or above (Hunt et al., 2014; Kross et al., 2015). Hence any further increase in LAI will not cause significant changes in NDVI. Shafian et al. (2018) reported that NDVI became invariant to changes in LAI above 2.5 in grain sorghum. Many other studies have reported similar exponential relationship between NDVI and LAI in row crops (Lee et al., 2017; Lelong et al., 2008; Zhang et al., 2006). The NDVI is a widely used vegetation index to estimate LAI and biomass yield (Foster et al., 2017; Freeman et al., 2007). The strong relationship between NDVI and LAI that we observed

in energy sorghum points to the utility of this index for non-destructive measurements of plant biophysical parameters and modeling applications.

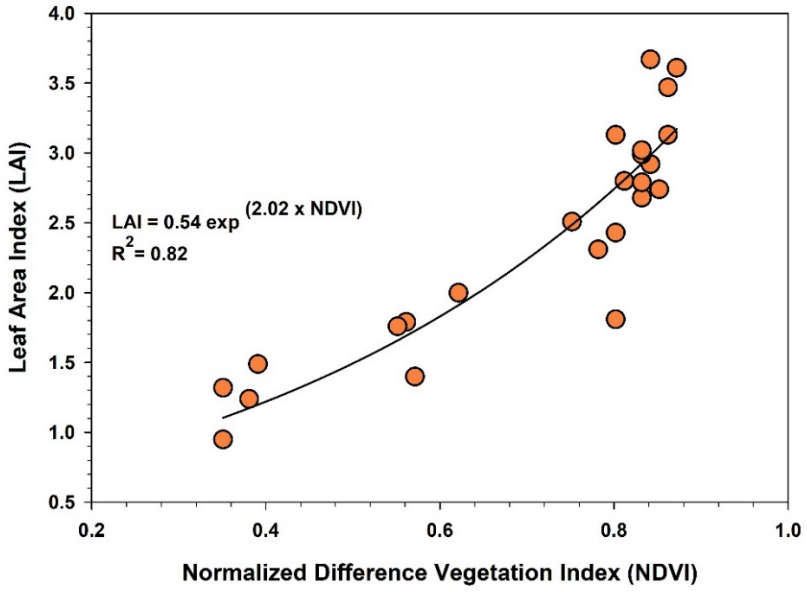

Figure 5.4. Relationship between leaf area index (LAI) and normalized difference vegetation index (NDVI) of energy sorghum hybrids. Each point represents the average value for individual plots.

Intercepted Photosynthetically Active Radiation and Light Extinction Coefficient

Canopy level photosynthesis is driven by *f*IPAR. A strong polynomial relationship ($R^2 = 0.82$) was observed between *f*IPAR and LAI of energy sorghum (Figure 5.5). Crop canopy intercepted about 50% of total PAR when LAI was about 1.5. As LAI approached 3, nearly 80 % of PAR was intercepted. Further increase in LAI did not increase *f*IPAR. Similar relationship was reported in biomass sorghum and miscanthus where more than 90% PAR was intercepted by canopy when LAI was 4 or higher (Meki et al., 2017; Vargas et al., 2002). The light extinction coefficient (k), estimated as the slope of the relationship between relative light transmission and LAI

(Figure 5.6), was similar for both hybrids. Previous studies have shown that the canopy photosynthesis is the highest for plants with lower k as more light penetrate to deeper layers (Hikosaka and Hirose, 1997). In those plants, as PAR is distributed more homogenously within the canopy, overall photosynthesis will increase especially when LAI is high. The findings related to PAR absorption and k presented in this study showed that the energy sorghum hybrids ES 5140 and ES 5200 are structurally adapted to maximize light absorption. The *k* values in our study also compared well with the values reported for biomass sorghum hybrids (*k* = 0.43 - 0.53) and corn (*k* = 0.39) (Li et al., 2018; Meki et al., 2017).

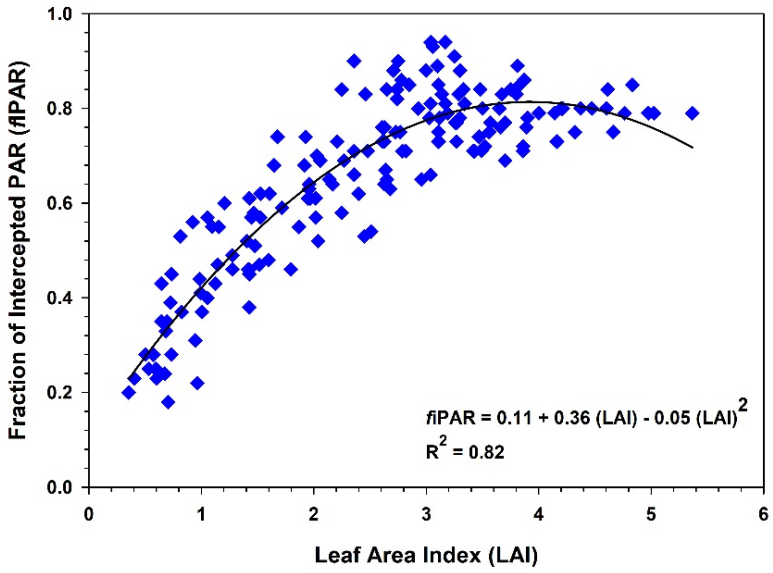

Figure 5.5. Relationship between leaf area index (LAI) and fraction of intercepted PAR of energy sorghum. Data include 2015 and 2017 growing seasons.

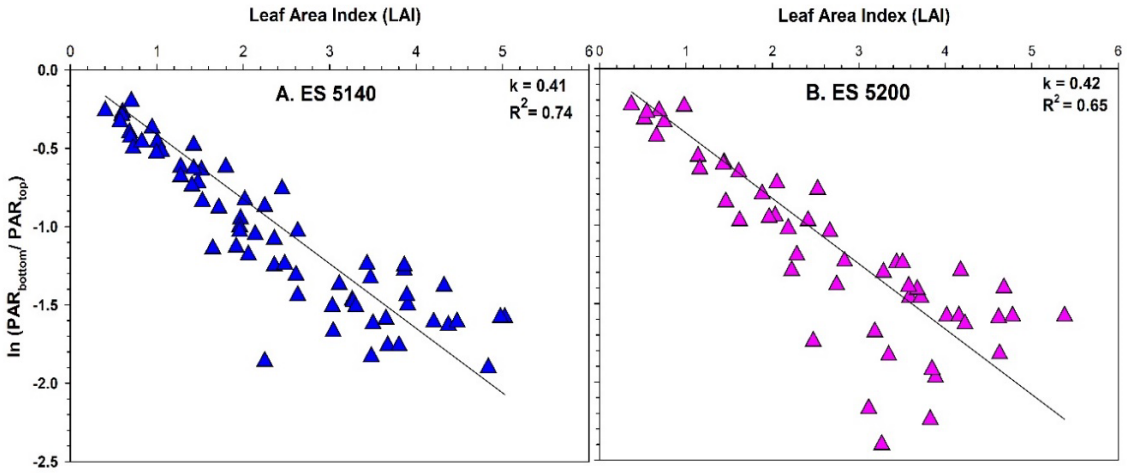

Figure 5.6. Relationship between leaf area index (LAI) and fraction of intercepted PAR of energy sorghum hybrids. *k* is slope of the line representing light extinction coefficient.

Biomass Yield

In 2015, additional irrigation resulted in almost double biomass production in high irrigation treatment (40.55 ± 1.26 t ha^{-1}) compared to low irrigation (20.39 ± 2.02 t ha^{-1}) and both hybrids yielded similarly within each irrigation treatment (Figure 5.7A). Although 2017 was a wet year, sugarcane aphids caused significant growth decline of both hybrids that year (discussed previously). There was no significant difference ($P > 0.05$) between biomass yields in high (average of 25.11 ± 2.49) and low irrigation (average of 21.53 ± 1.67) treatments. However, ES 5200 has higher dry biomass than ES 5140 in both high and low irrigation treatments (Figure 5.7B). One of the contributing factors could be that ES 5200 had higher stalk height (height from ground level to the collar of flag leaf) at harvest (334 ± 4.6 cm) than ES 5140 (323 ± 5.1 cm) in 2017 (unpublished data). Additionally, the LAI of ES 5200 was higher than ES 5140 although it the difference was not statistically significant. The biomass yield observed in our study

compares well with reported values in the literature. Studies have reported biomass yield of energy sorghums in the semi-arid Texas High Plains varying from 12 t ha^{-1} to 32 t ha^{-1} in response to irrigation and precipitation (Hao et al., 2014; Rooney et al., 2007; Tamang et al., 2011). A study in Temple, Texas reported biomass yield of 37.4 t ha^{-1} for energy sorghum hybrids (Meki et al., 2017). Yimam et al. (2015) reported biomass yield of ES 5200 varying from 4.4 - 32.5 t ha^{-1} depending on growing season precipitation in Oklahoma. Chavez et al. (2019) reported similar biomass yield of ES 5200 (32.8 t ha^{-1}) and ES 5140 (28 t ha^{-1}) as in our study in South Texas.

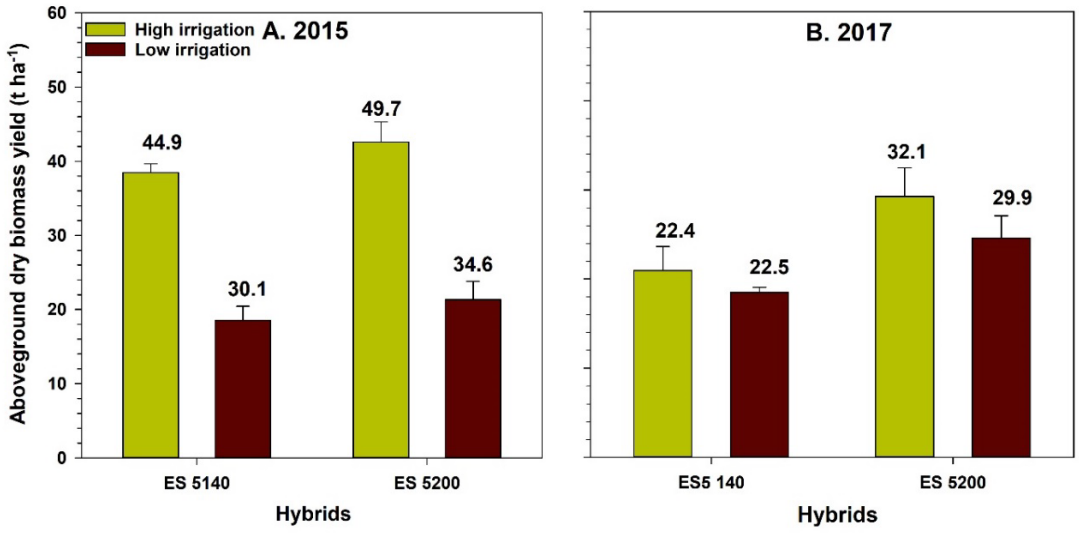

Figure 5.7. Aboveground dry biomass yield of energy sorghum hybrids at harvest in 2015 and 2017 growing season. Error bars in the bar graph are the standard error of the mean. Numbers on top of the bars shows the water use efficiency.

Water use efficiency (WUE), defined as the kg of aboveground dry biomass produced per hectare per mm of total water supply (rainfall and irrigation), was 47.26 kg ha^{-1} mm^{-1} in high irrigation plots and 33.1 kg ha^{-1} mm^{-1} in low irrigation plots in 2015.

In 2017, crop cultivar showed an effect on WUE (30.68 kg ha $^{-1}$ mm^{-1} in ES 5200) and (22.4 kg ha $^{-1}$ mm^{-1} in ES 5100). In a study conducted in Stillwater, Oklahoma, seasonal evapotranspiration (ET) based WUE estimates of biomass sorghum ranged from 9 - 49 kg ha^{-1} mm^{-1} (Yimam et al., 2015). Enciso et al. (2019) reported WUE ranging from 34.9- 58.7 kg ha^{-1} mm^{-1} in and Weslaco, Texas.

Biomass Composition

Plant tissue composition plays an important role in determining quantity of biofuel production. Table 5.2 summarizes the tissue composition of energy sorghum stem and leaves collected at harvest in 2017. Leaf tissues had higher cellulose (38%) and lignin (23-25%) contents compared to stem tissue (30-31% cellulose and 20% lignin). Hemicellulose contents was similar in leaf and stem tissues. Cellulose and hemicellulose content reported here are comparable to tissue compositions for energy sorghums reported in the literatures (Table 5.2). However, lignin content in our study is significantly higher than other studies. Crop cultivar, growth stage, growing environment, and management factors are some of the important factors affecting plant tissue composition. Additionally, method of compositional analysis also affects tissue component fractions (Hatfield and Fukushima, 2005). Early drying and senescence of leaves due to insect pest and abiotic stress, low fertility, and harvest after frost events may have increased the tissue lignin in our study.

Table 5.2. Stem, leaf, and inflorescence tissue composition of energy sorghum grown in Chillicothe Texas during 2015 and 2017. The values are presented as means ± standard deviation.

	Cellulose (%)	Hemi-cellulose (%)	Lignin (%)
Stem			
ES 5140	30.4±0.61	18.1±0.75	20.4±1.93
ES 5200	31.7±1.20	17.3±3.07	20.9±2.08
Leaf			
ES 5140	38.0±0.61	19.8±0.14	25.2±2.91
ES 5200	38.1±0.82	19.2±0.28	23.9±1.90
Literatures			
Rooney et. al, 2007[a]	29.3	26.3	7.6
Campi et al., 2016[b]	32.65	24.8	7.57
Nagaiah et al., 2012[c]	27-52	19-23	6-8
Jung et al., 2015[d]	31-35	23	17-20
Stefaniak et al., 2012[a]	21.3-37.7	11.6-20.4	8.9-20.6

Study locations: [a] Texas, USA [b] Trinitapoli, Italy [c] Hyderabad, India [d] Nigeria and Sudan

CONCLUSIONS

Two energy sorghum hybrids were evaluated under high and low irrigation in the semi-arid Texas Rolling Plains for their canopy development characteristics and biomass yield. Growing season irrigation affected canopy development parameters such as plant height, LAI and biomass yield in the dry year (2015). In the wet year, canopy development parameters and biomass were similar in both irrigation treatments; however, sugarcane aphid infestation caused yield decline. Both hybrids are structurally adapted to maximize canopy light interception as indicated by lower light extension coefficients (k) (0.41 in ES 5100 and 0.42 in ES 5200). Among the hybrids, ES 5200 had higher LAI, stalk height and biomass yield in the year with higher precipitation. Water use efficiency ranged from 22.4 – 47.26 kg ha^{-1} mm^{-1}. Among the two hybrids, ES 5200 showed relatively higher WUE (36.6 kg ha^{-1} mm^{-1}) than ES 5140 (30 kg ha^{-1} mm^{-1}).

CHAPTER VI

SUMMARY

Growing season water supply is a major limiting factor for biomass production in the Texas Rolling Plains. Significant portion of total land area in the region is categorized as marginal land therefore not suitable for agricultural use. Energy cane (*Saccharum spp*. hybrids) and biomass sorghum (*Sorghum bicolor* L. Moench) are high biomass yielding feedstock crops suitable for biomass production in the marginal lands. A study was conducted in Chillicothe, Texas from 2015 to 2017 to evaluate growth and yield performance of energy cane genotypes, model growth and biomass yield using crop modeling tool, simulate yield in future climatic conditions of increasing temperature and decreasing precipitation, and evaluate growth and biomass yield of two biomass sorghum hybrids. Experiment was laid out in a split plot design with irrigation as main plot factor and genotypes as the subplot factor. Experimental plots were irrigated to minimize the effect of severe drought. Low irrigation plots received 32-37% less irrigation water during feedstocks growing season. Energy cane plots were established in 2105 using second generation four energy cane genotypes (TUS11-62, TUS11-58, TCP10-4928, and Ho 02-113) whereas annual energy sorghum plots were established in 2015 and 2017. Plant growth data were collected from plant cane (in 2015), first ratoon (in 2016), and second ratoon (in 2017) from energy canes and plantings in 2015 and 2017 from energy sorghum. Separate energycane plots were established in 2016 using same genotypes using only high irrigation treatment arranged in randomized complete block design (RCBD).

Although growth characteristics (height, stalk density, and leaf area index) differed among genotypes, dry biomass yield at harvest was not significantly different among genotypes in the first and second ratoons. However, in the plant cane season (2016), TUS11-58 had the highest yield. The average biomass yield of plant cane, first, and second ratoons were 20.16, 40.37, and 26.4 t ha^{-1} respectively. A well-established root system as well as a longer growing period of ratoon (~8 months) compared to plant cane (~5.5 months) increased biomass yields in the first ratoon. However, low temperatures (-14 to -16°C) during the dormant phase prior to the emergence of second ratoon resulted in lower biomass yield of the second ratoon. The results indicate that low temperature tolerance as well as effective growing season duration are key factors regulating feedstock biomass yield in higher latitudes such as the Texas Rolling Plains.

A modeling experiment was conducted to simulate the biomass yield and growth characteristics of energy cane genotype used in the field experiment. The DSSAT - CANEGRO model was used to simulate the growth and yield performance of energycane genotypes. The model was adapted by optimizing the genotypic traits for biomass accumulation and partitioning, canopy-leaf, and tiller phenology characteristics. Overall results showed that the model was able to simulate final stalk height and aboveground biomass with percent error (PE) less than ±15% in the plant cane and first ratoon cycle. However, the model significantly overestimated stalk height and biomass in the second ratoon cycle. Similar results were observed when the model was used for simulating the growth of other energy cane genotypes in the experiment (TUS11-62, TUS11-58, and TCP10-4928). Low temperature during the overwintering period in the

second ratoon cycle (2017) significantly affected the regrowth and aboveground biomass production of all energy cane hybrids. Model may also serve as an effective tool to simulate the effect of changing temperature, precipitation, and irrigation treatments. However, inclusion of soil nutrient balance components, subsequent yield loss in ratoon due to weed, disease, pest would improve the estimation. Similarly, ability of model to run for multiple years from same planting and an account for rhizome ant tiller mortality due to sever winter in future would improve the accuracy of model prediction.

Evaluated CANEGRO Sugarcane model was used to simulate the impact of changing climate on energy cane biomass production in the Texas Rolling Plains. Effect of increase in daily maximum and minimum air temperatures, decrease in daily precipitation, and interaction between increasing temperature and decreasing precipitation were simulated from the baseline weather data during 1984-2017. Both increasing temperature and decreasing precipitation gradually reduced biomass yield. Increasing temperature from 0.5 ºC - 2ºC reduced biomass yield of plant cane by 4 - 17% in dry years, 3%- 14% in normal and wet years. Similarly, warming temperature decreased biomass yield of ratoon by 3% - 13%, increased biomass yield by 3% in normal years, and increased yield by 1% - 7%. Decrease in daily precipitation from 5% - 20% decreased the biomass yield of plant cane by 1% - 16% in dry years, 2% - 17% in normal years, and 1% - 18% in wet years. Similarly, decrease in daily precipitation from 5% - 20% decreased the biomass yield of ratoon by 2% - 17% in dry years, 2% - 20% in normal years, and 1% - 17% in wet years. When increase in temperature was combined with the decrease in precipitation, increase in temperature by 2°C and daily precipitation

decreased by 20% resulted higher biomass yield loss in both plant cane and ratoon. Maximum biomass yield loss ranged from 18% -24% of ratoon and 18% - 31% of plant cane in dry years. Thus, simulation modeling works as a guide to understand the effect of climatic variability on biomass yield of energycane in the future.

Energy sorghum study was conducted to evaluate the growth and yield performance of two energy sorghum hybrids. Light interception characteristics of the hybrids were also studied. Irrigation levels had significant effect on biomass yield in 2015. Additional water input in high irrigation treatment increased the plant height by 30%, water use efficiency (WUE) by 42%, and final biomass by 100% (40.55 t ha^{-1}) compared to low irrigation. In 2017, growth and biomass yield were similar in irrigation treatments; however, ES 5200 had higher biomass at harvest (26.9 t ha^{-1}). The low yield in 2017 was due to sugarcane aphid (*Melanaphis sacchari*) infestation. Plant height and leaf area index (LAI) were strongly related ($R^2 = 0.82$). An exponential relationship was observed between LAI and normalized difference vegetation index ($R^2 = 0.82$). Both sorghum hybrids showed similar light interception characteristics (light extinction coefficient of 0.41 in ES 5140 and 0.42 in ES 5022). Results from this study showed that energy sorghum has the potential to yield higher biomass in the Texas Rolling Plains with irrigation.

REFERENCES

Adhikari, P., S. Ale, J. P. Bordovsky, K. R. Thorp, N. R. Modala, N. Rajan, and E. Barnes. 2016. Simulating future climate change impacts on seed cotton yield in the Texas High Plains using the CSM-CROPGRO-Cotton model. *Agric Water Manage, 164*, 317-330.

Asseng, S., F. Ewert, P. Martre, R. P. Rötter, D. B. Lobell, D. Cammarano, B. A. Kimball, M. J. Ottman, G. Wall, and J. W. White. 2015. Rising temperatures reduce global wheat production. *Nature Climate Change, 5*(2), 143.

Attia, A., and N. Rajan. 2016. Within-season growth and spectral reflectance of cotton and their relation to lint yield. *Crop Sci, 56*(5), 2688-2701.

Attia, A., N. Rajan, S. S. Nair, P. B. DeLaune, Q. Xue, A. M. Ibrahim, and D. B. Hays. 2016a. Modeling cotton lint yield and water use efficiency responses to irrigation scheduling using Cotton2K. *Agron J, 108*(4), 1614-1623.

Attia, A., N. Rajan, Q. Xue, S. Nair, A. Ibrahim, and D. Hays. 2016b. Application of DSSAT-CERES-Wheat model to simulate winter wheat response to irrigation management in the Texas High Plains. *Agric Water Manage, 165*, 50-60.

Bai, Z., S. Mao, Y. Han, L. Feng, G. Wang, B. Yang, X. Zhi, Z. Fan, Y. Lei, and W. Du. 2016. Study on light interception and biomass production of different cotton cultivars. *PloS One, 11*(5), e0156335. doi:10.1371/journal.pone.0156335

Begum, M., and M. Islam. 2012. Effect of drought stress on yield and yield components of sugarcane. *Agroforestry and Environment, 6*(1), 105-109.

Bell, M., and A. Garside. 2005. Shoot and stalk dynamics and the yield of sugarcane crops in tropical and subtropical Queensland, Australia. *Field Crops Res, 92*(2-3), 231-248.

Berenguer, M., and J. Faci. 2001. Sorghum (Sorghum bicolor L. Moench) yield compensation processes under different plant densities and variable water supply. *European Journal of Agronomy, 15*(1), 43-55.

Bischoff, K., K. Gravois, T. Reagan, J. Hoy, C. Kimbeng, C. LaBorde, and G. Hawkins. 2008. Registration of 'L 79-1002'sugarcane. *Plant Registrations, 2*(3), 211-217.

Boote, K. J., M. J. Kropff, and P. S. Bindraban. 2001. Physiology and modelling of traits in crop plants: implications for genetic improvement. *Agricultural Systems, 70*(2-3), 395-420. doi:10.1016/S0308-521x(01)00053-1

Boote, K. J., M. I. Minguez, and F. Sau. 2002. Adapting the CROPGRO legume model to simulate growth of faba bean. *Agron J, 94*(4), 743-756.

Boschiero, B. N., Q. de Castro, S. Gustavo, A. E. Quintela da Rocha, H. C. Junqueira Franco, J. L. Nunes Carvalho, H. L. Soriano, J. Alves dos Santos, J. A. Bressiani, and O. T. Kölln. 2019. Biomass production and nutrient removal of energy cane genotypes in northeastern Brazil. *Crop Sci, 59*(1), 379-391.

Campi, P., A. Navarro, A. D. Palumbo, F. Modugno, C. Vitti, and M. Mastrorilli. 2016. Energy of biomass sorghum irrigated with reclaimed wastewaters. *European Journal of Agronomy, 76*, 176-185.

Carter, C. E., J. E. Irvine, V. McDaniel, and J. Dunckelman. 1985. Yield response of sugarcane to stalk density and subsurface drainage treatments. *Trans ASAE, 28*(1), 172-178. doi:10.13031/2013.32223

Carvalho, J. L. N., R. Otto, H. C. J. Franco, and P. C. O. Trivelin. 2013. Input of sugarcane post-harvest residues into the soil. *Scientia Agricola, 70*(5), 336-344.

Casler, M. D., S. Sosa, L. Hoffman, H. Mayton, C. Ernst, P. R. Adler, A. R. Boe, and S. A. Bonos. 2017. Biomass yield of switchgrass cultivars under high-versus low-input conditions. *Crop Sci, 57*(2), 821-832.

Chavez, J. C., J. Enciso, G. Ganjegunte, N. Rajan, J. Jifon, and V. P. Singh. 2019. Growth response and productivity of sorghum for bioenergy production in south Texas. *Transactions of the ASAB, 62*(5), 1207-1218.

Chavez, J. C., J. Enciso, M. N. Meki, J. Jeong, and V. P. Singh. 2018. Simulation of energy sorghum under limited irrigation levels using the EPIC model. *Transactions of the ASABE, 61*(1), 121-131.

Chiluwal, A., H. P. Singh, K. Sahoo, R. Paudel, W. F. Whithead, and B. P. Singh. 2019. Napiergrass has dual use as biofuel beedstock and animal fodder. *Agron J, 111*(4), 1752-1759.

Chiluwal, A., H. P. Singh, U. Sainju, B. Khanal, W. F. Whitehead, and B. P. Singh. 2018. Spacing effect on energy cane growth, physiology, and biomass yield. *Crop Sci, 58*(3), 1371-1384.

Chiu, Y. W., B. Walseth, and S. Suh. 2009. Water embodied in bioethanol in the United States. *Environ Sci Technol, 43*(8), 2688-2692. doi:10.1021/es8031067

Coelho, A. P., A. B. Dalri, J. A. Fischer Filho, R. T. d. Faria, L. S. Silva, and R. P. Gomes. 2020. Calibration and evaluation of the DSSAT/CANEGRO model for sugarcane cultivars under irrigation managements. *Revista Brasileira de Engenharia Agrícola e Ambiental, 24*(1), 52-58.

da Silva, J. A. 2017. The importance of the wild cane Saccharum spontaneum for bioenergy genetic breeding. *Sugar Tech, 19*(3), 229-240.

da Silva, J. A., N. Solis-Gracia, J. Jifon, S. C. Souza, and K. K. Mandadi. 2020. Use of bioreactors for large-scale multiplication of sugarcane (Saccharum spp.), energy cane (Saccharum spp.), and related species. *In Vitro Cellular Developmental Biology-Plant*. doi:10.1007/s11627-019-10046-y

da Silva, J. A. G., P. M. d. A. Costa, T. G. Marconi, E. J. d. S. Barreto, N. Solís-Gracia, J.-W. Park, and N. C. Glynn. 2018. Agronomic and molecular characterization of wild germplasm Saccharum spontaneum for sugarcane and energycane breeding purposes. *Scientia Agricola, 75*(4), 329-338.

da Silveira, L. C. I., B. P. Brasileiro, V. Kist, H. Weber, E. Daros, L. A. Peternelli, and M. H. P. Barbosa. 2015. Selection strategy in families of energy cane based on biomass production and quality traits. *Euphytica, 204*(2), 443-455.

Das, S., K. Teuffer, C. R. Stoof, M. F. Walter, M. T. Walter, T. S. Steenhuis, and B. K. Richards. 2018. Perennial grass bioenergy cropping on wet marginal land: impacts on soil properties, soil organic carbon, and biomass during initial establishment. *BioEnergy Research, 11*(2), 262-276. doi:10.1007/s12155-018-9893-4

de Carvalho, A. L., R. S. C. Menezes, R. S. Nóbrega, A. de Siqueira Pinto, J. P. H. B. Ometto, C. von Randow, and A. Giarolla. 2015. Impact of climate changes on potential sugarcane yield in Pernambuco, northeastern region of Brazil. *Renewable Energy, 78*, 26-34.

de Carvalho, V. S., and K. Tannous. 2017. Thermal decomposition kinetics modeling of energy cane Saccharum robustum. *Thermochimica Acta, 657*, 56-65.

de Silva, A., and W. de Costa. 2004. Varietal variation in growth, physiology and yield of sugarcane under two contrasting water regimes. *Tropical Agricultural Research, 16*, 1-12.

DOE. 2019a. Corn production and portion used for fuel ethanol. Retrieved from https://www.afdc.energy.gov/data/10339

DOE. 2019b. Renewable fuel standard. Retrieved from https://afdc.energy.gov/laws/RFS

Enciso, J., J. C. Chavez, G. Ganjegunte, and S. D. Zapata. 2019. Energy sorghum production under arid and semi-arid environments of Texas. *Water, 11*(7), 1344.

Energy Information Administration (EIA), 2018. Renewable energy. Retrieved from https://www.eia.gov/totalenergy/data/monthly/index.php#renewable

EPA. 2018a. Final renewable fuel standards for 2019 and the biomass-based diesel volume for 2020. Retrieved from https://www.epa.gov/renewable-fuel-standard-program/final-renewable-fuel-standards-2019-and-biomass-based-diesel-volume

EPA. 2018b. Overview for renewable fuel standard. Retrieved from https://www.epa.gov/renewable-fuel-standard-program/overview-renewable-fuel-standard

Erickson, J. E., A. Soikaew, L. E. Sollenberger, and J. M. Bennett. 2012. Water use and water-use efficiency of three perennial bioenergy grass crops in Florida. *Agriculture, 2*(4), 325-338.

Fageria, N., A. Moreira, L. Moraes, A. L. Hale, and R. P. Viator. 2013. Sugarcane and energycane. In B. P. Singh (Ed.), *Biofuel Crops: Production, Physiology and Genetics* (pp. 151-171). Boston, USA: CAB International

FAO. 2019. FAOSTAT Statistical Database. Retrieved from http://www.fao.org/faostat/en/#data/QC

Fedenko, J. R., J. E. Erickson, K. R. Woodard, L. E. Sollenberger, J. M. Vendramini, R. A. Gilbert, Z. R. Helsel, and G. F. Peter. 2013. Biomass production and composition of perennial grasses grown for bioenergy in a subtropical climate across Florida, USA. *BioEnergy Research, 6*(3), 1082-1093.

Fike, J. H., D. J. Parrish, D. D. Wolf, J. A. Balasko, J. T. Green Jr, M. Rasnake, and J. H. Reynolds. 2006. Long-term yield potential of switchgrass-for-biofuel systems. *Biomass Bioenergy, 30*(3), 198-206.

Fonteyne, S., H. Muylle, T. De Swaef, D. Reheul, I. Roldán-Ruiz, P. Lootens, and Products. 2016. How low can you go? Rhizome and shoot frost tolerance in miscanthus germplasm. *Industrial Crops and Products, 89*, 323-331.

Foster, A., V. Kakani, and J. Mosali. 2017. Estimation of bioenergy crop yield and N status by hyperspectral canopy reflectance and partial least square regression. *Precision Agriculture, 18*(2), 192-209.

Fouad, W. M., W. Hao, Y. Xiong, C. Steeves, S. K. Sandhu, and F. Altpeter. 2015. Generation of transgenic energy cane plants with integration of minimal transgene expression cassette. *Curr Pharm Biotechnol, 16*(5), 407-413.

Freeman, K. W., K. Girma, D. B. Arnall, R. W. Mullen, K. L. Martin, R. K. Teal, and W. R. Raun. 2007. By-plant prediction of corn forage biomass and nitrogen uptake at various growth stages using remote sensing and plant height. *Agron J, 99*(2), 530-536.

García, C. A., A. Fuentes, A. Hennecke, E. Riegelhaupt, F. Manzini, and O. Masera. 2011. Life-cycle greenhouse gas emissions and energy balances of sugarcane ethanol production in Mexico. *Applied Energy, 88*(6), 2088-2097.

Giamalva, M., S. Clark, and J. Stein. 1985. Conventional vs high fiber sugarcane. *American Society of Sugar Cane Technologists, 4*, 106-109.

Gordon, V. S., J. C. Comstock, H. S. Sandhu, R. A. Gilbert, S. G. Sood, P. Korndorfer, N. El-Hout, and R. Arundale. 2016. Registration of 'UFCP 87-0053'sugarcane for use as a biofuel feedstock. *Plant Registrations, 10*(3), 258-264.

Hale, A. L., E. O. Dufrene, T. L. Tew, Y.-B. Pan, R. P. Viator, P. M. White, J. C. Veremis, W. H. White, R. Cobill, and E. P. Richard. 2013. Registration of 'Ho 02-113'sugarcane. *Plant Registrations, 7*(1), 51-57.

Hao, B., Q. Xue, B. W. Bean, W. L. Rooney, and J. D. Becker. 2014. Biomass production, water and nitrogen use efficiency in photoperiod-sensitive sorghum in the Texas High Plains. *Biomass Bioenergy, 62*, 108-116.

Hatfield, R., and R. S. Fukushima. 2005. Can lignin be accurately measured? *Crop Sci, 45*(3), 832-839.

Hikosaka, K., and T. Hirose. 1997. Leaf angle as a strategy for light competition: Optimal and evolutionarily stable light-extinction coefficient within a leaf canopy. *Ecoscience, 4*(4), 501-507. doi:10.1080/11956860.1997.11682429

Hoffman, N., A. Singels, A. Patton, and S. Ramburan. 2018. Predicting genotypic differences in irrigated sugarcane yield using the CANEGRO model and independent trait parameter estimates. *European Journal of Agronomy, 96*, 13-21. doi:10.1016/j.eja.2018.01.005

Hoogenboom, G., C. H. Porter, V. Shelia, K. J. Boote, U. Singh, J. W. White, L. A. Hunt, R. Ogoshi, J. I. Lizaso, J. Koo, S. Asseng, A. Singels, L. P. Moreno, and J. W. Jones. 2019. Decision Support System for Agrotechnology Transfer (DSSAT) (Ver 4.7.5). DSSAT Foundation. Gainesville, Florida, USA. Retrieved from https://DSSAT.net

Huang, J., M. Ji, Y. Xie, S. Wang, Y. He, and J. Ran. 2016. Global semi-arid climate change over last 60 years. *Climate Dynamics, 46*(3), 1131-1150. doi:10.1007/s00382-015-2636-8

Huang, J. P., X. D. Guan, and F. Ji. 2012. Enhanced cold-season warming in semi-arid regions. *Atmospheric Chemistry & Physics Discussions, 12*(2), 5391–5398.

Hunt, E. R., C. S. Daughtry, S. B. Mirsky, and W. D. Hively. 2014. Remote sensing with simulated unmanned aircraft imagery for precision agriculture applications. *IEEE*

Journal of Selected Topics in Applied Earth Observations Remote Sensing, 7(11), 4566-4571.

iAIMS. 2020. iAIMS Climate Data. Retrieved from https://beaumont.tamu.edu/climaticdata/WeatherInfo.aspx?index=Info

Inman-Bamber, N. 1991. A growth model for sugar-cane based on a simple carbon balance and the CERES-Maize water balance. *South African Journal of Plant and Soil, 8*(2), 93-99.

Inman-Bamber, N., and G. Kiker. 1997. CANEGRO 3.10. DSSAT version 3.1 1998 distribution software. IBSNAT, University of Hawaii, Honolulu, Hawaii, USA.

Inman-Bamber, N. G. 1994. Temperature and seasonal effects on canopy development and light interception of sugarcane. *Field Crops Res, 36*(1), 41-51. doi:10.1016/0378-4290(94)90051-5

Jones, J. W., J. He, K. J. Boote, P. Wilkens, C. Porter, and Z. Hu. 2011. Estimating DSSAT cropping system cultivar-specific parameters using Bayesian techniques. In L. R. Ahuja & L. Ma (Eds.), *Methods of Introducing System Models into Agricultural Research* (pp. 365-394).

Jones, J. W., G. Hoogenboom, C. H. Porter, K. J. Boote, W. D. Batchelor, L. A. Hunt, P. W. Wilkens, U. Singh, A. J. Gijsman, and J. T. Ritchie. 2003. The DSSAT cropping system model. *European Journal of Agronomy, 18*(3-4), 235-265. doi:10.1016/S1161-0301(02)00107-7

Jones, M. R., and A. Singels. 2018. Refining the CANEGRO model for improved simulation of climate change impacts on sugarcane. *European Journal of Agronomy, 100*, 76-86.

Jung, S.-J., S.-H. Kim, and I.-M. Chung. 2015. Comparison of lignin, cellulose, and hemicellulose contents for biofuels utilization among 4 types of lignocellulosic crops. *Biomass Bioenergy, 83*, 322-327.

Khan, N. A., R. Bedre, A. Parco, L. Bernaola, A. Hale, C. Kimbeng, M. Pontif, and N. Baisakh. 2013. Identification of cold-responsive genes in energycane for their use in genetic diversity analysis and future functional marker development. *Plant Sci, 211*, 122-131.

Kim, M., and D. F. Day. 2011. Composition of sugar cane, energy cane, and sweet sorghum suitable for ethanol production at Louisiana sugar mills. *Industrial Microbiology Biotechnology, 38*(7), 803-807.

Knoll, J. E., W. F. Anderson, E. P. Richard, J. Doran-Peterson, B. Baldwin, A. L. Hale, and R. P. Viator. 2013. Harvest date effects on biomass quality and ethanol yield of new energycane (Saccharum hyb.) genotypes in the Southeast USA. *Biomass Bioenergy, 56*, 147-156. doi:10.1016/j.biombioe.2013.04.018

Knoll, J. E., W. F. Anderson, T. C. Strickland, R. K. Hubbard, and R. Malik. 2012. Low-input production of biomass from perennial grasses in the coastal plain of Georgia, USA. *Bioenergy Research, 5*(1), 206-214.

Knox, J. W., J. R. Díaz, D. Nixon, and M. Mkhwanazi. 2010. A preliminary assessment of climate change impacts on sugarcane in Swaziland. *Agricultural Systems, 103*(2), 63-72.

Ko, J., S. J. Maas, R. J. Lascano, and D. Wanjura. 2005. Modification of the GRAMI model for cotton. *Agron J, 97*(5), 1374-1379.

Kross, A., H. McNairn, D. Lapen, M. Sunohara, and C. Champagne. 2015. Assessment of RapidEye vegetation indices for estimation of leaf area index and biomass in corn and soybean crops. *International Journal of Applied Earth Observation Geoinformation, 34*, 235-248.

Langholtz, M. H., B. J. Stokes, and L. M. Eaton. 2016. *2016 Billion-ton report: Advancing domestic resources for a thriving bioeconomy, volume 1: economic availability of feedstocks*. Oak Ridge, TN: Oak Ridge National Laboratory, LLC for the US Department of Energy.

Lee, B., H. Kwon, A. Miyata, S. Lindner, and J. Tenhunen. 2017. Evaluation of a phenology-dependent response method for estimating leaf area index of rice across climate gradients. *Remote Sensing, 9*(1). doi:ARTN 2010.3390/rs9010020

Lelong, C. C. D., P. Burger, G. Jubelin, B. Roux, S. Labbe, and F. Baret. 2008. Assessment of unmanned aerial vehicles imagery for quantitative monitoring of wheat crop in small plots. *Sensors, 8*(5), 3557-3585. doi:10.3390/s8053557

Leon, R. G., R. A. Gilbert, and J. C. Comstock. 2015. Energycane (spp. × L.) biomass production, reproduction, and weed risk assessment scoring in the humid tropics and subtropics. *Agron J, 107*(1). doi:10.2134/agronj14.0388

Li, J., R. Xie, K. Wang, P. Hou, B. Ming, G. Zhang, G. Liu, M. Wu, Z. Yang, and S. Li. 2018. Response of canopy structure, light interception and grain yield to plant density in maize. *The Journal of Agricultural Science, 156*(6), 785-794.

Long, D., B. R. Scanlon, L. Longuevergne, A. Y. Sun, D. N. Fernando, and H. Save. 2013. GRACE satellite monitoring of large depletion in water storage in response to the 2011 drought in Texas. *Geophys Res Lett, 40*(13), 3395-3401.

Marin, F. R., J. W. Jones, F. Royce, C. Suguitani, J. L. Donzeli, J. P. Wander Filho, and D. S. Nassif. 2011. Parameterization and evaluation of predictions of DSSAT/CANEGRO for Brazilian sugarcane. *Agron J, 103*(2), 304-315.

Marin, F. R., J. W. Jones, A. Singels, F. Royce, E. D. Assad, G. Q. Pellegrino, and F. Justino. 2012. Climate change impacts on sugarcane attainable yield in southern Brazil. *Clim Change, 117*(1-2), 227-239. doi:10.1007/s10584-012-0561-y

Matsuoka, S., J. Ferro, and P. Arruda. 2009. The Brazilian experience of sugarcane ethanol industry. *In Vitro Cellular Developmental Biology-Plant, 45*(3), 372-381.

Matsuoka, S., and A. A. Franco-Garcia. 2011. Sugarcane underground organs: going deep for sustainable production. *Tropical Plant Biology, 4*(1), 22-30.

Matsuoka, S., A. J. Kennedy, E. G. D. d. Santos, A. L. Tomazela, and L. C. S. Rubio. 2014. Energy cane: its concept, development, characteristics, and prospects. *Advances in Botany, 2014*, 1-13.

Matsuoka, S., and R. Stolf. 2012. Sugarcane tillering and ratooning: key factors for a profitable cropping. In *Sugarcane: Production, Cultivation and Uses* (Vol. 5, pp. 137-157): Nova Science Publishers, Inc.

Meki, M. N., R. M. Ogoshi, J. R. Kiniry, S. E. Crow, A. H. Youkhana, M. H. Nakahata, and K. Littlejohn. 2017. Performance evaluation of biomass sorghum in Hawaii and Texas. *Industrial Crops and Products, 103*, 257-266. doi:10.1016/j.indcrop.2017.04.014

Modala, N. R. 2014. *Assessing the impacts of climate change on cotton production in the Texas High Plains and Rolling Plains.* Doctoral dissertation. Texas A&M University, College Station, Texas. Retrieved from https://oaktrust.library.tamu.edu/handle/1969.1/154084

Modala, N. R., S. Ale, N. Rajan, C. L. Munster, P. B. DeLaune, K. R. Thorp, S. S. Nair, and E. M. Barnes. 2015. Evaluation of the CSM-CROPGRO-Cotton model for the Texas rolling plains region and simulation of deficit irrigation strategies for increasing water use efficiency. *Transactions of the ASABE, 58*(3), 685-696.

Muir, J. P., M. A. Sanderson, W. R. Ocumpaugh, R. M. Jones, and R. L. Reed. 2001. Biomass production of 'Alamo'switchgrass in response to nitrogen, phosphorus, and row spacing. *Agron J, 93*(4), 896-901.

Na, C. I., J. R. Fedenko, L. E. Sollenberger, and J. E. Erickson. 2016a. Harvest management affects biomass composition responses of C4 perennial bioenergy grasses in the humid subtropical USA. *Global Change Biology Bioenergy, 8*(6), 1150-1161.

Na, C. I., L. E. Sollenberger, J. E. Erickson, K. R. Woodard, M. S. Castillo, M. K. Mullenix, J. M. Vendramini, and M. L. Silveira. 2015. Management of perennial warm-season bioenergy grasses. II. Seasonal differences in elephantgrass and

energycane morphological characteristics affect responses to harvest frequency and timing. *BioEnergy Research, 8*(2), 618-626.

Na, C. I., L. E. Sollenberger, J. E. Erickson, K. R. Woodard, M. O. Wallau, and N. C. Krueger. 2014. Biomass yield and composition of perennial bioenergy grasses at harvests following a freeze event. *Agron J, 106*(6). doi:10.2134/agronj14.0324

Na, C. I., L. E. Sollenberger, J. R. Fedenko, J. E. Erickson, and K. R. Woodard. 2016b. Seasonal changes in chemical composition and leaf proportion of elephantgrass and energycane biomass. *Industrial Crops and Products, 94*, 107-116. doi:10.1016/j.indcrop.2016.07.009

Nagaiah, D., P. Srinivasa Rao, and R. Prakasham. 2012. High biomass sorghum as a potential raw material for biohydrogen production: a preliminary evaluation. *Current Trends in Biotechnology Pharmacy, 6*(2), 183-189.

Naik, S. N., V. V. Goud, P. K. Rout, and A. K. Dalai. 2010. Production of first and second generation biofuels: a comprehensive review. *Renewable and Sustainable Energy Reviews, 14*(2), 578-597.

NASA-POWER. 2020. POWER Data. Retrieved from https://power.larc.nasa.gov/data-access-viewer/

OECD/FAO. 2015. *OECD-FAO Agricultural Outlook 2015*. Paris: OECD Publishing.

Peixoto, M. d. M., P. C. Friesen, and R. F. Sage. 2015. Winter cold-tolerance thresholds in field-grown Miscanthus hybrid rhizomes. *Experimental Botany, 66*(14), 4415-4425.

Pokhrel, P., N. Rajan, and J. Jifon. 2019. *Biomass yield variation in energycane genotypes ss affected by ratoon*. Paper presented at the ASA, CSSA and SSSA International Annual Meetings (2019), San Antonio, Texas.

Pokhrel, P., N. Rajan, J. Jifon, D. Menefee, M. Mikeska, and D. Zapata. 2017. *Agronomic performance of newly developed lignocellulosic bioenergy crops in Texas.* Paper presented at the Texas Plant Protection Conference (2017), College Station, TX.

Propheter, J. L., S. A. Staggenborg, X. Wu, and D. Wang. 2010. Performance of annual and perennial biofuel crops: yield during the first two years. *Agron J, 102*(2). doi:10.2134/agronj2009.0301

Rajan, N., S. J. Maas, and S. Cui. 2013. Extreme drought effects on carbon dynamics of a semiarid pasture. *Agron J, 105*(6), 1749-1760. doi:10.2134/agronj2013.0112

Rajan, N., S. J. Maas, and S. Cui. 2015. Extreme drought effects on summer evapotranspiration and energy balance of a grassland in the Southern Great Plains. *Ecohydrology, 8*(7), 1194-1204.

RFA. 2018a. 2017 U.S. ethanol exports and imports statistical summary. Retrieved from https://ethanolrfa.org/wp-content/uploads/2019/03/2018-US-Ethanol-Trade-Statistics-Summary.pdf

RFA. 2018b. Ethanol industry outlook. Retrieved from https://ethanolrfa.org/wp-content/uploads/2018/02/NECfinalOutlook.pdf

Rooney, W. L., J. Blumenthal, B. Bean, and J. E. Mullet. 2007. Designing sorghum as a dedicated bioenergy feedstock. *Biofuels Bioproducts & Biorefining-Biofpr, 1*(2), 147-157. doi:10.1002/bbb.15

Sanderson, M., R. Reed, W. Ocumpaugh, M. Hussey, G. Van Esbroeck, J. Read, C. Tischler, and F. Hons. 1999. Switchgrass cultivars and germplasm for biomass feedstock production in Texas. *Bioresour Technol, 67*(3), 209-219.

Sanford, G. R., L. G. Oates, S. S. Roley, D. S. Duncan, R. D. Jackson, G. P. Robertson, and K. D. Thelen. 2017. Biomass production a stronger driver of cellulosic ethanol yield than biomass quality. *Agron J, 109*(5). doi:10.2134/agronj2016.08.0454

Sannagoudar, M. S., R. Patil, and G. Rajanna. 2019. Calibration and evaluation of DSSAT-CERES model for kharif sorghum genotypes. *Experimental Agriculture International, 30*(3), 1-8.

Shafian, S., N. Rajan, R. Schnell, M. Bagavathiannan, J. Valasek, Y. Shi, and J. Olsenholler. 2018. Unmanned aerial systems-based remote sensing for monitoring sorghum growth and development. *PloS One, 13*(5).

Sharma, S., N. Rajan, S. Cui, K. Casey, S. Ale, R. Jessup, and S. Maas. 2017. Seasonal variability of evapotranspiration and carbon exchanges over a biomass sorghum field in the Southern U.S. Great Plains. *Biomass Bioenergy, 105*, 392-401. doi:10.1016/j.biombioe.2017.07.021

Sharma, S., N. Rajan, S. Cui, S. Maas, K. Casey, S. Ale, and R. Jessup. 2019. Carbon and evapotranspiration dynamics of a non-native perennial grass with biofuel

potential in the southern US Great Plains. *Agricultural and Forest Meteorology, 269*, 285-293. doi:10.1016/j.agrformet.2019.01.037

Shoemaker, C. E., and D. I. Bransby. 2010. *The role of sorghum as a bioenergy feedstock.* Paper presented at the Sustainable Alternative Fuel Feedstock Opportunities, Challenges and Roadmaps for Six US Regions. Proceedings of the Sustainable Feedstocks for Advanced Biofuel Workshop.

Shrestha, R., S. Thapa, Q. Xue, B. Stewart, B. Blaser, E. Ashiadey, J. Rudd, and R. Devkota. 2020. Winter wheat response to climate change under irrigated and dryland conditions in the US southern high plains. *Soil and Water Conservation, 75*(1), 112-122.

Silva, M. d. A., J. A. G. d. Silva, J. Enciso, V. Sharma, and J. Jifon. 2008. Yield components as indicators of drought tolerance of sugarcane. *Scientia Agricola, 65*(6), 620-627.

Singels, A., and C. N. Bezuidenhout. 2002. A new method of simulating dry matter partitioning in the CANEGRO sugarcane model. *Field Crops Res, 78*(2-3), 151-164. doi:Pii S0378-4290(02)00118-1, Doi 10.1016/S0378-4290(02)00118-1

Singels, A., M. Jones, F. Marin, A. Ruane, and P. Thorburn. 2014. Predicting climate change impacts on sugarcane production at sites in Australia, Brazil and South Africa using the CANEGRO model. *Sugar Tech, 16*(4), 347-355. doi:10.1007/s12355-013-0274-1

Singels, A., M. Jones, and M. van der BERG. 2008. DSSAT v 4.5 CANEGRO sugarcane plant module: Scientific documentation 2008. *International Consortium for Sugarcane Modelling*.

Singh, S., K. J. Boote, S. V. Angadi, K. Grover, S. Begna, and D. Auld. 2016. Adapting the CROPGRO model to simulate growth and yield of spring safflower in semiarid conditions. *Agron J, 108*(1), 64-72. doi:10.2134/agronj15.0272

Sissine, F. 2007. *Energy independence and security act of 2007: a summary of major provisions.* Paper presented at the Library of Congress Washington DC Congressional Research Service.

Sladden, S., D. Bransby, G. Aiken, and G. Prine. 1991. Biomass yield and composition, and winter survival of tall grasses in Alabama. *Biomass Bioenergy, 1*(2), 123-127.

Snider, J. L., R. L. Raper, and E. B. Schwab. 2012. The effect of row spacing and seeding rate on biomass production and plant stand characteristics of non-irrigated photoperiod-sensitive sorghum (Sorghum bicolor (L.) Moench). *Industrial Crops and Products, 37*(1), 527-535.

Sohl, T. L., B. M. Sleeter, K. L. Sayler, M. A. Bouchard, R. R. Reker, S. L. Bennett, R. R. Sleeter, R. L. Kanengieter, and Z. Zhu. 2012. Spatially explicit land-use and land-cover scenarios for the Great Plains of the United States. *Agric, Ecosyst Environ, 153*, 1-15.

Solomon, B. D., J. R. Barnes, and K. E. Halvorsen. 2007. Grain and cellulosic ethanol: History, economics, and energy policy. *Biomass Bioenergy, 31*(6), 416-425.

Sonkar, G., N. Singh, R. Mall, K. Singh, and A. Gupta. 2019. Simulating the impacts of climate change on sugarcane in diverse agro-climatic zones of northern India using CANEGRO-sugarcane model. *Sugar Tech, 22*, 460–472.

Sorghum-Checkoff. 2020. All About Sorghum. Retrieved from https://www.sorghumcheckoff.com/all-about-sorghum

Staggenborg, S. 2019. Forage and renewable sorghum end uses. In I. A. Ciampitti & P. V. V. Prasad (Eds.), *Sorghum: A State of the Art Future Perspetives* (Vol. 58, pp. 441-461). Madison, USA.

Stefaniak, T. R., J. A. Dahlberg, B. W. Bean, N. Dighe, E. J. Wolfrum, and W. L. Rooney. 2012. Variation in biomass composition components among forage, biomass, sorghum-sudangrass, and sweet sorghum types. *Crop Sci, 52*(4), 1949-1954. doi:10.2135/cropsci2011.10.0534

Steiner, J. 1986. Dryland grain sorghum water use, light interception, and growth responses to planting geometry. *Agron J, 78*(4), 720-726.

Stewart, B., S. Thapa, Q. Xue, and R. Shrestha. 2018. Climate change effect on winter wheat (Triticum aestivum L.) yields in the US Great Plains. *Soil and Water Conservation, 73*(6), 601-609.

Stokes, C. J., N. G. Inman-Bamber, Y. Everingham, and J. Sexton. 2016. Measuring and modelling CO2 effects on sugarcane. *Environ Model Software, 78*, 68-78.

Tamang, P., K. Bronson, A. Malapati, R. Schwartz, J. Johnson, and Moore-Kucera. 2011. Nitrogen requirements for ethanol production from sweet and photoperiod sensitive sorghums in the Southern High Plains. *Agron J, 103*(2), 431-440.

Tang, C., C. Sun, F. Du, F. Chen, A. Ameen, T. Fu, and G. H. Xie. 2018. Effect of plant density on sweet and biomass Sorghum production on semiarid marginal land. *Sugar Tech, 20*(3), 312-322.

Teruel, D., V. Barbieri, and L. Ferraro Jr. 1997. Sugarcane leaf area index modeling under different soil water conditions. *Scientia Agricola, 54*(SPE), 39-44.

Tew, T. L., and R. M. Cobill. 2008. Genetic improvement of sugarcane (Saccharum spp.) as an energy crop. In *Genetic Improvement of Bioenergy Crops* (pp. 273-294): Springer.

Thorp, K., S. Ale, M. Bange, E. Barnes, G. Hoogenboom, R. Lascano, A. McCarthy, S. Nair, J. Paz, and N. Rajan. 2014. Development and application of process-based simulation models for cotton production: A review of past, present, and future directions. *Cotton Science, 18*(1), 10-47.

Valentine, J., J. Clifton-Brown, A. Hastings, P. Robson, G. Allison, and P. Smith. 2012. Food vs. fuel: the use of land for lignocellulosic 'next generation' energy crops that minimize competition with primary food production. *Gcb Bioenergy, 4*(1), 1-19. doi:10.1111/j.1757-1707.2011.01111.x

Vargas, L., M. N. Andersen, C. Jensen, and U. Jørgensen. 2002. Estimation of leaf area index, light interception and biomass accumulation of Miscanthus sinensis 'Goliath'from radiation measurements. *Biomass Bioenergy, 22*(1), 1-14.

Viator, R., P. White Jr, A. Hale, and H. Waguespack. 2012. Screening for tolerance to periodic flooding for cane grown for sucrose and bioenergy. *Biomass Bioenergy, 44*, 56-63.

Viña, A., A. A. Gitelson, A. L. Nguy-Robertson, and Y. Peng. 2011. Comparison of different vegetation indices for the remote assessment of green leaf area index of crops. *Remote Sens Environ, 115*(12), 3468-3478.

Vose, J. M., B. D. Clinton, N. H. Sullivan, and P. V. Bolstad. 1995. Vertical leaf area distribution, light transmittance, and application of the Beer–Lambert Law in four mature hardwood stands in the southern Appalachians. *Canadian Journal of Forest Research, 25*(6), 1036-1043.

Vu, J. C. V., and L. H. Allen. 2009. Growth at elevated CO2 delays the adverse effects of drought stress on leaf photosynthesis of the C-4 sugarcane. *Plant Physiol, 166*(2), 107-116. doi:10.1016/j.jplph.2008.02.009

Waclawovsky, A. J., P. M. Sato, C. G. Lembke, P. H. Moore, and G. M. Souza. 2010. Sugarcane for bioenergy production: an assessment of yield and regulation of sucrose content. *Plant Biotechnol J, 8*(3), 263-276.

Wagle, P., and V. G. Kakani. 2014. Growing season variability in evapotranspiration, ecosystem water use efficiency, and energy partitioning in switchgrass. *Ecohydrology, 7*(1), 64-72.

Wang, Z., J. L. Heitman, T. J. Smyth, C. R. Crozier, A. Franzluebbers, S. Lee, J. Ronald, G. Z. Wang, J. L. Heitman, T. J. Smyth, and C. R. Crozier. 2017. Soil responses to bioenergy crop production in the North Carolina piedmont. *Agron J, 109*(4). doi:10.2134/agronj2017.02.0068

Whistance, J., W. Thompson, and S. Meyer. 2017. Interactions between California's low carbon fuel standard and the national renewable fuel standard. *Energy Policy, 101*, 447-455.

White, J. W. 1998. Modeling and crop improvement. In G. Y. Tsuji, G. Hoogenboom, & P. K. Thornton (Eds.), *Understanding Options for Agricultural Production* (pp. 179-188). The Netherlands: Kluwer Academic Publishers.

Wight, J., F. Hons, J. Storlien, T. Provin, H. Shahandeh, and R. Wiedenfeld. 2012. Management effects on bioenergy sorghum growth, yield and nutrient uptake. *Biomass Bioenergy, 46*, 593-604.

Willmott, C. J. 1981. On the validation of models. *Physical Geography, 2*(2), 184-194.

Wu, M., Y. Chiu, and Y. Demissie. 2012. Quantifying the regional water footprint of biofuel production by incorporating hydrologic modeling. *Water Resources Research, 48*. doi:Artn W10518, 10.1029/2011wr011809

Yang, J., J. Yang, S. Liu, and G. Hoogenboom. 2014. An evaluation of the statistical methods for testing the performance of crop models with observed data. *Agricultural Systems, 127*, 81-89.

Yang, Y., L. T. Wilson, J. Jifon, J. A. Landivar, J. da Silva, M. M. Maeda, J. Wang, and E. Christensen. 2018. Energycane growth dynamics and potential early harvest penalties along the Texas Gulf Coast. *Biomass Bioenergy, 113*, 1-14. doi:10.1016/j.biombioe.2018.03.003

Yimam, Y. T., T. E. Ochsner, and V. G. Kakani. 2015. Evapotranspiration partitioning and water use efficiency of switchgrass and biomass sorghum managed for biofuel. *Agric Water Manage, 155*, 40-47.

Zhang, Y., C. Liu, Y. Lei, Y. Tang, Q. Yu, Y. Shen, and H. Sun. 2006. An integrated algorithm for estimating regional latent heat flux and daily evapotranspiration. *Int J Remote Sens, 27*(1), 129-152. doi:10.1080/01431160500159743

Zhao, D., M. Irey, C. LaBorde, and C.-J. Hu. 2017. Identifying physiological and yield-related traits in sugarcane and energy cane. *Agron J, 109*(3). doi:10.2134/agronj2016.10.0585